

Microenvironmental advancement and miniaturization of human in vitro bone models

Citation for published version (APA):

Vis, M. A. M. (2023). *Microenvironmental advancement and miniaturization of human in vitro bone models*. [Phd Thesis 1 (Research TU/e / Graduation TU/e), Biomedical Engineering]. Eindhoven University of Technology.

Document status and date:

Published: 19/06/2023

Document Version:

Publisher's PDF, also known as Version of Record (includes final page, issue and volume numbers)

Please check the document version of this publication:

- A submitted manuscript is the version of the article upon submission and before peer-review. There can be important differences between the submitted version and the official published version of record. People interested in the research are advised to contact the author for the final version of the publication, or visit the DOI to the publisher's website.
- The final author version and the galley proof are versions of the publication after peer review.
- The final published version features the final layout of the paper including the volume, issue and page numbers.

[Link to publication](#)

General rights

Copyright and moral rights for the publications made accessible in the public portal are retained by the authors and/or other copyright owners and it is a condition of accessing publications that users recognise and abide by the legal requirements associated with these rights.

- Users may download and print one copy of any publication from the public portal for the purpose of private study or research.
- You may not further distribute the material or use it for any profit-making activity or commercial gain
- You may freely distribute the URL identifying the publication in the public portal.

If the publication is distributed under the terms of Article 25fa of the Dutch Copyright Act, indicated by the "Taverne" license above, please follow below link for the End User Agreement:

www.tue.nl/taverne

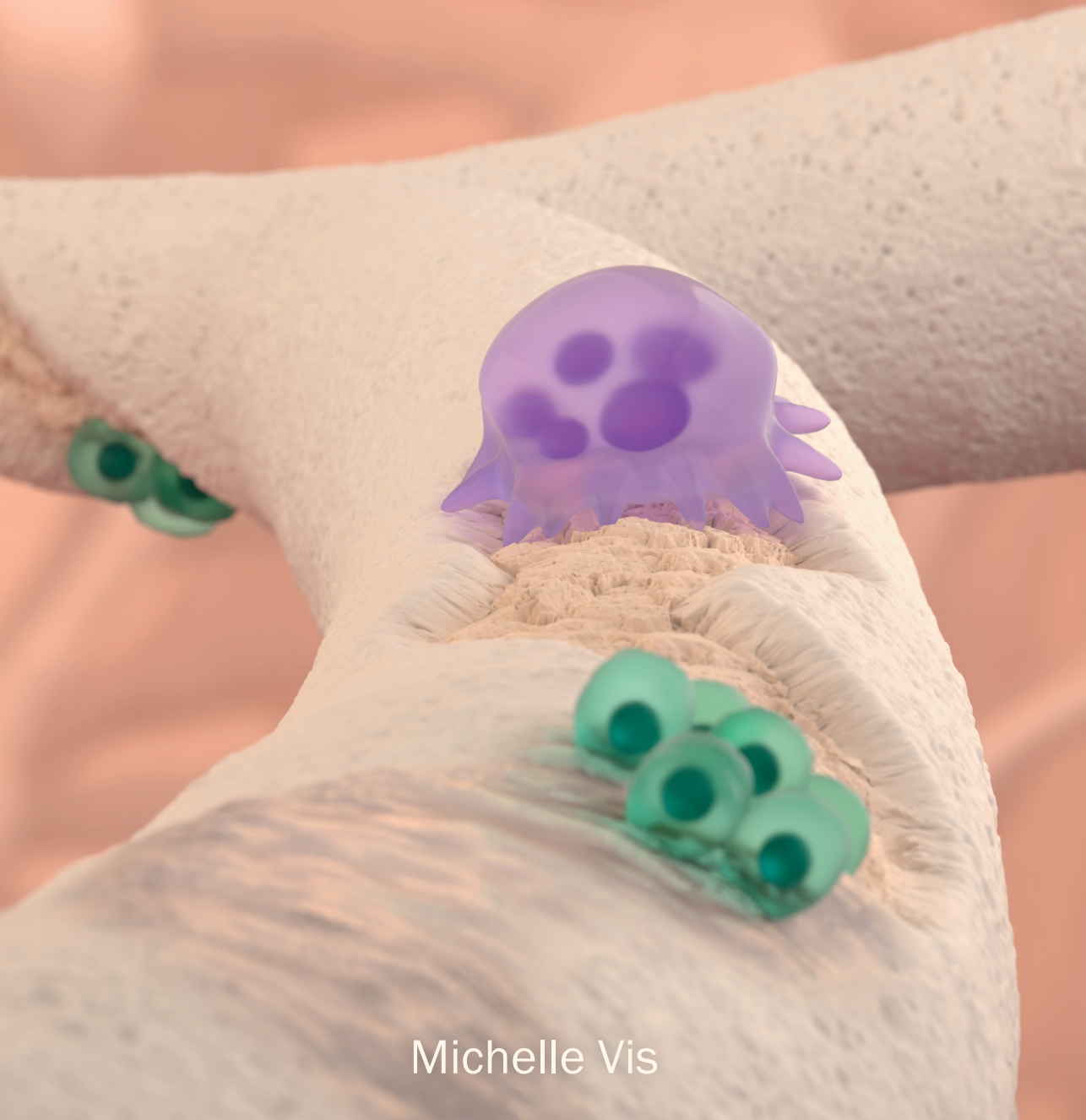
Take down policy

If you believe that this document breaches copyright please contact us at:

openaccess@tue.nl

providing details and we will investigate your claim.

Microenvironmental advancement
and miniaturization of human
in vitro bone models



Michelle Vis

Microenvironmental advancement and miniaturization of human *in vitro* bone models

Michelle Vis

A catalogue record is available from the Eindhoven University of Technology Library

ISBN: 978-90-386-5757-8

© Copyright 2023, M.A.M. Vis

All rights reserved. No part of this book may be reproduced, stored in a database or retrieval system, or published, in any form or in any way, electronically, mechanically, by print, photo print, microfilm or any other means without prior written permission by the author.

Cover design by Milan van Wezel, ICMS Animation Studio

Printed by ADC Dereumaux

This work is part of the research program TTW with project number TTW 016.Vidi.188.021, which is (partly) financed by the Netherlands Organization for Scientific Research (NWO).

Financial support for printing this thesis by Anna Fonds, Leiden, the Netherlands Society for Biomaterials and Tissue Engineering (NBTE) and the department of Biomedical Engineering of Eindhoven University of Technology for the publication of this thesis is gratefully acknowledged.

Microenvironmental advancement and miniaturization of human *in vitro* bone models

PROEFSCHRIFT

ter verkrijging van de graad van doctor aan de Technische Universiteit Eindhoven,
op gezag van de rector magnificus prof. dr. S.K. Lenaerts, voor een commissie
aangewezen door het College voor Promoties, in het openbaar te verdedigen op
maandag 19 juni 2023 om 16:00 uur

door

Michelle Anna Maria Vis

geboren te Brunssum

Dit proefschrift is goedgekeurd door de promotoren en de samenstelling van de promotiecommissie is als volgt:

Voorzitter	prof.dr. M. Merkx
Promotoren	dr. S. Hofmann prof. dr. K. Ito
Promotiecommissieleden	prof.dr. J.M.J. den Toonder prof. dr. G.C. Reilly (Sheffield University) prof.dr. J. Klein-Nulend (ACTA) dr. J.J.J.P. van den Beucken (Radboud UMC) dr. E. Farrell (Erasmus MC)

Het onderzoek dat in dit proefschrift wordt beschreven is uitgevoerd in overeenstemming met de TU/e Gedragscode Wetenschapsbeoefening.

Table of contents

Summary	1
Samenvatting	3
1. General introduction	6
2. Osteoblast-osteoclast cocultures: A systematic review and map of available literature	14
<i>Part 1: Enhancing the microenvironment for in vitro bone remodeling</i>	36
3. Impact of culture medium on cellular interactions in <i>in vitro</i> coculture systems	38
4. A dialysis medium refreshment cell culture set-up for an osteoblast-osteoclast coculture	50
<i>Part 2: Miniaturizing in vitro bone remodeling models</i>	70
5. Towards bone-remodeling-on-a-chip: self-assembling 3D osteoblast-osteoclast coculture in a microfluidic chip	72
6. Osteogenic differentiation on a chip using pumpless bidirectional fluid flow	106
7. General discussion	124
Bibliography	132
Scientific output	144
Curriculum Vitae	146
Dankwoord (Acknowledgements)	147

Summary

Healthy bone is maintained by the process of bone remodeling. An unbalance in this process leads to pathologies such as osteoporosis. Animal models are often used to study bone pathologies. However, data from animals frequently fail to predict the results obtained in human clinical trials. Human *in vitro* models are emerging as alternatives as they address the principle of reduction, refinement, and replacement of animal experiments (3Rs). Osteoblast-osteoclast cocultures are often used to study bone physiology, bone diseases and drugs in these models. In this thesis, we studied ways to advance the microenvironment for *in vitro* bone remodeling models as creating the right environment for both osteoblasts and osteoclasts simultaneously remains a challenge. Moreover, we explored methods to miniaturize our *in vitro* bone remodeling models. The emergence of organ-on-chip, which utilizes microfluidic technology to simulate the natural environment of tissues, has enabled scientists to miniaturize tissue engineered constructs. This technology has great potential to improve the accuracy and efficiency of bone tissue engineering, as well as to provide insights into the underlying mechanisms of healthy and diseased bone.

The use of osteoblast-osteoclast cocultures is not always clearly mentioned in the title and abstract in literature, making it difficult to identify these studies. As a result, researchers are all developing their own methods, leading to many methodological differences and incomparable results. Therefore, we systematically identified all osteoblast-osteoclast coculture studies that have been published before the year 2020 in Chapter 2. Differences in methods were mapped systematically, giving comprehensive details on cells, culture conditions and analytical techniques for using and studying osteoblast-osteoclast cocultures. In this way, researchers can quickly identify publications relevant to their specific needs and easily validate and compare their work with existing literature.

Coculturing of cells in *in vitro* tissue models is widely used to study how they interact with each other. This asks for a highly specific environment meeting the requirements of all involved cell types and therefore requires a great deal of optimization. We provided steps that can guide optimization of culture medium composition and volume in cocultures with a particular focus on cell communication via the cells' secretome in Chapter 3. The effect of medium exchange on cells is often an overlooked topic but particularly important for this type of cell communication. Medium exchange leads to loss of valuable auto- and paracrine factors produced by the cells but is necessary for nutrient supply and to prevent waste product accumulation. Thus, it remains the gold standard in cell culture applications. We proposed a method based on dialysis to reduce loss of the cells' secretome during culture medium exchange in Chapter 4. With our custom-made simple dialysis culture system, human mesenchymal stromal cells (MSCs) were differentiated into osteoblasts and monocytes (MCs) into osteoclasts while the secretome was maintained via dialysis. We showed an increased osteoblastic and osteoclastic activity in the dialysis groups compared to the standard non-dialysis groups. This culture system showed the potential to create a more efficient microenvironment compared to standard culture methods, allowing for cell

interactions via secreted factors in mono- and cocultures. In addition, the system could be applied for many other tissue types.

In the second part of this thesis, we explored methods to miniaturize our *in vitro* bone remodeling model. At the moment, no complete *in vitro* model for bone-remodeling exists. Microfluidic chips offer great possibilities, particularly because of the dynamic culture options, which are crucial for *in vitro* bone formation. We developed a bone-on-a-chip coculture system in which human MSCs were differentiated into osteoblasts and self-assembled into scaffold free bone-like tissues with the shape and dimensions of human trabeculae in Chapter 5. Human MCs were able to attach to these tissues and to fuse into multinucleated osteoclast-like cells, establishing the coculture. Furthermore, a set-up was developed allowing for long-term (35 days) on-chip cell culture with benefits including continuous fluid-flow, low bubble formation risk, easy culture medium exchange inside the incubator and live-cell imaging options. In Chapter 6, we investigated the use of gravity-driven bidirectional flow for bone-on-a-chip devices. Perfusion set-ups require specialized pumps and tubing and can be rather complex. Gravity-driven flow could offer an alternative as it is simpler, requiring only a rocking plate which is readily available in most laboratories. The rocking motion enables a bidirectional flow inside the chip channel. We studied the effect of bidirectional flow on osteogenic differentiation of MSCs by comparing it with static cultures and our previous pump system with unidirectional flow. A clear benefit of flow compared to static cultures was seen in terms of extracellular matrix production and mineralization by the cells. With Chapter 5 and 6 we provided two different methods for dynamic culturing of bone-on-a-chip devices, of which each has its own advantages and can be selected based on the specific goals of the research project.

To conclude, this thesis provides strategies for the microenvironmental advancement and miniaturization of human *in vitro* bone remodeling models. Moreover, we are the first to show a fully human, 3D, direct osteoblast-osteoclast coculture on a chip. Our work is not only of interest for bone tissue engineering applications but could also be used with many other tissue types. First, the dialysis system could be used for the proliferation and differentiation of different cell types. Second, the microfluidic chip set-up could be combined with any type of microfluidic chip and used for dynamic fluid flow cultures. With this thesis we aimed to hand out tools for improvement of *in vitro* models, with the ultimate goal of replacing, reducing, and refining the use of animal models. We believe that *in vitro* models will provide reliable and predictive alternatives to animal testing in the future.

Samenvatting

Gezonde botten worden in stand gehouden door een proces genaamd bot remodelering. Wanneer dit proces uit balans raakt, ontstaan er ziektes zoals bijvoorbeeld osteoporose. Diermodellen worden vaak gebruikt om ziektes in bot te onderzoeken, maar helaas voorspellen deze modellen niet voldoende hoe de ziektes verlopen bij mensen. Menselijke *in vitro* modellen zijn hiervoor een alternatief. “*In vitro*” staat vrij vertaald voor “in een reageerbuis”, in dit geval duidend op het maken van weefsels in het laboratorium. Voor het nabootsen van botweefsel gebruiken we de botcellen genaamd osteoblasten en osteoclasten die we gelijktijdig kweken in zogenaamde coculturen. In deze scriptie hebben we manieren onderzocht om de micro-omgeving voor *in vitro* bot remodeleringsmodellen te verbeteren, omdat het creëren van de juiste omgeving voor zowel osteoblasten als osteoclasten tegelijkertijd een uitdaging blijft. Bovendien hebben we methoden onderzocht om onze *in vitro* bot remodeleringsmodellen te miniaturiseren. De opkomst van organen-op-*een-chip*, waarbij microfluidische technologie gebruikt wordt om het natuurlijke milieu van weefsels na te bootsen, heeft wetenschappers in staat gesteld om in het laboratorium gemaakte weefsels te miniaturiseren. Deze technologie heeft een grote potentie om de nauwkeurigheid en efficiëntie van botweefseltechnologie te verbeteren, evenals om inzicht te geven in de onderliggende mechanismen van gezond en ziek bot.

In de wetenschappelijk literatuur wordt de toepassing van osteoblast-osteoclast coculturen niet altijd duidelijk vermeld in de titel en samenvatting, waardoor het lastig is om deze studies te identificeren. Als gevolg hiervan ontwikkelen onderzoekers hun eigen methoden, wat leidt tot veel methodologische verschillen en niet te vergelijken resultaten. Daarom identificeerden we systematisch alle osteoblast-osteoclast cocultuur studies die voor het jaar 2020 zijn gepubliceerd in hoofdstuk 2. Verschillen in methoden werden systematisch in kaart gebracht, waardoor uitgebreide details over cellen, culturomstandigheden en analysetechnieken voor het gebruik en onderzoek van osteoblast-osteoclast coculturen beschikbaar kwamen. Op deze manier kunnen onderzoekers snel publicaties vinden die relevant zijn voor hun specifieke behoeften en hun werk gemakkelijk valideren en vergelijken met bestaande literatuur.

Coculturen van cellen in weefselmodellen wordt veel gebruikt om te onderzoeken hoe cellen met elkaar communiceren. Hiervoor is een zeer specifieke omgeving nodig die aan de vereisten van alle betrokken celtypen voldoet en daarom is er veel optimalisatie nodig. We hebben manieren aangegeven die kunnen helpen bij optimalisatie van cultuurmedium compositie en -volume in coculturen met een focus op celcommunicatie via door de cel uitgescheiden stoffen in hoofdstuk 3. Het effect van mediumwissel op cellen wordt vaak over het hoofd gezien, maar is vooral belangrijk voor dit type celcommunicatie. Mediumwissel leidt tot verlies van waardevolle factoren die door de cellen worden geproduceerd, maar is noodzakelijk voor het verstrekken van voedingsstoffen en het verwijderen van afvalstoffen. Het blijft daarom de gouden standaard in celkweek. We hebben in hoofdstuk 4 een methode ontwikkeld, gebaseerd op dialyse, om verlies van door de cel uitgescheiden stoffen tijdens de mediumwissel te verminderen. Met ons zelfgemaakte eenvoudige dialysesysteem

hebben we menselijke mesenchymale stromale cellen (MSC's) gedifferentieerd tot osteoblasten en monocyt (MC's) tot osteoclasten, terwijl de uitgescheiden stoffen behouden bleven via dialyse. We zagen een verhoogde osteoblastische en osteoclastische activiteit in de dialysegroepen in vergelijking met de standaardgroepen zonder dialyse. Dit systeem toont het potentieel om een efficiëntere micro-omgeving te creëren in vergelijking met standaard cultuurmethoden, waardoor cel interacties via uitgescheiden factoren in mono- en coculturen mogelijk worden gemaakt. Het systeem kan op veel andere weefseltypen worden toegepast.

In de tweede helft van deze scriptie hebben we methoden onderzocht om onze botweefsel modellen te miniaturiseren. Op dit moment bestaat er geen compleet model voor bot remodelering. Microfluidische chips bieden grote mogelijkheden, met name vanwege de dynamische cultuurmogelijkheden, die cruciaal zijn voor *in vitro* botvorming. In hoofdstuk 5 hebben we een bot-op-een-chip cocultuur ontwikkeld waarin menselijke MSCs werden gedifferentieerd tot osteoblasten en zichzelf vormden tot driedimensionale botachtige weefsels. Menselijke MCs konden zich aan deze weefsels hechten en fuseren tot meerkernige osteoclastachtige cellen. Verder werd een opstelling ontwikkeld waarmee lange-termijn (35 dagen) celweek in de chip mogelijk is, met als voordelen een continue vloeistofstroom, een lage risicovorming op luchtbellen, een gemakkelijke vervanging van het cultuurmedium in de incubator en opties voor het live bekijken van de cellen. In hoofdstuk 6 hebben we onderzocht hoe zwaartekracht-gedreven bidirectionele stroming voor bot-op-een-chip kan worden gebruikt. Perfusiesystemen vereisen gespecialiseerde pompen en slangen en kunnen redelijk complex zijn. Zwaartekracht gedreven vloeistofstroming kan een alternatief bieden, omdat deze eenvoudiger is en alleen een wiegende beweging vereist. De wiegende beweging maakt een bidirectionele vloeistofstroming in het chipkanaal mogelijk. We hebben de invloed van bidirectionele vloeistofstroom op osteogene differentiatie van MSCs bestudeerd door het te vergelijken met statische kweekmodellen. Er was duidelijk een voordeel van vloeistofstroom in vergelijking met statische kweekmodellen wat betreft de productie van extracellulaire matrix en mineralisatie door de cellen. Met hoofdstuk 5 en 6 bieden we twee verschillende methoden voor het dynamisch kweken van bot-op-een-chips, waarvan elk zijn eigen voordelen heeft en kan worden geselecteerd op basis van de specifieke doelen van het onderzoeksproject.

Concluderend biedt deze scriptie strategieën voor de micro-omgevingsverbetering en miniaturisering van menselijke *in vitro* bot remodeleringsmodellen. Bovendien zijn we de eersten die een volledig menselijke, driedimensionale, directe osteoblast-osteoclast cocultuur op een chip laten zien. Ons werk is niet alleen van belang voor toepassingen in botweefseltechnologie, maar kan ook worden gebruikt met vele andere weefseltypen. Ten eerste kan het dialyse-systeem worden gebruikt voor de proliferatie en differentiatie van verschillende celtypen. Ten tweede kan de opstelling worden gecombineerd met elk type microfluidische chip en worden gebruikt voor dynamische kweekmodellen. Met deze scriptie hebben we als doel gereedschappen aan te bieden voor verbetering van *in vitro* modellen, met als ultieme doel het vervangen, verminderen en verfijnen van het gebruik van diermodellen. We geloven dat *in vitro* modellen in de toekomst betrouwbare en voorspellende alternatieven zullen bieden voor dierproeven.

Chapter 1

General introduction

Preface

The adult skeleton has around 213 bones.¹ In the Netherlands, an estimated 100,000 to 120,000 fragility fractures occur annually, the equivalent of at least 11 broken bones per hour.² The underlying cause of these fragility fractures is osteoporosis, a metabolic bone disease that causes bones to become weak and fragile. The number of these fractures is expected to rise by more than a third over the next 15 years due to aging of the population.² Animal models are often used to study bone pathologies such as osteoporosis. However, animal models are costly, time-consuming and ethically questionable.³ Moreover, data from animals frequently fail to predict the results obtained in human clinical trials.^{3,4} The concept of tissue engineering has enabled scientists to develop biological substitutes of human tissues in the laboratory. With tissue engineering, so called human *in vitro* models can be created that mimic natural bone-related functions. These human *in vitro* models provide the invaluable opportunity to explore bone physiology and pathology, promising the ability to further understand bone diseases and develop new drugs.

1.1 Bone tissue

Bone is a complex and dynamic tissue that is essential for the structural integrity of the human body. It is composed of cells, extracellular matrix, and minerals and is responsible for providing support and protection, allowing movement, and serving as a calcium, phosphate and growth factor storage. Bones are composed of a dense outer layer known as cortical bone and a highly porous inner layer known as trabecular bone (Figure 1.1A). Bone matrix is made up of organic (~30-40%) and inorganic (~60-70%) components.⁵ The organic matrix consists mainly of collagen type 1 and serves as a template for mineralization.^{5,6} The inorganic matrix consists of mineral salts, mainly hydroxyapatite. These small, tightly packed, needle like crystals mineralize the collagen fibers, resulting in a mineralized bone matrix with unique mechanical properties.

The smallest functional unit of bone is called a basic multicellular unit (Figure 1.1B).⁷ In this unit, three cell types work together: osteoblasts, osteocytes, and osteoclasts. Osteoblasts are cube-shaped bone forming cells that secrete the immature bone matrix, called osteoid.⁸ Osteoblasts that remain on the bone surface are flatly shaped and called bone lining cells. When osteoblasts embed themselves in the secreted matrix and become completely surrounded by it, they differentiate into osteocytes. Osteocytes are stellate shaped cells that function as mechanosensors that monitor and maintain the matrix. Osteocytes are able to transform mechanical strain into chemical signaling to regulate bone formation and resorption.^{8,9} For bone resorption, osteoclasts are recruited to the bone matrix.⁸ When active, osteoclasts appear as giant multinucleated cells with a ruffled border that is in direct contact with the bone. At this contact point, bone is degraded via enzymes and acids. Together, the cells in the basic multicellular unit cooperate in a process of continuous bone formation and resorption, called bone remodeling, to maintain bone health.

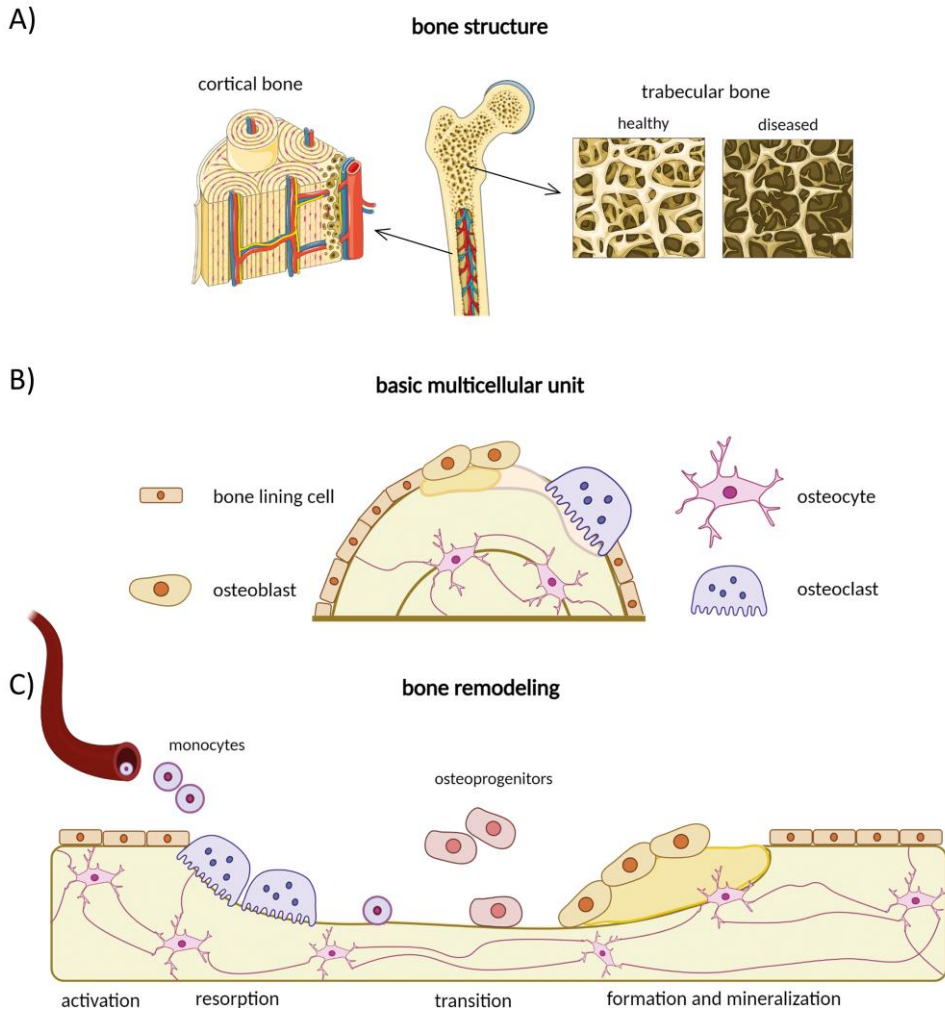


Figure 1.1 A) Overview of the structure of long bones comprising of cortical bone and trabecular bone. B) The basic multicellular unit with bone lining cells, osteoblasts, osteocytes, and osteoclasts. C) The bone remodeling process divided in several steps: activation, resorption, transition and formation and mineralization. This image was created with use of BioRender and Servier Medical Art.

1.2 Bone remodeling

Bone has the power to regenerate and repair itself. In order to do so, a process referred to as bone remodeling plays an important role. Bone remodeling is initiated in response to changes in biomechanical loading or to replace old, damaged bone with new bone and takes place continuously during a lifetime. This process is vital for the maintenance of healthy bones and helps to prevent fractures and other bone-related injuries.¹⁰ In remodeling, the balance between bone formation and resorption is important. In healthy bone, this process is in equilibrium, called homeostasis. In certain bone diseases, the balance is disturbed,

which could either result in too much (e.g. osteopetrosis) or too little bone tissue (e.g. osteoporosis).

Bone remodeling comprises four phases (Figure 1.1C): In the activation phase, pre-osteoclasts are recruited from the blood circulation. They attach to the bone surface and fuse into multinucleated osteoclasts. Next, the resorption phase is initiated. Osteoclasts start to resorb old or damaged bone tissue. Minerals are hereby released into the blood. Thereafter, the transition phase takes place in which the osteoclasts leave the bone surface. Macrophages clean the surface and osteoprogenitor cells are attracted. In the formation phase, these osteoprogenitors differentiate into osteoblasts that secrete new collagen matrix and control its mineralization.¹¹ This phase is important for maintaining bone strength and density. Cortical bone turnover is around 2–3% per year, which is sufficient to maintain bone strength.¹ Trabecular bone presents a higher turnover rate of around 20% per year because of its role in calcium and phosphorus metabolism.^{1,12}

1.3 Bone tissue engineering

Tissue engineering (TE) is the interdisciplinary field that applies the principles of engineering and life sciences towards the development of functional biological substitutes for damaged tissues.¹³ Advances in TE have produced various strategies for fabricating living human tissues, including bone. Traditionally, bone tissue engineering has been focused on creating grafts for patients with extensive bone damage, utilizing scaffolds, progenitor cells, mechanical stimuli, and soluble factors.⁶ The development of these grafts generated methods to manipulate cells and grow three-dimensional tissues. With this, TE also provided the opportunity to grow *in vitro* tissues that could function as a model to monitor diseases and to test drugs in the laboratory.

1.4 *In vitro* bone models

In vitro models are engineered tissues made in the laboratory using cells and optionally also biomaterials. By using human cells, these models are hopefully able to represent human tissue behavior in healthy and diseased states. At the moment, animal models are often used to study bone pathologies, but animal models are costly, time-consuming and ethically questionable.³ In addition, the lack of human relevant models has led to a high rate of failure for therapeutic drugs in the clinic and increased healthcare costs.³ There is a growing interest in exploring alternative preclinical models.^{3,4} Human *in vitro* models are emerging in search for alternatives to animal models as they address the principle of reduction, refinement, and replacement of animal experiments (3Rs).¹⁴ The challenge remains to recreate functional bone tissue while being isolated from the natural environment of the body. *In vitro* bone models potentially represent powerful tools for the development of new treatments for bone disorders and diseases.

1.5 Bone-on-a-chip

One of the recent successes in the pursuit to create human *in vitro* models is the use of organ-on-chip microfluidic culture devices.³ These devices are lined with living cells cultured under fluid flow and can simulate organ-level physiology and pathophysiology with high

fidelity.³ Organ-on-chip devices promise several advantages over traditional *in vitro* culture techniques such as small volumes of cells, samples and reagents leading to decreased costs and options for parallel and real-time analysis. Additionally, structural and dynamic cues are readily integrated. Particularly the dynamic culture options are of interest for culturing bone cells, as in their natural environment these cells experience a regular mechanical loading regime.

Organ-on-chip devices have been reported for many different tissue types. Chips with several tissue types can even be coupled to create a body-on-a-chip, which enables capturing of both the efficacy of a drug and the potential toxicity in other organs.¹⁵ To date, bone-on-a-chip models have not been abundantly reported, probably because of the highly complex bone microenvironment and multicellularity.¹⁶ To study the bone remodeling process accurately, all involved cell types (osteoblasts, osteoclasts and osteocytes) need to be present. These cell types all have different lifespans from days to months and may not be located at the remodeling site simultaneously.^{16–20} Bone-on-a-chip models offer opportunities to remove these spatial and temporal restrictions and are therefore of interest to study bone remodeling.

1.6 Thesis outline

In this thesis we aim to provide strategies for advancement and miniaturization of human *in vitro* bone remodeling models. The thesis is divided into two parts. In the first part, we studied ways to advance the microenvironment for *in vitro* bone remodeling as creating the right environment for the coculture of osteoblasts and osteoclasts remains a challenge. In the second part, we explored methods to miniaturize our *in vitro* bone remodeling models into bone-on-a-chip systems.

To study bone remodeling *in vitro*, a coculture of osteoblasts and osteoclasts is needed. The use of these cocultures is not always clearly mentioned in the title and abstract in literature, making it difficult to identify these studies. As a result, researchers are all developing their own methods, leading to many methodological differences and incomparable results. Therefore, we systematically identified all osteoblast-osteoclast coculture studies that have been published before the year 2020 in **Chapter 2**. Comprehensive details on cells, culture conditions and analytical techniques were mapped systematically and made openly available in a database. In this way, researchers can quickly identify publications relevant to their specific needs and easily validate and compare their work with existing literature.

Part 1: Enhancing the microenvironment for *in vitro* bone remodeling

Coculturing of cells in *in vitro* tissue models is widely used to study how they interact with each other. This asks for a highly specific environment meeting the requirements of all involved cell types and therefore requires a great deal of optimization. We provided steps that can guide optimization of culture medium composition and volume in cocultures with a particular focus on cell communication via the cells' secretome in **Chapter 3**. The effect of medium exchange on cells is often an overlooked topic but particularly important for this type of cell communication. Medium exchange leads to loss of valuable auto- and paracrine factors produced by the cells but is necessary for nutrient supply and to prevent waste

product accumulation. We proposed a method based on dialysis to reduce loss of the cells' secretome during culture medium exchange in **Chapter 4**. This culture system showed the potential to create a more efficient microenvironment compared to standard culture methods, allowing for cell interactions via secreted factors in mono- and cocultures. In addition, the system could be applied for many other tissue types.

Part 2: Miniaturizing *in vitro* bone remodeling models

At the moment, no complete *in vitro* model for bone-remodeling exists that contains all needed cell types and their interactions. Microfluidic chips offer great possibilities, particularly because of the dynamic culture options which are crucial for *in vitro* bone formation. We developed a bone-on-a-chip coculture system in which human MSCs were differentiated into osteoblasts and self-assembled into scaffold-free bone-like tissues with the shape and dimensions of human trabeculae in **Chapter 5**. Human MCs were able to attach to these tissues and to fuse into multinucleated osteoclast-like cells, establishing the coculture. Furthermore, a set-up was developed allowing for long-term (35 days) on-chip cell culture with benefits including continuous fluid-flow, low bubble formation risk, easy culture medium exchange inside the incubator and live-cell imaging options. In **Chapter 6**, we investigated the use of gravity-driven bidirectional flow for bone-on-a-chip devices. Perfusion set-ups are needed for dynamic culturing, but require specialized pumps and tubing and can be rather complex. Bidirectional gravity-driven flow could offer an alternative as it is simpler, requiring only a rocking plate which is readily available in most laboratories. Furthermore, bidirectional flow can better recapitulate the multidirectional movement of the interstitial fluid within the native bone. We studied the effect of bidirectional flow on osteogenic differentiation of MSCs by comparing it with static cultures and our previous pump system with unidirectional flow. A clear benefit of flow compared to static cultures was seen in terms of extracellular matrix production and mineralization by the cells. With Chapter 5 and 6 we provided two different methods for dynamic culturing of bone-on-a-chip devices, of which each has its own advantages and can be selected based on the specific goals of the research project.

The main findings of this thesis are presented and discussed in **Chapter 7** and potential future directions are described.

Chapter 2

Osteoblast-osteoclast cocultures: A systematic review and map of available literature

The contents of this chapter are based on:

Stefan J. A. Remmers^a, Bregje W. M. de Wildt^{a*}, **Michelle A. M. Vis^{a*}**, Eva S. R. Spaander^a, Rob B. M. de Vries^b, Keita Ito^a, Sandra Hofmann^a (2021) *PLOS ONE* 16(11): e0257724. <https://doi.org/10.1371/journal.pone.0257724>

^a *Department of Biomedical Engineering and Institute for Complex Molecular Systems (ICMS), Eindhoven University of Technology, Eindhoven*

^b *Department for Health Evidence, SYRCLE, Radboud Institute for Health Sciences, Radboud UMC, Nijmegen*

* both authors contributed equally

Abstract

Drug research with animal models is expensive, time-consuming and translation to clinical trials is often poor, resulting in a desire to replace, reduce, and refine the use of animal models. One approach to replace and reduce the use of animal models is to use *in vitro* cell-culture models. To study bone physiology, bone diseases and drugs, many studies have been published using osteoblast-osteoclast cocultures. The use of osteoblast-osteoclast cocultures is usually not clearly mentioned in the title and abstract, making it difficult to identify these studies without a systematic search and thorough review. As a result, researchers are all developing their own methods, leading to conceptually similar studies with many methodological differences and, as a consequence, incomparable results. The aim of this study was to systematically review existing osteoblast-osteoclast coculture studies published up to 6 January 2020, and to give an overview of their methods, predetermined outcome measures (formation and resorption, and ALP and TRAP quantification as surrogate markers for formation and resorption, respectively), and other useful parameters for analysis. Information regarding these outcome measures was extracted and collected in a database, and each study was further evaluated on whether both the osteoblasts and osteoclasts were analyzed using relevant outcome measures. From these studies, additional details on methods, cells and culture conditions were extracted into a second database to allow searching on more characteristics. The two databases presented in this publication provide an unprecedented amount of information on cells, culture conditions and analytical techniques for using and studying osteoblast-osteoclast cocultures. They allow researchers to identify publications relevant to their specific needs and allow easy validation and comparison with existing literature. Finally, we provide the information and tools necessary for others to use, manipulate and expand the databases for their needs.

2.1 Introduction

Bone is a highly dynamic tissue with mechanical and metabolic functions that are maintained by the process of bone remodeling by bone forming osteoblasts (OBs), bone resorbing osteoclasts (OCs), and regulating osteocytes. In healthy tissue, bone resorption and formation are in equilibrium, maintaining the necessary bone strength and structure to meet the needs of the body. In diseases such as osteoporosis and osteopetrosis this equilibrium is disturbed, leading to pathological changes in bone mass that adversely affect the bone's mechanical functionality.²¹

Studies on bone physiology, bone disease and drug development are routinely performed in animal models, which are considered a fundamental part of preclinical research. The use of animals raises ethical concerns and is generally more time consuming and expensive than *in vitro* research. Laboratory animals are also physiologically different from humans. Their use in pre-clinical studies often leads to poor translation of results to human clinical trials^{22,23} and subsequent failure of promising discoveries to enter routine clinical use.^{24,25} These limitations and the desire to reduce, refine and replace animal experiments gave rise to the development of *in vitro* models.^{26,27} Over the last four decades, significant progress has been made towards developing OB-OC coculture models.

The development of *in vitro* OB-OC cocultures started with a publication of T.J. Chambers in 1982, where the author induced quiescence of isolated tartrate resistant acid phosphatase (TRAP)-positive rat OCs with calcitonin and reversed their quiescence by co-culturing them with isolated rat OBs in direct contact.²⁸ At that time, studies involving OCs resorted to the isolation of mature OCs by disaggregation from fragmented animal bones. The first account of *in vitro* osteoclastogenesis in coculture was realized in 1988 when Takahashi and co-authors cultured mouse spleen cells and isolated mouse OBs in the presence of $1\alpha,25$ -dihydroxyvitamin D3 and found TRAP-positive dentine-resorbing cells.²⁹ The herein described methods were used and adapted to generate OCs for the following decade. Most of the studies published until this point in time used cocultures as a tool for achieving osteoclastogenesis, as opposed to a model for bone remodeling. At that time, a coculture of OBs with spleen cells or monocytes was the only way of generating functional OCs *in vitro*. It wasn't until 1999 that Suda discovered Receptor Activator of Nuclear Factor Kappa Ligand (RANKL) and Macrophage Colony Stimulating Factor (M-CSF) as the necessary and sufficient proteins required for differentiating cells from the monocyte/macrophage lineage into functioning OCs.³⁰⁻³³ This discovery marked the start of coculture models developed for studying bone remodeling.

In recent years, many research groups have ventured into the realm of OB-OC cocultures with the intent of studying both formation and resorption, but each group seems to be individually developing the tools to suit their needs resulting in many functionally related experiments that are methodologically completely different. In addition, the use of such methods is often not clearly stated within title and abstracts. Simple title/abstract searches such as 'OB + OC + coculture' show only a fraction of available studies using OB-OC

cocultures. Finding and comparing different coculture approaches and their results is thus complicated which forces each group to develop and use their own methods.

The aim of this study was to conduct a systematic review of all OB-OC cocultures published up to January 6, 2020. With this systematic review, we aimed at identifying all existing OB-OC coculture studies and analyze these within two comprehensive databases, allowing researchers to quickly search, sort and select studies relevant for their own research. Database 1 contains all OB-OC coculture studies in which at least one relevant primary outcome measure was investigated (formation and/or resorption) or secondary outcome measure (alkaline phosphatase (ALP) and/or tartrate resistant acid phosphatase (TRAP) quantification as surrogate markers for formation and resorption, respectively) (Supplementary Information S2.1). A sub-selection of studies that investigated these relevant outcome measures on both OBs and OCs in the coculture was included in Database 2, accompanied by additional details on methods, culture conditions and cells (Supplementary Information S2.2). The collection of the two databases will further be referred to as a systematic map.

2.2 Methods

For this systematic map a structured search protocol was developed using the SYRCLÉ protocol format.³⁴ The protocol and search strings were made publicly available before completion of study selection via Zenodo to ensure transparency of the publication.³⁵ In short, three online bibliographic literature sources were consulted with a comprehensive search query and the resulting publications were combined and screened using a four-step procedure (Figure 2.1): 1) identification of OB-OC cocultures, 2) identification of relevant outcome measures, 3) categorization in Databases 1 and 2 (Figure 2.2), 4) search for additional articles in the reference lists of studies included in Database 2 and relevant reviews.

2.2.1 Database Search

The online bibliographic literature sources Pubmed, Embase (via OvidSP) and Web of Science were searched on January 6, 2020 with a predefined search query consisting of the following components: ([OBs] OR ([OB precursors] AND [bone-related terms])) AND ([OCs] OR ([OC precursors] AND [bone-related terms])) AND [coculture], where each component in square brackets represents a list of related thesaurus and free-text search terms. The full search strings can be found via Zenodo.³⁵ The results of all three searches were combined. Conference abstracts and duplicates were removed using the duplicate removal tools of Endnote X7 and Rayyan web-based systematic review software.³⁶ The entire screening and data collection process was performed independently by two researchers.

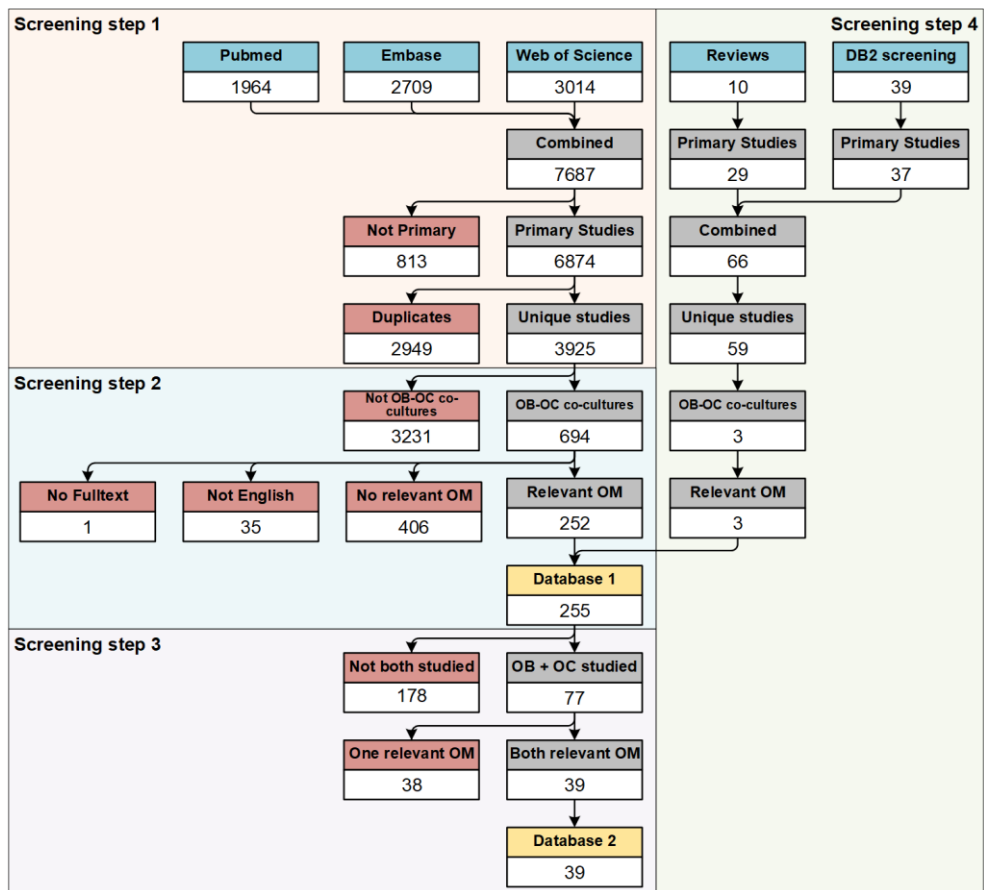


Figure 2.1 Flow diagram of systematic literature search and screening. Screening step 1: Hits from 3 online bibliographic literature sources were combined, primary studies were selected, and duplicates were removed. Title and abstracts were screened for the presence of OB-OC cocultures. Screening step 2: OB-OC cocultures were screened in full text for relevant outcome measures. All studies in which at least one relevant outcome measure was studied were included into Database 1. Screening step 3: Papers in which both cell types were studied with relevant outcome measures were included into Database 2. Screening step 4: Papers included into Database 2 and reviews were screened for potentially missing relevant studies and identified studies were screened in the same manner as above. Each screening step within the screening steps is marked with a colored header. Blue header: used as input for the review. Grey header: selection step. Red header: excluded studies. Yellow header: Database as presented in this systematic map.

2.2.2 Screening step 1: Identification of OB-OC cocultures

This step was performed to identify and extract OB-OC cocultures from the complete list of studies identified from the three online bibliographic literature sources after automatic removal of conference abstracts and duplicates. Using Rayyan web-based systematic review software, the titles and abstracts were screened for the presence of primary studies using OB-OC cocultures.³⁶ Reviews, theses, chapters, and conference abstracts that were not automatically detected were excluded at this point. Potentially relevant reviews were saved separately to serve as an additional source of studies that could have been missed by the systematic search.

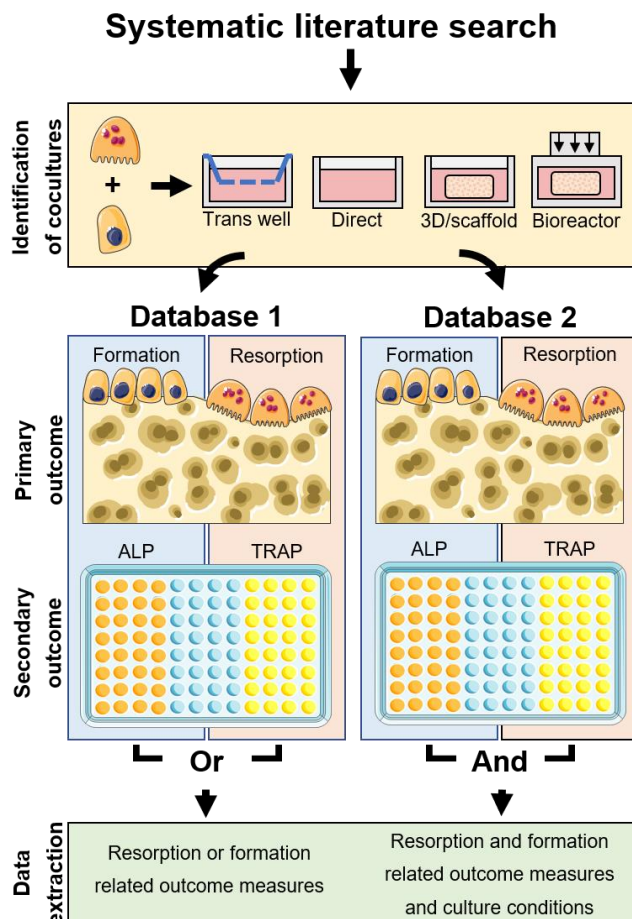


Figure 2.2 Schematic overview of Databases 1 and 2. All identified studies were searched for OB-OC cocultures, where coculture was defined as OB and OC being present simultaneously and able to exchange biochemical signals. In addition to direct-contact cultures, cultures such as transwell cultures, 3D or scaffold cultures and bioreactor cultures were allowed as well. OB-OC coculture studies which used relevant outcome measures were included into Database 1. Of these, only the relevant outcome measures were analyzed. All studies where relevant outcome measures were used for both OB and OC were included into Database 2 as well. Of these, cells and culture conditions were analyzed. The figure was modified from Servier Medical Art, licensed under a Creative Common Attribution 3.0 Generic License (<http://smart.servier.com>, accessed on 2 July 2021).

In the selection process, coculture was defined as the simultaneous (assumed) presence of OBs and OCs (or OB-like and/or OC-like cells) within the same culture system at a moment during the described experiment such that the cells were able to communicate either via soluble factors in the medium and/or direct cell-cell contact. Both primary cells and cell lines of any origin were admitted including heterogeneous cell populations if these were clearly defined and expected to result in a biologically relevant number of the desired cell type. The presence of progenitor cells (such as monocytes or mesenchymal stem/stromal cells) was allowed only if these were either verified or expected to differentiate into OBs and/or OCs.

Studies using a single animal or human donor for both cell types were allowed, but only if the two (progenitor) cell types were at one point separated, counted, and reintroduced in a controlled manner. Trans-well systems (no physical contact but shared medium compartment with or without membrane), scaffolds (3-dimensional porous structure of any material including decellularized matrix), and bioreactor culture systems (culture exposed to physical stimuli such as rotation, mechanical loading or fluid flow) were included. Conditioned media experiments were excluded because these do not allow real-time two-way exchange of cell signals. Explant-, organ- and other *ex vivo* cultures were excluded, except when these were used solely to generate decellularized matrix.

When the study used any type of OB-OC coculture as defined above, the study was included. When, based on the title and abstract, it was possible that there was a coculture but this was not described as such, the full-text publication was screened.

2.2.3 Screening step 2: Identification of relevant outcome measures in the coculture experiments

This step was used to identify cocultures that specifically investigated relevant outcome measures related to bone remodeling: formation or resorption (primary outcome measures), or quantitative measurements of activity markers ALP or TRAP in a dedicated assay (secondary outcome measures). The primary outcome measures of resorption and formation were chosen because these are the processes that are directly affected in bone diseases. Formation/resorption measurement was defined as any method that directly measures the area or volume of (tissue) mineralization by OBs or resorption by OCs or any method that measures by-products or biochemical markers that directly and exclusively correlate to formation/resorption respectively. The secondary outcome measures of ALP and TRAP were included because these are regarded as viable alternatives for the direct measurement of formation and resorption. The measurement of ALP and TRAP was defined as the detection of either the enzymatic activity or the direct quantification of these proteins present. Polymerase Chain Reaction (PCR) and Immuno-histological stainings (with or without image analysis) were not considered relevant outcome measures. The full texts of the studies identified in screening step 1 were screened for experimental techniques and outcome measures. Studies in which for at least one of the cell types a relevant outcome measure was used were selected to be used in Database 1 (Supplementary Information S2.1). Publications written in languages other than English with no translation available and publications where the full text could not be found were excluded at this point.

2.2.4 Screening step 3: Categorization within Database 1

This step made the distinction between studies from screening step 2 on how OBs or OCs were studied in each publication. Each study was categorized into one of five categories within Database 1: 1) A relevant outcome measure was measured in both OBs and OCs in the coculture. These studies were also included in the in-depth screening for Database 2 (Supplementary Information S2.1). 2) and 3) Both cell types were studied, but relevant outcome measures were only measured in OCs or OBs respectively. 4) and 5) Only OCs or OBs respectively were studied in coculture, the other cell type was neglected.

2.2.5 Screening step 4: Review and reference list screening

To find additional studies that may have been missed during bibliographic searches, relevant review articles and studies labeled as category 1 were screened for additional unique relevant publications. Identified publications were screened as before.

2.2.6 Database 1 generation and analysis – All cocultures with relevant outcome measures

All information related to the relevant outcome measures was collected and organized in Database 1. For resorption, additional information on the resorbed substrate, the methodological procedure and quantification of results was collected. For formation, additional information on the type of analysis, the methodological procedure and quantification of results was collected. For both ALP and TRAP, additional information on the mechanism of the biochemical assay, whether it was conducted on lysed cells or supernatant, and information regarding the quantification was collected. In addition, the following information was collected, whether: the authors described their setup as a model specifically for remodeling, the experiment was conducted in 3D, the experiment applied bioreactors, more than 2 cell types were cultured simultaneously, the culture used a trans-well setup, the culture used PCR and components in the supernatant of the culture were analyzed by ELISA or a similar quantification method. Finally, a column for additional remarks was introduced for details that did not fit in another column. Studies where the authors are color coded in pink were those found through screening step 4. Studies categorized as category 1 in screening step 3 were selected for use in Database 2 and had their title color coded in orange.

2.2.7 Database 2 generation and analysis – All cocultures in which both cell types had relevant outcome measures.

Additional information was collected from studies in which relevant outcome measures were studied on both OBs and OCs (Category 1 studies). The species,³⁷ origin (cell line or primary) and cell type²⁶ of both the OBs and OCs, seeding numbers, densities³⁸ and ratios³⁹ were collected or calculated. The culture surface (bio-)material,⁴⁰ sample size, culture duration, medium refreshing rate, environmental conditions and pre-culture duration⁴¹ were collected if available. The medium components⁴² and supplements were extracted, as well as medium components of any monoculture prior to the coculture. Finally, the tested genes of all studies applying PCR and any proteins studied with ELISA or other supernatant analyses executed on the coculture were noted.

2.2.9 Quality assessment and scripting

Database 1 only reports the methods used for analyzing relevant outcome measures, Database 2 the culture conditions, cells and materials. The data obtained or the results described in the publications are not included in the databases. Quality assessment in Database 1 and 2 is thus limited to assessing the completeness of the necessary elements of the collected methodological details, to the extent that the description of used methods is complete enough to be properly represented in Database 1 and 2 and related figures and tables. Publications in which information was missing are here represented as 'not reported' if no information was provided, 'reference only' if no information was provided but another study was referenced. In database 1 'undefined kit' was used, when a commercial kit was

used but the content or methodology was not further described. Instances of missing information can easily be identified in figures, tables and databases, but were not further used in this systematic map. Studies where information was missing were still used for other analyses for which the corresponding provided information was present. If studies were missing information critical to reproduce the outcome measures in database 2 (for example seeding ratio's, culture surface material, medium or supplement information, critical steps in analyses), the cells in the database missing this information were labeled in red. If the missing information was not critical for the outcome measures but necessary for replication of the study (for example sample size, medium refresh rate, control conditions), the cells were labeled in orange.

Several scripts were written in Excel Visual Basics programming language to analyze and process both databases. On sheet 2 "Data" of both Database 1 and 2 excel file, the statistical data and collected information are presented in the form of lists and tables together with the buttons to re-run the analyses based on the reader's requirements. The scripts are integrated within the excel file and can be used only when the file is saved as a 'macro-enabled' file (.xlsm). For information on using the databases see Supplementary Information S2.3.

2.3 Results

2.3.1 Search results

From three online bibliographic literature sources, 7687 studies were identified (Pubmed: 1964, Embase via OvidSP: 2709, Web of Science: 3014). 6874 studies remained after removing conference abstracts, and 3925 unique studies remained to be screened after duplicate removal.

2.3.2 Studies included into Database 1 and 2

After screening step 1, 694 studies remained as OB-OC cocultures. A list of these studies is available as a supplementary file (S2.4). Screening step 2 further excluded one study because of missing full text, 35 studies because they were in a language other than English and 406 studies because no relevant outcome measure was used. The qualifying 252 studies were included in Database 1. Screening step 3 revealed that in 77 of the 252 studies in Database 1 both the OB and OC were studied. In 39 of these, both OB and OC were studied using relevant outcome measures. These 39 studies were included in Database 2.

Screening step 4 identified 34 unique studies from the reference lists of the included 39 studies of Database 2, and identified another 25 unique studies from the 10 identified review publications. These additional 59 studies were screened as described previously and resulted in an additional 3 OB-OC cocultures with only relevant outcome measures measured on one cell type, resulting in a total of 255 studies with relevant outcome measures on at least one cell type for Database 1, and still 39 studies in which relevant outcome measures were studied in both cell types for Database 2. A detailed overview of the search and selection process is shown in Figure 2.1.

2.3.3 Publications per year

The publications included in Database 1 were published between 1983 and 2019, with a peak in publications around the year 2000, followed by a slight but steady increase until now (Figure 2.3A). The peak roughly coincides with the discovery that M-CSF and RANKL were both necessary and sufficient to induce osteoclastic differentiation in monocytes in 1999.⁴³ The included publications in Database 2 span the time between 1997 and 2019, with only 8 publications before 2010 (Figure 2.3B). This coincides with the progress in development of *in vitro* cocultures of OBs and OCs, moving beyond cocultures with OBs to generate OCs, and moving towards cocultures of OBs and OCs to study for example cell-cell interactions.²⁶

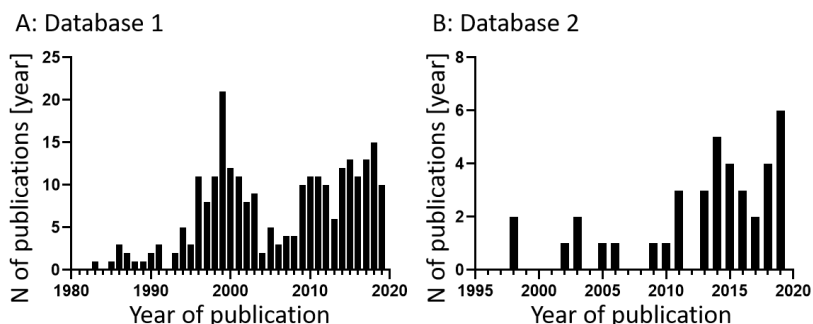


Figure 2.3 Relevant publications per year. A) All 255 publications that contain relevant outcome measures counted by year ranging from 1983 to 2019 (Database 1). B) The 39 selected publications of Database 2 counted by year ranging from 1998 to 2019 (Database 2).

2.3.4 Database 1 results

Database 1 provides an overview of all OB-OC coculture studies published until January 6, 2020 in which at least one relevant outcome measure was studied. Of the 255 studies included, resorption was analyzed in 181 studies, formation was analyzed in 37 studies and both were analyzed in 16 studies. ALP was analyzed in 42 studies, TRAP was analyzed in 61 studies and both were analyzed in 22 studies (Table 2.1). An overview of all reported methods to study the relevant outcome measures (resorption, formation, TRAP and ALP) can be found in the Supplementary Information S2.5.

Table 2.1 Combinations and frequencies of primary and secondary outcome measures. This table can be referenced to identify the number of studies using any combination of primary and secondary outcome measures. All 255 studies that investigate at least one of the primary or secondary outcome measures are represented exactly once in this table. Each study is represented by a combination of primary outcome measures (horizontal) and secondary outcome measures (vertical). Marginal totals of each row and column are counted under 'total' with the grand total in the bottom-right cell.

Combinations of primary and secondary outcome measures in each study		Primary outcome measures				Total
		No resorption or formation	Resorption only	Formation only	Resorption and formation	
Secondary outcomes measures	No ALP or TRAP	0	151	14	9	174
	ALP only	16	0	2	2	20
	TRAP only	23	9	3	4	39
	ALP + TRAP	14	5	2	1	22
	Total	53	165	21	16	255

2.3.5 Database 2 results

Database 2 provides an overview of experimental details such as culture conditions used for cocultures.

2.3.5.1 Osteoblasts

Database 2 included 39 studies. Table 2.2 presents the cell types at the start of the coculture (Table 2.2). Most studies used human primary cells. Almost half of the studies started the coculture with OBs, the others started with progenitor cells. As a result of ambiguous isolation methods and nomenclature which is subjective and can evolve over time, some cell descriptions in Table 6 might refer to identical cell populations.⁴⁴ This systematic map reflects the nomenclature used by the authors or extrapolated from the description and does not further interpret the provided information.

Except for the oldest 6 studies that used chicken and rat cells, all studies used human or mouse cells, most of which were primary cells. While the studies using rat and mouse cells mostly directly introduced OBs (either isolated as such or differentiated before seeding), those that used human cells predominantly introduced progenitor cells.⁴⁴ Those that used primary OBs purchased expandable human OBs⁴⁵ or used OBs⁴⁶, undefined expanded bone cells⁴⁷, or differentiated MSCs⁴⁸ from bones obtained during a surgical procedure.

Table 2.2 Osteoblast origins and occurrences. From Database 2, the origin of the cells that were used as OB was extracted. Each column represents a different cell type of OB-like cells or their precursors. Each row represents a different source of cells, differentiating between both the origin species and whether the cells are primary cells or cell lines. Incremental totals are presented in the last row and column.

Cell Origin	Osteoblasts	Mesenchymal stem cells	Mesenchymal stromal cells	Stromal cells	Stromal vascular Fraction	Osteoprogenitor cells	Per-row Total
Human primary	4	9	2	6	1		22
Human cell line	1						1
Mouse primary	3	2					5
Mouse cell line	4						4
Rat primary	3					1	4
Chicken primary				2			2
Reference only	1						1
Total	16	11	2	8	1	1	39

OB Seeding densities ranged from 0.9×10^3 cells/cm² to 60×10^3 cells/cm² with a mean of 11×10^3 cells/cm² (N = 26) in 2D (Figure 4A) and from 0.3×10^3 cells/cm³ to 7×10^3 cells/cm³ with a mean of 15×10^6 cells/cm³ (N = 6) in 3D (Figure 2.4D).

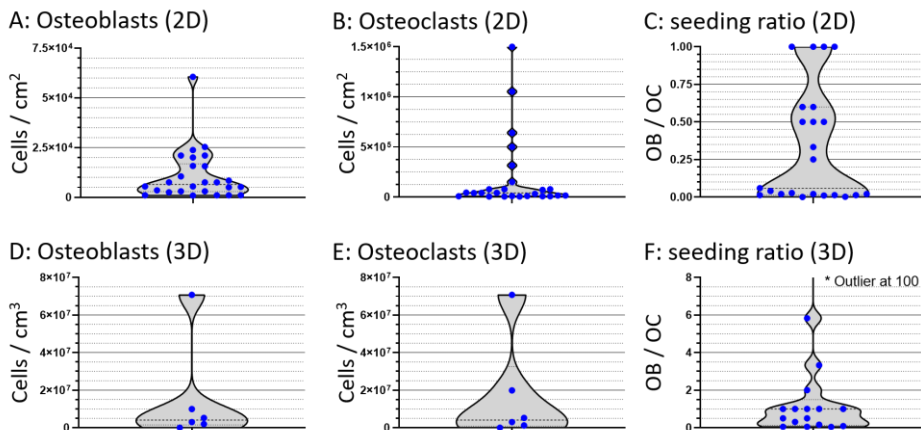


Figure 2.4 Seeding densities and seeding ratios. Violin plots of 2D and 3D seeding ratios of OB (A+D), OC (B+E) and respective seeding ratios in cocultures (C+F). Values are calculated based on reported seeding numbers of the cells or precursors thereof per surface area or volume. No distinction was made between different (precursor) cell types in these figures, resulting in a considerable spread in data that could be attributed to proliferation and cell fusion after seeding. The ranges along the Y-axis are not the same for each figure. Each seeding density of each study is represented by a blue dot.

2.3.5.2 Osteoclasts

Out of the 39 studies in Database 2, 20 used human primary cells, the others used animal primary cells or any type of cell line for resorption (Table 2.3). Cultures were mostly initiated with OC progenitors: 16 studies introduced monocytes, 11 introduced mononuclear cells, the rest used other precursors.

The 6 oldest included studies used chicken and rat cells, all others used mouse or human cells. With only one exception combining a mouse ST-2 cell line with human monocytes, all studies used cells of exclusively a single species for the OB and OC source.⁴⁹ Only one study claimed to introduce OCs directly into coculture but failed to provide any information regarding the cell source and was therefore ignored from further investigation.

The OC seeding density ranged from 5×10^3 cells/cm² to 15×10^6 cells/cm² with a mean of 190×10^3 cells/cm² (N = 25) in 2D (Figure 2.4B) and from 20×10^3 cells/cm³ to 70×10^6 cells/cm³ with a mean of 17×10^6 cells/cm³ (N = 6) in 3D (Figure 2.4E). Seeding ratios of OB:OC in 2D varied highly and ranged from 1:1500 to 1:1 (Figure 2.4C). Seeding ratios of OB:OC in 3D ranged from 100:1 to 1:25 (Figure 2.4F).

Table 2.3 Osteoclast origins and occurrences. From Database 2, the origin of cells used as OC was extracted. Each column represents a different cell type of OC-like cell or a precursor. Each row represents a different source of cells, differentiating between both the origin species and whether the cells are primary cells or cell lines. Incremental totals are presented in the last row and column.

Cell Origin	Monocytes	Mononuclear cells	Macrophages	Osteoclast precursors	Osteoclasts	Spleen cells	Total
Human primary	10	6	1	3			20
Human cell line	4						4
Mouse primary	2		2	2			6
Mouse cell line			2				2
Rat primary		3				1	4
Chicken primary		2					2
Reference only					1		1
Total	16	11	5	5	1	1	39

2.3.5.3 Coculture medium composition and culture conditions

The behavior of cells is highly dependent on their environment, of which the biochemical part is predominantly determined by the culture medium composition. The main components of typical culture media are a base medium, fetal bovine serum (FBS) and specific supplements such as OB and OC supplements. Eight different base (or complete) media were reported (Figure 2.5A), with α MEM and DMEM accounting for approximately 80% of all studies. FBS content ranged from 0% to 20%, with most studies using 10% (Figure 2.5B). Those without supplemented FBS used forms of complete media of which the composition was not described, but possibly including a type of serum or equivalent serum-free supplements.

M-CSF concentration was reported in 11 studies and ranged from 10 ng/ml to 100 ng/ml with a mean of 39,82 ng/ml (Figure 2.5C). RANKL concentration was reported in 14 studies and ranged from 10 ng/ml to 100 ng/ml with a mean of 49 ng/ml. OB supplements were recalculated to molarity if necessary (Figure 2.5D). Ascorbic Acid (AA) (also referred to as ascorbic acid-2-phosphate, L-ascorbic acid or L-ascorbate-2-phosphate) concentration was reported in 19 studies and ranged from 0.05 mM to 0.57 mM, with a mean of 0.18 mM and one outlier at 200 mM that was disregarded for this calculation. Dexamethasone was used in 13 studies and was used in 2 different molarities: 6 times at 10^{-7} M and 7 times at 10^{-8} M. β -Glycerophosphate (β GP) concentration was reported in 17 studies, and ranged from 1 mM to 46 mM, with a mean of 13 mM.

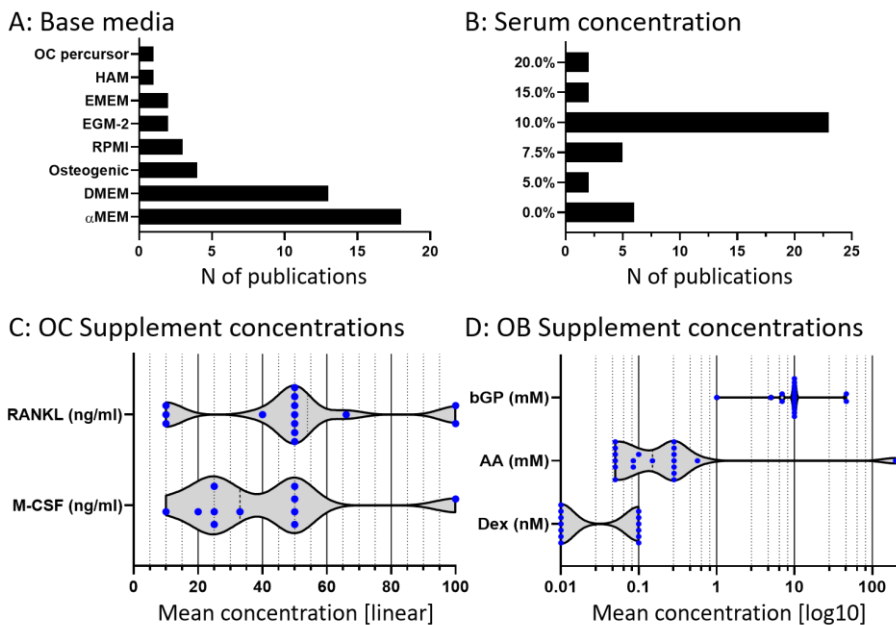


Figure 2.5 Medium components used by studies in Database 2. A) The occurrence of all identified base and complete media used during the coculture phase of each study. B) Serum concentrations during the coculture phase of each study. C) OC supplements administered during the coculture phase of each study. Please note that the x-axis has a linear distribution. D) Osteogenic supplements during the coculture phase of each study. Please note that the x-axis has a logarithmic scale. Individual concentrations or molarities are shown as blue dots.

2.4 Discussion

In recent years, many research groups have ventured into the realm of OB-OC cocultures with the intent of studying both formation and resorption. Due to a lack of standardization within the field and the difficulty of finding publications based on methods instead of results, each group seems to be individually developing the tools to suit their needs resulting in many functionally related experiments that are methodologically different. The use of OB-OC cocultures is usually not clearly mentioned in the title and abstract, making it difficult to find these studies without a systematic search and thorough review. The aim of this study was to generate a systematic map to give an overview of existing osteoblast-osteoclast coculture studies published up to 6 January 2020, and present their methods, predetermined outcome measures and other useful parameters for analysis in 2 databases which can be filtered, sorted, searched and expanded.

The Database 1 contains all OB-OC coculture studies in which at least one relevant primary outcome measure (formation and/or resorption) or secondary outcome measure (ALP and/or TRAP quantification) was investigated. A sub-selection of studies that have relevant outcome measures investigated on both OBs and OCs in the coculture are shown in Database 2, accompanied by additional details on methods, culture conditions and cells.

2.4.1 Resorption and formation

To study resorption, 2D bone and dentine discs remain the most-used method although alternatives such as osteological coatings offer new and easy ways of quantification. To measure bone formation, 2D nodule stainings were the most frequently used. Combined with Alizarin Red dye release these provide an easy way to quantify mineralization.⁵⁰

Compared to 2D cultures however, 3D cultures are under-represented in this systematic map. Only 24 studies were labeled as 3D cocultures in Database 1, the first being published only in 2006.⁵¹ From these we learn that studying 3D resorption and formation remains a challenge, with the only identified viable options for quantification being μ CT imaging⁵² and supernatant analysis techniques such as NTx,⁵³ CTx,⁵⁴ and CICP.⁵⁵ Because of their non-destructive nature, they can be used to measure the same sample repeatedly and prior to destructive techniques. μ CT it is well suited to monitor mineralized volume change within the same samples over a longer period of time^{52,56,57}. Registering consecutive images can even show both formation and resorption events within the same set of images of the same sample if both mineralizing OBs and resorbing OCs were present.⁵⁷ The use of μ CT leads to both quantification and visualization of mineralization. The supernatant analysis methods measure bone turnover markers are used in the clinic and can quantify resorption and formation by analyzing the liberated collagen fragments in the supernatant⁵⁸

2.4.2 ALP and TRAP

ALP and TRAP are the two major markers for indirectly quantifying OB and OC activity that were included into Database 1. ALP makes phosphates available to be incorporated into the matrix⁵⁹ and TRAP has been associated with migration and activation of OC.⁶⁰ Their presence is not conclusive proof that formation and resorption are occurring because ALP is expressed already in differentiating MSCs⁶¹ and TRAP is expressed on monocytes as well.⁵⁷ Still, there is a correlation between their presence and that of OB and OC activity. These enzymes can be measured both after lysis of the cells or within the culture supernatant. The former allows the quantification of enzyme per DNA content when combined with a DNA assay, whereas the latter allows the monitoring of relative enzyme release over time. The most frequently used methods are the pNPP-based methods where ALP and TRAP directly convert a substrate into a measurable compound. Naphthol-based methods⁶² rely on a similar principle, and show an increased specificity for TRAP isoform 5B in particular.⁶³ The main advantage of these methods is that they use the inherent enzymatic activity of ALP and TRAP, reducing the complexity and cost of the assay. However, the reliance on the inherent enzymatic activity of the enzymes is also a practical limitation as inherent activity can be affected by for example freeze-thaw cycles and long-term storage, which is a likely occurrence when monitoring ALP or TRAP release over time. A workaround would be to analyze the samples directly after collection. Another risk is that both ALP and TRAP are phosphatases. Assays that rely on their inherent phosphatase activity may show cross-reactivity of other phosphatases, although this can largely be mitigated by controlling the pH during the test.

Immunoenzymatic assays such as ELISA detect the presence and not the activity of these enzymes instead.⁶⁴ These methods have the capacity to detect low protein concentrations

because each individual protein can be labeled with an excess of new enzymes each capable of converting substrate. In the case of TRAP, ELISA kits exist that are specific for TRAP isoform 5b which is expressed almost exclusively in OCs,⁶⁵ whereas isoform 5a is also expressed by macrophages and dendritic cells.⁶⁶ While in a coculture with pure populations of OB and OC this distinction would not be relevant, macrophages, macrophage-like cells and macrophage precursors⁶⁷ can be used as precursors for OCs⁶⁸, and thus express isoform 5a in coculture. Whether this negatively affects the results is another matter that can only be determined by comparison between the two assay types.

To conclude, pNPP based methods are the most frequently used methods for detecting ALP and TRAP due to their affordability and simplicity. However, immunoenzymatic detection methods are more sensitive and specific, and do not rely on the intrinsic enzymatic activity of ALP and TRAP which can be affected by freeze-thaw cycles, long-term storage, and could show cross-reactivity with other phosphatases.

2.4.3 Osteoclasts

Osteoclastic resorption is an integral part of *in vivo* bone maintenance. Old and damaged bone tissue is resorbed and replaced by OBs with new bone tissue. There is a clear preference in the studies identified for Database 2 for using human cells to generate OCs, most notably monocytes and mononuclear cells. These have in the past two decades proven to be a reliable and relatively straight-forward precursor population for OCs,²⁶ they can be obtained from human blood donations, and are thought to be better representatives for studying human physiology than cells of animal origin.^{22,23}

The choice of using precursors versus differentiated OCs is forced sharply into one direction because of both biological and experimental limitations. The extraction of OCs from bone is possible but cumbersome, requires access to fresh bone material and generally does not yield relevant numbers of OCs. Generating OCs from circulating precursors is easier. However, OCs have an average life span of approximately 2 weeks.^{69,70} some of which would already be lost if OCs would be created prior to the actual experiments. In contrast to most cells, differentiation happens by fusion of several precursors into a single OC. Fused multinucleated OCs can become large and hard to handle without being damaged. For those reasons they are usually differentiated from precursors within the actual experiments.

Thanks to the discovery of M-CSF and RANKL being sufficient to induce osteoclastic differentiation,⁴³ OCs can currently be obtained *in vitro* without the need for OBs. Where in the past researchers used spleen cells for this, the studies included in this systematic map predominantly use (blood-derived) mononuclear cells, monocytes, or macrophages as precursor cells.

There are *caveats* and risks associated with each cell source. Animal cells introduce a between-species variation and can respond differently than human cells.³⁷ Human donor cells tend to exhibit large between-donor variation compared to cell lines⁷¹ and the number of cells acquired is limited and variable.⁷² The large variation between donors again highlights the need for patient-specific disease models instead of generic bone models. By using cells of a single diseased donor, the reaction of that patient's cells on potential

treatment options can be studied. Immortalized cell-lines are more practical than primary cells but result in immortal OC-like cells. While these can greatly reduce between-experiment and between-lab variation, they are also physiologically less relevant. While these risks and characteristics do not discredit any source as a viable source of OCs for any experiment, the results of the corresponding studies should be interpreted with these characteristics in mind.

2.4.4 Osteoblasts

OBs are the bone forming cells, and together with bone resorbing OCs they keep the bone mass and bone strength in equilibrium. The preference for the use of human primary cells identified in the studies included in Database 2 can be explained by the good availability of donor material, expandability of OB precursors, and because human cells better reflect human physiology than cells from other species.^{22,23} The choice of OB progenitors versus OBs is not as crucial here as it is with OCs. MSCs, the most commonly used precursors, have a tri-lineage potential and differentiate into OBs on a 1-1 ratio.⁷³ The advantage of osteoprogenitors such as MSCs is that these are capable of extensive proliferation before differentiation. Using progenitors allows studying osteoblastogenesis in addition to bone formation. When the effect of an intervention on mineralization but not osteogenesis is under investigation, care must be taken that the intervention is not applied before differentiation has been achieved.

The advantage of directly introducing OBs instead of precursors, whether obtained directly from primary material or pre-differentiated *in vitro*, is that these do not need to be differentiated within the experiment anymore, and any experimental conditions affect only mature OBs and not osteoblastogenesis in parallel. OBs or to-be-differentiated MSCs isolated from bone marrow or orthopedic surgery are the most common source of primary human OBs. Healthy human donor OBs are scarce because these persons rarely undergo bone surgeries or get bone biopsies. Whether the use of OBs from diseased donors affects experimental results needs to be elucidated. On the other hand, using patient cells to create a personalized *in vitro* disease model is the first step towards personalized medicine, especially if all cells are of that same patient. Finally, the risks of using animal cells the introduction of a between-species variation. While none of these risks directly discredit any of the methods obtaining OBs, the results must be interpreted with these risks and characteristics in mind.

2.4.5 Culture conditions

The success of a cell-culture experiment is dependent on the culturing conditions. For many cell-types, optimal culture conditions have been established. During coculture experiments however, the needs of two or more cell types need to be met. Medium components and factors may be needed in different concentrations, as they can be beneficial to one cell type but inhibitory to the other.⁷⁴

There is a clear preference for medium based on DMEM and α MEM, but many factors influence the choice of base medium. Base media are chosen based on the intended cell type, recommendations by a manufacturer or supplier of either cells or medium, preferred effect on cells, interaction with other supplements, and earlier experience. These factors

make direct comparison of experimental results within literature virtually impossible. Additionally, none of the studies mentioned why they specifically chose the base media they used.

Another variable in medium composition is FBS (or FCS). It is known to have batch-to-batch- and between-brand differences which can impact the results of an experiment tremendously.⁷⁵ However, no study explains why each type and concentration of FBS was chosen.

When osteoblastic or osteoclastic supplements were used, the concentrations were within the same orders of magnitude in all studies, except for AA. Only 2 studies used all 5 of the supplements indexed in this study (AA, β GP, Dexamethasone, M-CSF and RANKL) and many combinations of supplements have been registered in this map. OC supplements RANKL and M-CSF are both necessary and sufficient for osteoclastogenesis.⁴³ However, OBs can produce RANKL and M-CSF themselves to trigger differentiation and therefore the supplements are not necessarily required in coculture.²⁹ Each osteoblastic supplement contributes to a specific function. Dexamethasone upregulates osteogenic differentiation, β GP acts as a phosphate source, and AA is a co-factor involved in collagen synthesis.⁷⁶ Depending on the type of (progenitor) cells introduced, the aim of the experiment and other methodological details, their inclusion could be necessary. Finally, many studies used or omitted specific supplements related to their research question regarding the activity of OBs or OCs or used less common supplements for differentiation such as vitamin D3, human serum or Phorbol 12-myristate 13-acetate.

What is seldom addressed however, is the compromise that must be made in choosing the right supplements and concentrations. Adding too high doses of supplements could cause an excess of these signals in the culture medium, effectively overshadowing any other ongoing cell-signaling over the same pathway by other cells. This is of critical importance when the goal is not to achieve only OB and/or OC activity, but a self-regulating system with experimental conditions or interventions that are expected to affect this system. Here, it may be beneficial to experiment with lower concentrations of factors, supplemented only during critical phases of the cells' development or differentiation.

The choice of medium in a coculture is most likely going to be a compromise and must be based on the exact research question to be addressed, where the advantages and disadvantages of base media and supplements for both cell types are carefully weighed.

2.4.6 Seeding densities and seeding ratios

Using the correct seeding densities plays a major role in proliferation and cell function of OBs^{38,77} and osteoclastic differentiation.⁷⁸ The seeding densities reported in this map show an enormous spread. Many factors could have influenced these numbers. For example, some studies report the numbers prior to expansion, others expand the cells in (co-)culture. Similarly, the percentages of relevant precursor cells in heterogenous cell populations can vary widely. The cell numbers present and OB:OC ratio most likely even change during a coculture due to ongoing cell-division, differentiation, fusion and different expected life spans

and corresponding cell death. Regrettably, the available documentation of exact cell numbers introduced is often lacking, and open to some interpretation.

Animal type, cell type, cell line versus primary cells and even passage number may also directly influence the choice of seeding densities in addition to various experimental choices. At the same time, the purpose of the experiment and more specifically the purpose of the cells and type of interaction or result required should determine the necessary seeding density. The combination of all these factors suggests that there in fact is no ideal seeding density, and that the best seeding density for a certain experiment can only be determined by taking all the above factors into account, learning from others that did similar experiments, and most importantly verifying assumptions and predictions in the lab.

Looking at the cell seeding ratio, here reported as number of seeded OB/OB-precursors per seeded OC/OC-precursor, outliers can be normalized against their seeded counterparts. In 2D studies, there are never more OBs/OB-precursors than OCs/OC-precursors. At most, they are seeded at a 1:1 OB:OC ratio. Even though in human bone tissue the ratio of OB:OC is estimated to be approximately 7:1, higher OC numbers than OB numbers are seen.⁷⁹ OB precursors can still proliferate, whereas OC precursors usually still need to fuse together to form mature OC or OC-like cells. In 3D we do not see the same trend, with ratio's ranging from 1:20 to 100:1. These differences are again affected by the same factors that influence individual OB and OC seeding densities, further enhanced by the extra layer of complexity that are inherent to 3D cultures. As with the individual seeding densities, these factors prevent us from determining an ideal seeding ratio.

2.4.7 Limitations

While the authors took great care to construct a series of search queries fine-tuned for each of the three online bibliographic literature sources, the authors cannot be certain that all relevant OB-OC cocultures have been included into the two databases. The search was limited by the necessary addition of a 'coculture' search element. Coculture studies without any indication thereof in the title or abstract simply cannot be identified through the initial search. To compensate for this, screening step 4, searching through identified reviews and publications included into Database 2, was executed. Publications in languages other than English were excluded because none of the researchers involved in data curation and analysis were fluent in the remaining languages. Consequently, relevant publications might have been excluded based on language.

The quality of reporting in included studies is lacking in many cases. Missing information for reproducing the methods of the studies was identified, and only 13 out of 39 studies included in Database 2 did not miss at least a high-level description of all indexed characteristics.

This systematic map is not intended to provide a definitive answer to the question of how to set up the perfect OB-OC coculture. Instead, it allows searching through all relevant coculture studies looking for specific matching experimental characteristics or culture details that may be applicable to one's own research. For this, it contains the possibility to search, sort and filter through many relevant characteristics. This allows one to find relevant studies

that may have already (partly) studied one's research question, or that can be used as a guide to design comparable experiments.

2.5 Conclusion

With this systematic map, we have generated an overview of existing OB-OC coculture studies published until January 6, 2020, their methods, predetermined outcome measures (formation, resorption, ALP and TRAP quantification), and other useful parameters for analysis. The two constructed databases are intended to allow researchers to quickly identify publications relevant to their specific needs, which otherwise would have not been easily available or findable. The presented high-level evaluation and discussion of the major extracted methodological details provides important background information and context, suggestions and considerations covering most of the used cell sources, culture conditions and methods of analysis. Finally, this map includes the instructions for others to expand and manipulate the databases to answer their own more specific research questions.

Author contributions

SR, RdV and SH contributed to the conceptualization and methodology. SR, BdW, MV and ES contributed to data curation and analysis. SR wrote the software. SR and BdW contributed to the preparation of the figures. SR, BdW and SH contributed in supervision. SR wrote the original manuscript. All authors contributed to manuscript revision and approved the submitted version. SR and SH acquired funding for this research.

Funding

SR was supported by ZonMw More Knowledge with Fewer Animals Program (MKMD), project number 114024141. S.R. and S.H. were financially supported by the European Union's Seventh Framework Program (FP/2007-2013), Grant agreement No. 336043 (project REMOTE). BdW, MV and SH were financially supported by the research program TTW with project number TTW 016.Vidi188021, which is (partly) financed by the Netherlands Organization for Scientific Research (NWO).

Supplementary information

S2.1 Database 1. This database contains all studies in which at least one relevant outcome measure was investigated. Characteristics of outcome measures and descriptive statistics are listed in this database.

S2.2 Database 2. This database contains all studies in which at least one relevant outcome measure was investigated for both OB and OC. Characteristics of cells, methods and culture conditions, and descriptive statistics are listed in this database.

S2.3 Using the databases. Document providing instructions on how to operate the databases, how to add publications and expand the analyses with more elements.

S2.4 List of all OB-OC cocultures. List containing the initial 694 OB-OC cocultures obtained after screening, before full-text investigation and exclusion based on outcome measures.

S2.5 Results of database 1. Extensive information and tables on all resorption and formation methods extracted from Database 1, described in the results section of the original publication.



A fluorescence microscopy image showing a porous, interconnected network of fibers or cells. The structure is stained with two different dyes: a bright red dye that highlights the main structural components and a blue dye that appears to stain specific cells or regions within the network. The overall appearance is that of a complex, three-dimensional scaffold.

Part 1

Enhancing the microenvironment for
in vitro bone remodeling

Chapter 3

Impact of culture medium on cellular interactions in *in vitro* coculture systems

The contents of this chapter are based on:

Michelle A. M. Vis^a, Keita Ito^a, Sandra Hofmann^a (2020) *Frontiers Bioengineering and Biotechnology* DOI: 10.3389/fbioe.2020.00911

^a *Department of Biomedical Engineering and Institute for Complex Molecular Systems (ICMS) Eindhoven University of Technology, Eindhoven*

Abstract

Coculturing of cells in *in vitro* tissue models is widely used to study how they interact with each other. These models serve to represent a variety of processes in the human body such as development, homeostasis, regeneration, and disease. The success of a coculture is dependent on a large number of factors which makes it a complex and ambiguous task. This review article addresses co-culturing challenges regarding the cell culture medium used in these models, in particular concerning medium composition, volume, and exchange. The effect of medium exchange on cells is often an overlooked topic but particularly important when cell communication via soluble factors and extracellular vesicles, the so-called cell secretome (CS) is being studied. Culture medium is regularly exchanged to supply new nutrients and to eliminate waste products produced by the cells. By removing medium, important CSs are also removed. After every medium change, the cells must thus restore their auto- and paracrine communication through these CSs. This review article will also discuss the possibility to integrate biosensors into cocultures, in particular to provide real-time information regarding media composition. Overall, the manner in which culture medium is currently used will be re-evaluated. Provided examples will be on the subject of bone tissue engineering.

3.1 Introduction: *In vitro* tissue models

Before culturing of cells was possible, animals were used to study human physiology and pathophysiology, in particular in medical and pharmaceutical industries¹⁴. Animal models frequently failed to capture important facets of human physiology and pathophysiology and thus failed to mimic true human responses.⁸⁰ The possibility to culture human cells increased our insight into healthy and diseased states of the human body.^{81,82} First, cells were cultured in monolayers which in some cases lacked the complexity needed to study diseases and responses to drugs thoroughly.⁸³⁻⁸⁵ Three-dimensional (3D) models enabled the creation of a cell environment closer to the natural microenvironment, increasing the potential to predict physiological responses and also increasing complexity. For example, different 3D *in vitro* models to study osteocytes were established recently, mimicking their native environment and showing superior morphology and behavior compared to monolayer cultures, enabling future development of human disease models.⁸⁵

The approach for the design of *in vitro* tissue models originates from tissue engineering.^{13,86} TE combines cells, scaffolds, growth factors and mechanical stimuli to create tissues *in vitro*. Traditionally, TE has focused on the creation of tissue grafts for implantation. More recently, TE has been applied to develop *in vitro* tissue models. In contrast to tissue grafts that need clinically relevant sizes of engineered tissue, *in vitro* models aim to resemble the smallest functional unit of a tissue. Such *in vitro* models show potential to study processes of the human body such as development,⁸⁷ homeostasis,⁸⁸ regeneration,⁸⁹ and disease.⁹⁰

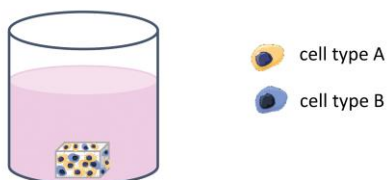
The development of 3D human *in vitro* models depends on the ability to partially recreate the complexity of the native microenvironment that defines cues (physical, chemical, and biological) for cell function, proliferation, and differentiation⁸⁰. The challenge is to define the aspects of the microenvironment which are important in order to engineer the smallest functional unit that captures the interaction between key cues in the cell system which it controls⁸⁰. Research has shifted toward improving *in vitro* models by increasing their complexity in order to understand how mature intricate tissues form.⁸² An increase in complexity can be accomplished by culturing different cell types together in one culture, called coculturing.

3.2 Cocultures with the application for *in vitro* tissue models

Coculturing of cells is widely used to study interactions between cell populations in many fields including (but not limited to) synthetic biology,⁹¹ ecology,⁹² TE both 2D and 3D,^{93,94} and multi-organ microphysiological systems.⁹⁵ Models have been developed for a variety of tissues such as lung,⁹⁶ intestine,⁹⁷ kidney,⁹⁸ bone,⁸⁸ embryo,⁹⁹ ovary,¹⁰⁰ neuron-glia,¹⁰¹ and liver.¹⁰² Cocultures can be used to represent both physiological and pathological tissue states. Ideally, human, or even patient-specific cells are used to create cellular environments that are more representative for humans rather than animal derived cells.⁸⁶ Most coculture studies involve two cell types, owing to an increased complexity in establishing a stable system when more cell types are involved.⁹¹ There are also studies reporting the use of three¹⁰³⁻¹⁰⁵ or even four cell types.^{106,107}

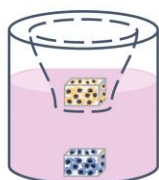
Different strategies to coculture cells in 3D exist, each allowing for a different degree of contact between the cell types. Through this contact, the cells are able to stimulate each other. Direct cocultures facilitate physical contact between the different cell types which allows for communication through their surface receptors and gap junctions, defined as juxtacrine communication (Figure 3.1A). Indirect cocultures incorporate a physical separation between cell types, such as a semi-permeable membrane in the form of a transwell system, only enabling signaling via the cell secretome (CS; Figure 3.1B-I). In addition, in indirect co-cultures, conditioned medium is frequently used (Figure 3.1B-II). Medium is first used for culturing one cell type and then transferred to the second cell type. The medium contains the CS of the first cell type, which then affects the second cell type. Conditioned medium contains numerous CSs that may positively and/or negatively regulate cell behavior.¹⁰⁸ The mechanisms that support the effect of these CSs remain insufficiently defined and are highly dependent on the cell source.¹⁰⁹

A) direct coculture



B) in-direct coculture

I) transwell system



II) conditioned medium

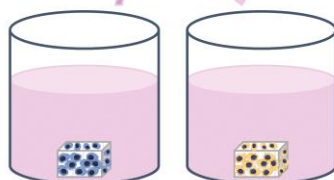


Figure 3.1 A) Direct cocultures facilitate physical contact between the different cell types which allows for communication through their surface receptors. B) Indirect cocultures incorporate a physical separation between cell types only allowing for communication via cell secretomes. I) Physical separation in the form of a transwell system using a semi-permeable membrane. II) Conditioned medium is first collected from one cell type and then transferred to the other cell type. The medium contains the cell secretome of the first cell type, which then affects the second cell type.

Cell secretomes ensure cell-cell communication and comprise of soluble factors and cell-derived membranous structures. These so-called extracellular vesicles (EVs), are nanosized particles (exosomes, 30–100 nm; microvesicles, 50–2000 nm)¹¹⁰ that transfer proteins, bioactive lipids between cells. Moreover, EVs are also capable of transferring RNA between cells, called exosomal RNA or esRNA.^{111,112} EVs are present in biological fluids and are involved in multiple physiological and pathological processes.¹¹³ For example, EVs derived from osteogenically committed mesenchymal stromal cells were shown to induce osteogenic commitment of homotypic cells without further supplementation.¹¹⁰ EVs are widely studied for their potential as a cell-free therapeutic method for regeneration of numerous tissue types.

Subsequently, EVs might be used to study cellular interactions *in vitro* omitting the requirement for a coculture experiment and thus overcoming coculture challenges. The biggest challenge of using EVs lies within the development of purification and characterization protocols.¹¹⁴

Overall, cocultures are versatile models to create cellular environments in which interactions between different cell types can be studied *in vitro*. These interactions can take place by direct contact and by exchange of soluble factors and EVs. This review article will focus on steps that can guide optimization of medium composition and volume in cocultures with a particular focus on cell communication via the CS.

3.3 General considerations regarding culture medium in cocultures

3.3.1 Selecting culture medium composition

In cell culturing, culture medium is added to nourish the cells. Culture medium is a liquid nutritive substance consisting of a mixture of base medium, serum, and regulating factors. Firstly, base medium fills the nutritional requirements of the cells. The first base medium was developed in 1959 and was defined as the Minimal Essential Medium (MEM), including 13 amino acids, 8 vitamins, 6 ionic species, and glucose.¹¹⁵ Secondly, serum, such as fetal bovine serum (FBS) contains important basic proteins including growth factors and hormones for maintaining cell survival, growth, and proliferation.¹¹⁶ FBS is a complex and natural mixture that is extracted from fetal blood. The use of FBS is controversial due to quality and reproducibility issues as well as animal welfare concerns which is elaborately reviewed elsewhere.¹¹⁷ Thirdly, regulating factors such as growth factors are added to the medium to guide specific and desired cell behavior such as proliferation and differentiation into a particular cell lineage. These factors are key in cell cultures as they predominantly determine cell fate. Establishing a functional and precise mixture of these culture medium ingredients is of great importance for creating *in vitro* tissue models.

Each cell type has specific needs according to its function and requires a corresponding specific medium composition. When two or more different cell types are cultured together, choosing the right medium becomes a challenge.⁹¹ Several approaches are possible, such as mixed medium, supplemented medium and partitioned culture environments (Figure 3.2A). In a mixed medium, the medium of all used cell types is combined, possibly in different ratios. With this method, the original medium supplements might interfere with the other cell type, which is particularly important when culturing progenitor cells as these cells yet have to differentiate into the desired cell type. For instance, in a coculture of precursors of osteoblasts and osteoclasts, the osteogenic supplements dexamethasone and β -glycerophosphate are needed for osteoblast differentiation and maturation, while these supplements have been shown to inhibit monocyte differentiation into osteoclasts.¹¹⁸⁻¹²⁰ An optimum dosage of supplements has to be found in order to obtain both functional osteoblast and functional osteoclasts. Another approach could be to use a general base medium, supplemented with the soluble factors that stimulate both cell types without negatively affecting either of them.¹²¹ This method makes it possible to modulate the medium more specifically than by just mixing two media types. The disadvantage is that it is time

consuming to find suitable supplements and to optimize the combination. Additionally, a culture method that enables two physically partitioned medium flows can be used. In this way, both cell types receive their specific medium while cell-cell contact is still possible.¹²² However, this is a complicated and precise method that can mostly be performed in 2D and for certain cell types.

In multi-organ microphysiological systems, the challenge of finding the right medium is even more difficult as a variety of cell types may each have their own optimal medium and supplements. For example, in a device combining liver, lung, kidney, and adipose tissue, it was shown that addition of transforming growth factor β 1 (TGF- β 1) supported the growth of lung cells but inhibited the growth of liver cells.¹⁰⁶ They overcame this by using gelatin microspheres that released TGF- β 1 locally to support the lung compartment while in the circulation, low TGF- β 1 levels could be maintained.¹⁰⁶

Just as important, one cell type in a co-culture naturally provides CSs that influence the other cell type. As a result, medium supplements might have to be altered in concentration or might be fully omitted.¹²¹ For example, osteoclasts in mono-culture are derived from mononuclear cells by addition of macrophage colony-stimulating factor and receptor activator of nuclear factor kappa-B ligand. Both molecules are naturally produced by osteoblasts.¹²³ Thus, in a coculture with osteoblasts, no additional cytokines may be needed for osteoclast formation.^{121,124}

Medium optimization is crucial but is laborious and time-consuming because of the enormous number of possible combinations. Parallel assays using micro/nano-scale devices hold great promise for evaluation and optimization of a multitude of options.¹²⁵ For example, a sensitive platform for optimum culture media investigation was developed in which image-based profiling was combined with microdevices to achieve high-throughput evaluation of culture medium conditions.¹²⁵ Advances in this field could be of great value to ease the inconvenience of medium optimization.

3.3.2 The effect of culture medium volume

Medium volume is of importance as a higher volume leads to lower concentrations of the CS (Figure 3.2B). In bone cell cultures, osteoblastic mineral deposition and fusion of osteoclast-precursors into osteoclasts were shown to be dependent on the medium volume.¹²⁶ When culturing cells, often the medium volume suggested by the manufacturer of culture plastics is used. However, this volume is not optimized for specific cell types. For example, low culture medium volumes not only have been shown to be beneficial for culturing cell types such as neuron-like cells¹²⁷ and adipose derived mesenchymal stem cells,¹²⁸ they are also more economical. On the other hand, some culturing conditions, for example in bioreactors, might require minimal volumes to operate, which makes volume optimization impracticable. In these cases, it should be recognized that the medium volume may impact a variety of cell culture aspects.¹²⁶

Medium volume is influenced by cell culture aspects such as nutrient supply, dilution, or concentration of waste products and metabolites, and changes in oxygen level.¹²¹ Studies have demonstrated that the oxygen concentration in medium decreases with increasing

medium depth, leading to altered cell growth characteristics.^{129,130} Moreover, it has been recognized that cell proliferation and differentiation are largely influenced by the concentration of CSs.¹²⁶ With different medium volumes these CSs become either more or less concentrated resulting in faster or slower proliferation and differentiation of these cells. Thus, cells might function differently when cultured in different medium volumes. Again, optimization is key but laborious and, in some cases, even impracticable. Therefore, one should be aware of the effects of medium volume. Certainly, when unexplainable results are encountered and when protocols are adjusted to up- or down-scale experiments.

3.4 The effect of medium exchange on cell-cell interactions

3.4.1 Waste accumulation problem

Medium is exchanged regularly to maintain nutrients and growth factors consumed by the cells and to eliminate waste products produced by the cells. Mammalian cells use glucose for energy and produce lactate as a metabolite.¹³¹ *In vitro*, every cell type needs a narrow pH range within 0.2 to 0.4 pH units of its optimum to grow.¹³² The production of lactic acid should not exceed the buffering capacity of the medium, because lowering the pH can inhibit cell growth.^{131,133–135} Also, high ammonium concentrations as a by-product of glutamine catabolism can be toxic to cells causing cytosol vacuolization and subsequent cell death.^{134,136} Exchanging the medium prevents these waste product accumulation effects.

However, after every medium exchange, also the CS is removed, and the cells must make a new effort to restore their communication by producing fresh molecules. This effort could negatively influence their behavior, not representing their natural state. The influence of medium exchange was for example investigated by measuring actin microfilament structure directly before and after medium exchange.¹³⁷ Medium exchange led to a rapid disturbance of stress fiber formation and disconnection of cell-cell contacts. Frequent medium exchange is also economically disadvantageous as medium can contain expensive additives such as growth factors and animal serum.¹³⁴ However, medium exchange cannot be prevented as nutrient deprivation and waste accumulation would lead to inevitable cell death.

3.4.2 Systems for culture medium re-use

Driven by economical motives, re-use of medium was first described in 1977 by adding fresh nutrient supplements to used medium.¹³⁸ However, due to the accumulation of waste products, the medium could only be re-used once. A second re-use caused cell death. To overcome this issue, other cell culture systems were developed in which medium was dialyzed to remove waste products. In addition, dialysis could be used to harvest cell products such as antibodies.¹³⁹ The principle of dialysis relies on the exclusion of molecules based on their size (Figure 3.2C). Fresh medium contains low molecular weight (MW) molecules such as nutrients, amino acids, and vitamins. Depending on the chosen MW cut-off, the dialysis membrane allows for exchange of those molecules. In this way waste products can diffuse out of the culture medium while nutrients and vitamins diffuse back in. High MW components such as growth factors are retained in the medium compartment.

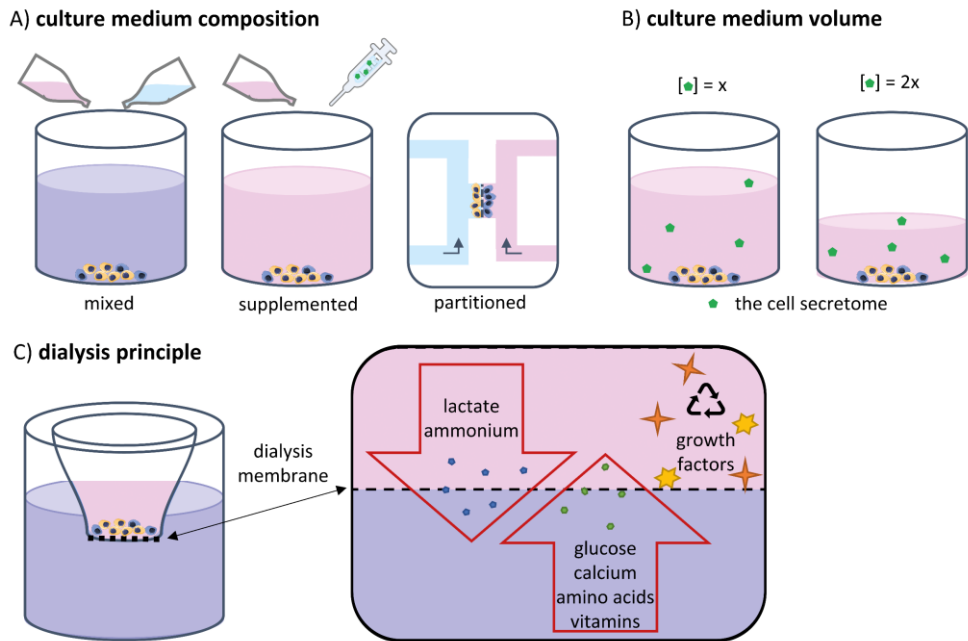


Figure 3.2 A) Several approaches for co-culture medium optimization have been tested, such as mixed medium, supplemented medium, and fluidically partitioned culture environments. B) The culture medium volume has an influence on the concentration of the cell secretome. C) The principle of dialysis of culture medium relies on the size of the components in the medium. Depending on the chosen MW cut-off, the dialysis membrane allows for exchange of low MW proteins, amino acids, vitamins, lactate, and ammonium while high MW components such as growth factors, are retained in cell culture insert.

The first dialysis system cultures were rather complex and large. For example, a bioreactor was developed using a 5 liter medium vessel coupled to a 2 liter perfusion system.¹⁴⁰ Several fluid streams were connected to control waste removal, medium recycling, and nutrient supply. For the elimination of toxic waste products, a hollow fiber microfiltration system was used while nutrients were supplied by adding concentrated solutions. Most previous studies focused on mass production, generally using large scale reactors.^{141,142} Recently, a simpler dialysis culture system was presented that does not require the use of pumps and vessels.¹⁴³ A deep well culture plate including an insert with a dialysis membrane was used (Figure 3.2C). Successful and continuous glucose supply and lactate removal through the dialysis membrane were shown. The retaining of cytokines and autocrine factor enabled to promote endodermal differentiation of induced pluripotent stem cells (iPSCs) without daily cytokine addition. This dialysis system for re-using culture medium still is not frequently applied and mainly used for proliferation and differentiation processes of (costly) iPSCs studies.¹⁴²⁻¹⁴⁴ Use of these dialysis systems in other cell culturing fields requires optimization. For example, the size of medium components should be known and taken into account as high MW proteins, which are also found in FBS, will not be able to cross the dialysis membrane. In our opinion, medium dialysis could not only reduce culture costs, it could also contribute to a more physiological environment for cell proliferation and differentiation. This would especially be

true for cocultures where the interaction between different cell types is investigated, by retaining the communication factors produced by the cells.

3.5 Implementation of biosensors

Combining biology and technology advances cell culturing at a rapid pace. Addition of biosensors to cell cultures is one of these beneficial combinations. Biosensors show potential for monitoring of the microenvironments in *in vitro* systems and aim at providing real-time information regarding cell viability, growth and metabolism.¹⁴⁵⁻¹⁴⁷ For example, on-line measurement of dissolved oxygen was applied for medium optimization of mammalian cell cultures.¹⁴⁸ An oxygen sensor immobilized at the bottom of each well in a 96 wells plate was successfully used to optimize the concentration of glucose, glutamine and inorganic salts. This method was highly cost effective and time efficient, automatically analyzing many samples in one go in small medium volumes.

In order to maintain cell viability, experimental validity and reproducibility, it is essential that metabolite levels are maintained within physiological limits.¹³⁰ For example, fluctuations in oxygen and glucose concentration can affect cell growth, differentiation and signaling.¹³⁰ Multiplexed sensing, recording, and processing of real-time data could provide novel insights into the optimal nutrients and culture conditions needed to grow cells.¹⁴⁷ Furthermore, real-time data analytics can be used to respond to changes in culture conditions in a closed feedback loop, adjusting inputs to obtain desired results.¹⁴⁷ Sensors could provide help in determining the status of the cell culture. For example, medium composition can be tracked for the CS as a stem cell differentiates to determine how differentiation is progressing. Accordingly, growth factors can be removed or added to encourage further differentiation.¹⁴⁷

It needs to be mentioned that while the technology is available, not many user-friendly and affordable techniques have been implemented into *in vitro* tissue cultures. Particularly techniques developed for continuous detection of biomolecules at low physiological concentrations require thorough understanding of electrochemistry, electrical engineering, and/or optics. Implementation will require a closer collaboration between researchers of different fields, willing to combine each other's expertise, requirements, and possibilities.

3.6 Conclusion

Investigating cell-cell interactions through CSs requires complex tissue cultures where different cell types are being co-cultured. Coculturing asks for a highly specific environment meeting the requirements of all involved cell types and therefore requires a great deal of optimizing. Advances in this field bring us closer to *in vitro* models that can be used to study physiological and pathological cell-cell interactions and will allow for the development of drugs that interact with cells. We highly recommend to reconsider today's method of complete medium exchange to provide a more physiological environment to the cells. Combining current *in vitro* culturing techniques with existing technological inventions such as dialysis and biosensors could lead toward the goal of developing more complex, reproducible, nature-like *in vitro* tissue models.

Author Contributions

MV and SH contributed to the conception of the review. MV wrote the first draft of the manuscript. All authors contributed to manuscript revision, read, and approved the submitted version.

Funding

The authors gratefully acknowledge the financial support for MV and SH by the research program TTW with project number TTW 016.Vidi.188.021, which is financed by the Dutch Organization for Scientific Research (NWO).

Conflict of Interest

The authors declare that the research was conducted in the absence of any commercial or financial relationships that could be construed as a potential conflict of interest.

Acknowledgments

The authors gratefully acknowledge Professor Menno Prins and Paul Vernooij for sharing their knowledge on biosensors and for their contribution to the discussions about implementation of biosensors in the cell biology field.

Chapter 4

A dialysis medium refreshment cell culture set-up for an osteoblast-osteoclast coculture

The contents of this chapter are based on:

Michelle A. M. Vis^a, Bregje W.M. de Wildt^a, Keita Ito^a, Sandra Hofmann^a (2023) *Biotechnology and Bioengineering*, 120, 1120-1132. <https://doi.org/10.1002/bit.28314>

^a *Department of Biomedical Engineering and Institute for Complex Molecular Systems (ICMS) Eindhoven University of Technology, Eindhoven*

Abstract

Culture medium exchange leads to loss of valuable auto- and paracrine factors produced by the cells. However, frequent renewal of culture medium is necessary for nutrient supply and to prevent waste product accumulation. Thus it remains the gold standard in cell culture applications. The use of dialysis as a medium refreshment method could provide a solution as low molecular weight molecules such as nutrients and waste products could easily be exchanged, while high molecular weight components such as growth factors, used in cell interactions, could be maintained in the cell culture compartment. This study investigates a dialysis culture approach for an *in vitro* bone remodeling model. In this model, both the differentiation of human mesenchymal stromal cells (MSCs) into osteoblasts and monocytes (MCs) into osteoclasts is studied. A custom-made simple dialysis culture system with a commercially available cellulose dialysis insert was developed. The data reported here revealed increased osteoblastic and osteoclastic activity in the dialysis groups compared to the standard non-dialysis groups, mainly shown by significantly higher alkaline phosphatase (ALP) and tartrate-resistant acid phosphatase (TRAP) activity, respectively. This simple culture system has the potential to create a more efficient microenvironment allowing for cell interactions via secreted factors in mono- and cocultures and could be applied for many other tissues.

4.1 Introduction

In conventional cell and tissue culture strategies, cells/tissues are surrounded by culture medium containing various nutrients and stimulants. This culture medium is exchanged regularly to maintain nutrient and stimulant levels upon cell consumption and to eliminate waste products produced by the cells.¹⁴⁹ While in culture, the cells also actively produce and secrete a variety of macromolecules to maintain their microenvironment. By changing the medium, these important molecules for auto- and paracrine signaling are lost. After every medium change the cells must make a new effort to restore their communication through these molecules. This effort could considerably influence the cell's behavior. However, frequent renewal of the medium is necessary to provide sufficient nutrients and prevent waste product accumulation, which has been shown to inhibit cell growth.¹³⁴

To overcome this waste accumulation problem, cell culture systems have been developed in which culture medium was filtered or dialyzed to remove waste products.^{150,151} The principle of dialysis relies on the exclusion of molecules based on their size.¹⁴⁹ Fresh medium contains low molecular weight (MW) molecules such as nutrients, amino acids, and vitamins. Depending on the chosen MW cut-off (MWCO), the dialysis membrane allows for exchange of those molecules. In this way waste products can diffuse out of the culture medium while nutrients and vitamins can diffuse back in. High MW components such as growth factors produced by the cells or added to the medium are retained in the medium compartment.¹⁴⁹

This dialysis culture principle has already been reported in 1958 by G.G Rose who introduced the concept of using a cellophane membrane to divide the tissue culture part from the culture medium exchange part.^{150 151} He kept advancing the set-up and eventually engineered a 12-chambered tissue culture system with dialysis membranes.¹⁵² Decades later, E.A. Vogler reported a cell culture device based on Rose's work and showed long-term cell culture (30 days) of a variety of mammalian cells (epithelioid (canine), fibroblastic (monkey), hybridoma, primary thymocytes and splenocytes (all murine)) in the stable culture environment created by dialysis.¹⁵³ Vogler's group further expanded this idea of "simultaneous growth and dialysis" and over the years reported work in the field of bone tissue engineering and breast cancer metastasis with cell cultures ranging from two-dimensional (2D) to three-dimensional (3D).^{154,155,156,157}

Currently, dialysis for re-use of culture medium is not frequently reported. It is remarkable that these techniques are not used more often in cell culture systems while they have the potential to improve cell function tremendously. Dialysis cultures have both economic and biological benefits. The economic benefits come from the fact that less of the costly macromolecules for cell proliferation and differentiation are needed in the culture medium. The biological benefit originates from the maintenance of the cells' secretome over time, which leads to a more stable cell culture environment. This seems particularly imperative for studies investigating cell-cell-communication via cell-secreted macromolecules or extracellular vesicles. Through the retention of those factors in the medium, dialysis cultures could be beneficial for the proliferation and differentiation process of many cell types, particularly for the culture of *in vitro* tissue models. These models aim at representing the *in*

vivo situation as closely as possible in order to for example test the effect of drugs on cells. It is hypothesized that a microenvironment providing more stability through less fluctuations could contribute to the efficacy and reliability of such models.

In the most recent study of Krishnan *et al.*, Vogler's bioreactor was used to create a 3D bone remodeling model with murine osteoblasts and osteoclasts cultured over a period of 2-10 months.¹⁵⁷ With a goal towards *in vitro* bone-remodeling models for drug testing and personalized medicine, a human model would be preferred over a murine model due to interspecies differences. Moreover, a 2-10 month culture period would generate practical issues for high throughput drug testing. Therefore, we propose a fully human 3D bone-remodeling model, including the use of human platelet lysate (hPL) instead of the generally used fetal bovine serum (FBS).¹⁵⁸ We present a simple, cost-effective method for incorporating dialysis into the cell culture. A silk fibroin (SF) scaffold will be integrated to reduce the amount of time needed to create the 3D bone tissue (Figure 4.1A).

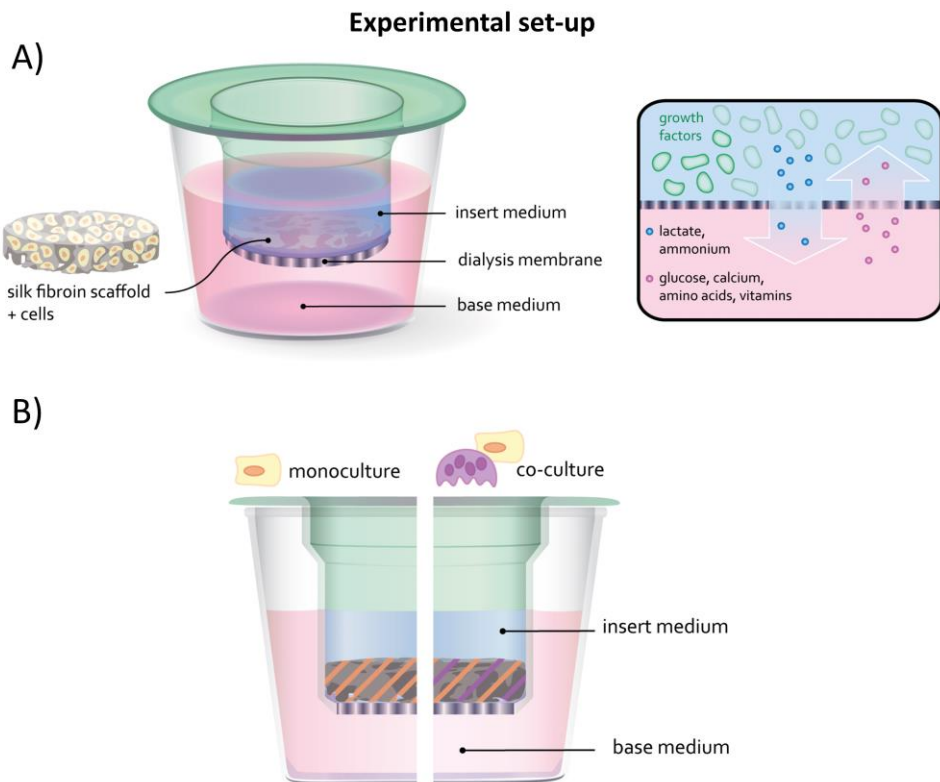


Figure 4.1 Experimental set-up: A) A silk fibroin scaffold was seeded with cells and cultured in a custom-made dialysis culture dish. The dialysis membrane ensured retaining of high molecular weight growth- and communication factors in the cell culture insert. Nutrients and waste products of low molecular weight can pass the dialysis membrane and will be supplied and removed by diffusion across the membrane. B) In the monoculture experiment the silk fibroin scaffold is seeded with MSCs. In the coculture experiment the scaffold is seeded with MSCs and MCs.

For *in vitro* bone tissue formation, the extracellular matrix (ECM) production by the cells is of uttermost importance. Osteoblasts produce collagen type 1 ECM that is mineralized both intrafibrillarly and extrafibrillarly.⁶ The cells' secretome is essential in this process. Continuous removal or periodic exchange of culture medium considerably disturbs these mineralization processes, making it difficult to induce *in vitro* bone tissue formation.¹⁵⁴ Therefore, in this study, a dialysis culture approach is investigated for an *in vitro* bone remodeling model by differentiation of human mesenchymal stromal cells (MSCs) into osteoblasts and monocytes (MCs) into osteoclasts (Figure 4.1B). A custom-made simple dialysis culture system with a commercially available cellulose dialysis insert is developed. It is believed that the dialysis of culture medium could contribute to a more efficient and more physiological environment for cell proliferation and differentiation, as the cells' secretome remains in the culture.

4.2. Materials and Methods

4.2.1 Fabrication of the silk fibroin scaffolds

Silk fibroin scaffolds were produced as previously described.^{159,160} Briefly, *Bombyx mori* L. silkworm cocoons were degummed by boiling in 0.2M Na₂CO₃ for 1 hour. Dried silk was dissolved in 9M LiBr and dialyzed against ultra-pure water (UPW) using SnakeSkin Dialysis Tubing (MWCO: 3.5 kDa; Thermo Fisher Scientific, Breda, The Netherlands). Dialyzed silk solution was snap frozen in liquid nitrogen (-190 °C), lyophilized, and dissolved in 1,1,1,3,3,3-Hexafluoro-2-propanol (HFIP, FCB125463, FluoroChem), resulting in a 17% (w/v) solution. One milliliter silk-HFIP solution was added to 2.5 g NaCl with a granule size between 250 and 300 µm in a Teflon container and allowed to air dry. Silk-salt blocks were immersed in 90% methanol in UPW for 30 minutes to induce β-sheet formation.¹⁶¹ NaCl was extracted in UPW for 2 days. Scaffolds were cut into disks of 1 mm height, punched with a 5-mm diameter biopsy punch, and autoclaved in phosphate buffered saline (PBS) at 121°C for 20 min for sterilization.

4.2.2 Fabrication of the dialysis culture plates

A holder with 48 holes was custom-made (poly carbonate, designed in Inventor Professional, Autodesk) to fit a 48-wells plate (677180, Greiner) (Figure 4.2). The holder was autoclaved at 121°C for 20 min and placed on top of a 48-wells plate in a biosafety cabinet. Slide-a-lyzer mini dialysis devices (0.1 mL, 69590, Thermo Fisher scientific) with a MWCO of 20 kDa were sterilized using UV-light on both sides for 15 minutes each. The mini dialysis devices were carefully placed in the holder. All membranes were pre-wetted using sterile PBS which was pipetted in both the base and the insert of the wells (Figure 4.1). Later, the PBS was removed and replaced with the appropriate cell culture medium.

4.2.3 Monoculture: isolation, expansion and cultivation of MSCs

MSC isolation and characterization from human bone marrow (Lonza, Walkersville, MD, USA) was performed as previously described.¹⁶² MSCs were frozen at passage 3 with 1.25*10⁶ cells/ml in freezing medium containing FBS (BCBV7611, Sigma-Aldrich) with 10% dimethylsulfoxide (DMSO, 1.02952.1000, VWR, Radnor, PA, USA) and stored in liquid nitrogen until further use. Before experiments, MSCs were thawed and seeded at a density of 2.5*10³ cells/cm² in expansion medium containing DMEM (high glucose, 41966, Thermo

Fisher Scientific), 10% FBS (BCBV7611, Sigma Aldrich), 1% Antibiotic Antimycotic (anti-anti, 15240, Thermo Fisher Scientific), 1% Non-Essential Amino Acids (11140, Thermo Fisher Scientific), and 1 ng/mL basic fibroblastic growth factor (bFGF, 100-18B, PeproTech, London, UK) at 37 °C and 5% CO₂. After 9 days, cells were detached using 0.25% trypsin-EDTA (25200, Thermo Fisher Scientific) and directly used for experiments at passage 4. A dynamic seeding process was used as previously described.¹⁶³ Briefly, SF scaffolds were incubated with a cell suspension (3×10⁵ cells/4 mL expansion medium) in 50-mL tubes placed on an orbital shaker at 150 rpm for 6 hours in an incubator at 37°C and 5% CO₂. Next, the samples were transferred to the dialysis wells plates and incubated at 37°C and 5% CO₂ for a total 4 weeks in osteogenic monoculture medium containing DMEM (low glucose, 22320, Thermo Scientific), 10% human platelet lysate¹⁵⁸ (hPL, PE20612, PL BioScience, Aachen, Germany), 1% Anti-Anti, 0.1 μM dexamethasone (D4902, Sigma-Aldrich), 0.05 mM ascorbic acid-2-phosphate (A8960, Sigma-Aldrich), 10 mM β-glycerophosphate (G9422, Sigma-Aldrich). The insert of the dialysis wells plates contained the scaffold and 200 μL osteogenic medium, the base contained 500 μL osteogenic medium. Medium was changed according to Table 4.1. The culture was maintained for 28 days.

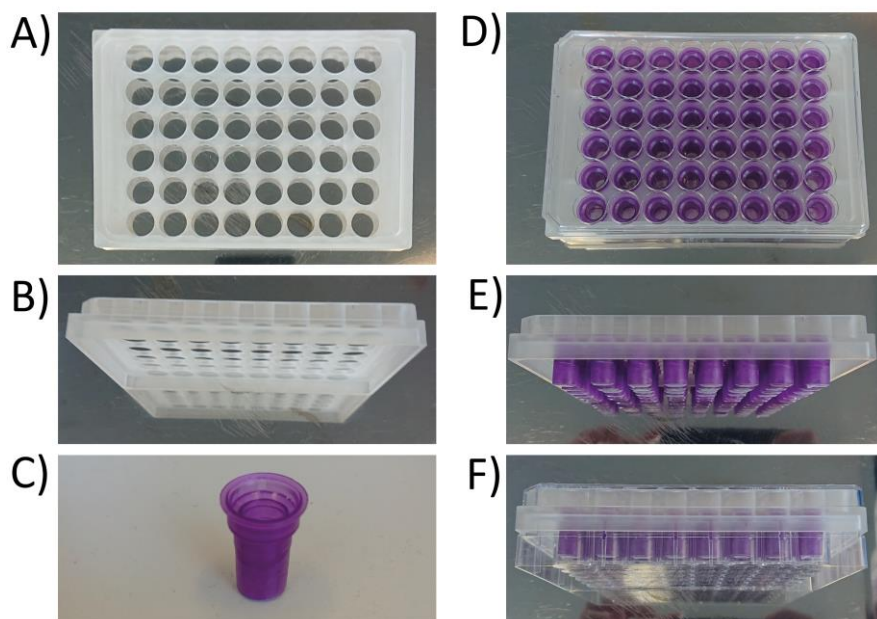


Figure 4.2 The custom-made holder for the 48 wells plate. A) top view, B) side view, C) dialysis cup, D) top view of holder filled with dialysis cups, E) side view of holder filled with dialysis cups, F) holder with cups in 48 wells plate.

4.2.4 Coculture: isolation of monocytes and cultivation of MSCs + monocytes



Human peripheral blood buffy coats from healthy volunteers under informed consent were obtained from the local blood donation center (agreement NVT0320.03, Sanquin, Eindhoven, the Netherlands). The buffy coats (~ 50 mL) were diluted to 200 mL in 0.6 % (w/v) sodium citrate in PBS adjusted to pH 7.2 at 4 °C (citrate-PBS), after which the peripheral mononuclear

cell fraction was isolated by carefully layering 25 mL diluted buffy coat onto 13 mL Lymphoprep (07851, StemCell technologies, Cologne, Germany) in separate 50 mL centrifugal tubes, and centrifuging for 20 min with lowest brake and acceleration at 800×g at RT. Human peripheral blood mononuclear cells (PBMCs) were collected, resuspended in citrate-PBS and washed 4 times in citrate-PBS supplemented with 0.01% bovine serum albumin (BSA, 10735086001, Sigma-Aldrich, Zwijndrecht, The Netherlands) to remove all Lymphoprep. PBMCs were frozen in liquid nitrogen in freezing medium containing RPMI-1640 (RPMI, A10491, Thermo Fisher Scientific), 20% FBS (BCBV7611, Sigma-Aldrich) and 10% DMSO and stored in liquid nitrogen until further use. Prior to experiments, monocytes (MCs) were isolated from PBMCs using manual magnetic activated cell separation (MACS). PBMCs were thawed, collected in medium containing RPMI, 10% FBS (BCBV7611, Sigma-Aldrich) and 1% penicillin-streptomycin (p/s, 15070063, Thermo Fisher Scientific), and after centrifugation resuspended in isolation buffer (0.5% w/v BSA in 2mM EDTA-PBS). The Pan Monocyte Isolation Kit (130-096-537, Miltenyi Biotec, Leiden, The Netherlands) and LS columns (130-042-401, Miltenyi Biotec) were used according to the manufacturer's protocol. After magnetic separation, the cells were directly resuspended in osteogenic coculture medium (α MEM 41061, 10% hPL, 1% Anti-Anti with 0.1 μ M dexamethasone, 0.05 mM ascorbic acid-2-phosphate, 10 mM β -glycerophosphate) spiked with 50 ng/mL macrophage colony stimulating factor (M-CSF, 300-25, PeproTech). The cells were counted and 1.9×10^6 monocytes were resuspended in 20 μ L coculture medium and per scaffold added on top of the scaffolds that had previously been seeded with MSCs as described above (in 4.2.4). After 1.5 hour incubation at 37 °C and 5% CO₂, the rest of the 180 uL medium was added to the insert. 500 uL medium was added to the base. Medium was changed according to Table 4.11. After 2 days, 50 ng/mL receptor activator of NF κ -B ligand (RANKL, 310-01, PeproTech) was added to the coculture medium and maintained for the rest of the culture. The culture was maintained for 28 days.

4.2.5 Glucose Assay

A glucose assay was used to measure the glucose concentration in the medium at day 7, 14, 21 and 28 in both the insert and the base (n=3). The glucose concentration was measured to ensure passage of glucose as a nutrient component over the dialysis membrane during the 28 day culture period. The method was adapted from Hulme *et al.*¹⁶⁴ Briefly, on the day of assay, a buffer/chromophore reagent was prepared by mixing an equal volume (3.5 mL) of 4-aminoantipyrine (10 mM, 06800, Sigma-Aldrich) and N-ethyl-N-sulfopropyl-m-toluidine (10 mM, E8506, Sigma-Aldrich) with 3.0 mL of 0.8 M sodium phosphate buffer at pH 6.0. 100 μ L of this reagent was added to 10 μ L horseradish peroxidase (1.6 units/mL, 77332, Sigma-Aldrich) and 2 μ L of sample/standard (0–1.25 mM D-glucose (15023-21, Thermo Fisher) in wells of a 96-well plate. The reaction was initiated by the addition of 10 μ L glucose oxidase (2.7 units/mL, G7141-10KU, Sigma-Aldrich) and after 30 min incubation at room temperature in the dark, absorbance was measured at 550 nm using a plate reader (Synergy HTX, Biotek). Glucose concentration of each sample was then calculated using a standard curve.

Table 4.1 Overview of group name, culture medium type, medium change schedule and explanation

culture type		group name	medium type	medium change		explanation
monoculture 	negative control	mono-cntr-	control	insert + base	3x/week	no osteogenic differentiation expected
	positive control	mono-standard	osteogenic monoculture	insert + base	3x/week	medium change according to the gold standard
	dialysis	mono-dialysis	osteogenic monoculture	insert	never	retainment of cells' secretome in the cell culture compartment
			base	3x/week		
coculture 	positive control	co-standard	osteogenic coculture	insert + base	3x/week	medium change according to the gold standard
	dialysis	co-dialysis	osteogenic coculture	insert	never	retainment of cells' secretome in the cell culture compartment
				base	3x/week	

4.2.6 Lactate Assay

A lactate assay was used to measure the lactate concentration in the medium at day 7, 14, 21 and 28 in both the insert and the base (n=3). The lactate concentration was measured to ensure passage of lactate as a metabolic waste product over the dialysis membrane during the 28 day culture period. The methods was adapted from Salvatierra *et al.*¹⁶⁵ Briefly, a reaction mix was prepared containing 5 mg/mL of β -Nicotineamide Adenine Dinucleotide (N7004, 1G, Sigma-Aldrich), 0.2 M glycine buffer (G5418, Sigma-Aldrich), and 22.25 units/mL of L-Lactic Dehydrogenase (L3916, Sigma-Aldrich). A standard curve was prepared using 20 mM lactate stock solution by adding sodium L-lactate (L7022, Sigma-Aldrich) to dH₂O. Equal parts (40 μ L) of the reaction mix and each sample/standard were mixed in a 96-well plate. After 30 minutes of incubation at 37°C, absorbance was measured at 340 nm using a plate reader (Synergy HTX, Biotek). Lactate concentration of each sample was then calculated using a standard curve.

4.2.7 Cell metabolic activity

PrestoBlue assay was used to analyze and track the metabolic activity of the MSCs and MCs in the SF scaffold. Briefly, at days 7, 14, 21 and 28, samples (n=4 per group) were transferred to a clean 48 wells plate filled with 200 μ L of 10 v/v % PrestoBlue reagent (A13262, Thermo

Fisher) in the appropriate medium (mono or coculture) and incubated for 1 h at 37 °C. In a 96-well assay plate 100 µL of the PrestoBlue solution was added in duplo per sample and the absorbance was measured at 570 and 600 nm. Dye reduction rate was calculated according to manufacturer's instructions.

4.2.8 Cell-associated alkaline phosphatase activity

Alkaline phosphatase (ALP) was used to indirectly quantify osteoblast activity. At days 7, 14, 21 and 28, after the Presto Blue assay (see 2.7 Cell metabolic activity) scaffolds (n=4 per group) were washed in PBS and disintegrated in 0.5 mL of 0.2% (v/v) Triton X-100 and 5 mM MgCl₂ solution using steel beads and a Mini Beadbeater™ (Biospec). The remaining solution was centrifuged at 3000g for 10 minutes. In a 96-well assay plate, 80 µL of the supernatant was mixed with 20 µL of 0.75M 2-amino-2-methyl-1-propanol buffer (A65182, Sigma-Aldrich) and 100 µL 100 mM p-nitrophenylphosphate solution (71768, Sigma-Aldrich) and incubated for 10 minutes, before adding 100 µL 0.2M NaOH stop solution. Absorbance was measured at 405 nm using a plate reader (Synergy HTX, Biotek) and these values were converted to ALP activity (converted p-nitrophenyl phosphate in µmol/ml/min) using standard curve absorbance values.

4.2.9 DNA assay

The solution obtained for the ALP activity assay (see 2.8) after disintegration of the scaffold was further used to measure the amount of DNA as an attribute for cell number. In each Eppendorf tube, 340 µL of liquid remained after the ALP measurements. Next, 340 µL of papain (280 µg/mL, p4762, Sigma-Aldrich) in digestion buffer was added and the samples were incubated overnight at 60 °C under constant shaking in a shaking Eppendorf tubes water bath. The DNA content of the supernatant was determined using the Qubit HS dsDNA Assay Kit (Q32854, Invitrogen, Thermo Fisher) according to the manufacturer's instructions. The calculated ALP activity was normalized by the DNA content.

4.2.10 Tartrate-resistant acid phosphatase activity

Tartrate-resistant acid phosphatase (TRAP) was used to indirectly quantify osteoclast activity. Supernatant medium samples of both the insert and the base were taken at medium change and stored at -80 °C at day 7, 14, 21, and 28. 100 µL pNPP buffer (1 mg/mL p-nitrophenylphosphate, 0.1 mol/L sodium acetate, 0.1 % (v/v) Triton-X-100 in PBS, first adjusted to pH 5.5, then supplemented with 30 µL/mL tartrate solution (Sigma Aldrich)) and 20 µL culture medium or nitrophenol standard in PBS were incubated in 96-well assay plates at 37 °C. After 90 min, 100 µL 0.3 mol/L NaOH was added to stop the reaction. Absorbance was read at 405 nm using a plate reader and absorbance values were converted to TRAP activity (converted p-nitrophenyl phosphate in µg/ml) using standard curve absorbance values.

4.2.11 Immunohistochemistry

At day 28, scaffolds (n=4 per group) were washed with PBS and immersed first in 5% and then in 35% sucrose solution in PBS at room temperature for 10 min each. The scaffolds were embedded in cryomolds containing Tissue-Tek OCT compound (Sakura, The Netherlands), snap frozen in liquid nitrogen, cut into 10 µm thick sections using a Cryotome Cryostat (Leica

biosystems), and mounted on Superfrost Plus microscope slides (Thermo Fisher Scientific). Next, sections were immunostained after washing with PBS-tween, fixing in 10% neutral-buffered formalin for 10 min at room temperature, washing again with PBS-tween, permeabilizing in 0.5% Triton X-100 in PBS for 10 min and blocking in 10% normal goat serum in PBS for 30 min. Cells were incubated with DAPI, Phalloidin and immunostainings (Table 4.2) in PBS for 1 h. Images were taken with either a Zeiss Axio Observer 7 (collagen type-1 images) or a Leica TCS SP5X (RUNX-2 and osteopontin images).

Table 4.2 List of all dyes and antibodies used

Antigen	Source	Catalogue No	Label	Species	Concentration/Dilution
DAPI	Sigma-Aldrich	D9542			0.1 µg/mL
Atto 647 conjugated Phalloidin	Sigma-Aldrich	65906			50 pmol
Collagen type-1	Abcam	Ab34710		Rabbit	1:200
RUNX-2	Abcam	Ab23981		Rabbit	1:500
Osteopontin	Thermo Fisher	14-9096-82		Mouse	1:200
Anti-rabbit (H+L)	Molecular Probes	A11008	Alexa 488	Goat	1:200
Anti-mouse IgG1 (H+L)	Molecular Probes	A21127	Alexa 555	Goat	1:200

4.2.12 Histology

Cryosections made as described (2.11 Immunohistochemistry) were washed with PBS, fixed in 10% neutral-buffered formalin for 10 min at room temperature, washed again with PBS, and stained with Alizarin Red (2% in distilled water, A5533, Sigma-Aldrich) for 15 minutes to identify mineralization. Sections were imaged using a Zeiss Axio Observer Z1 microscope.

4.2.13 Scanning electron microscopy

Constructs for scanning electron microscopy (SEM) (n=4 per group for cocultures) were fixed at day 14 in 2.5 % glutaraldehyde for 24 h at 4 °C, dehydrated with a graded ethanol series (2 × 50 %, 70 % and 95 %, 3 × 100 % 10-15 min each) followed by a graded 1,1,1-Trimethyl-N-(trimethylsilyl)silanamine (HMDS)/ethanol series (1 : 2, 1 : 1, 2 : 1, 3 × 100 % HMDS 15 min each), dried at room temperature overnight and sputter coated with 5 nm gold (Q300TD, Quorum Technologies Ltd, Laughton, UK) prior to imaging with SEM (Quanta600, FEI Company, Eindhoven, the Netherlands) with a spot size of 3.0, 10.00 kV, working distance 10 mm. Images were colored using Adobe Photoshop 2022.

4.2.14 Statistical analysis

Statistical analyses were performed, and graphs were prepared in GraphPad Prism (version 9.4.0, GraphPad, La Jolla, CA, USA) and R (version 4.0.2). Data were tested for normality in distributions with Shapiro-Wilk tests and for equal variances with Levene's tests. Glucose, lactate (Figure 4.3) and TRAP data (Figure 4.6) were normally distributed without equal variances and differences were therefore tested with Welch's t-tests and presented with mean and standard deviation. Cell metabolic activity data (Figure 4.4) was not normally distributed and without equal variances and differences were tested with Mann-Whitney tests and presented with median and interquartile range. ALP (Figure 4.5) data was normally distributed and variances were equal and differences were tested with two-way ANOVA and Tukey post hoc test for multiple comparisons and presented as mean and standard deviation.

4.3 Results

4.3.1 Functionality of the dialysis membrane: continuous passage of glucose and lactate

To test whether the dialysis membrane did not clog over time, glucose and lactate passage over the membrane were measured over the culture period of 28 days in the monoculture. Measurements were taken from the cell culture media of both the insert and the base of the dialysis system (Figure 4.1). Free passage of glucose and lactate molecules over the membrane was indicated by non-significant differences of the measured amount of glucose and lactate between the insert and the base medium in all groups (Figure 4.3A-D).

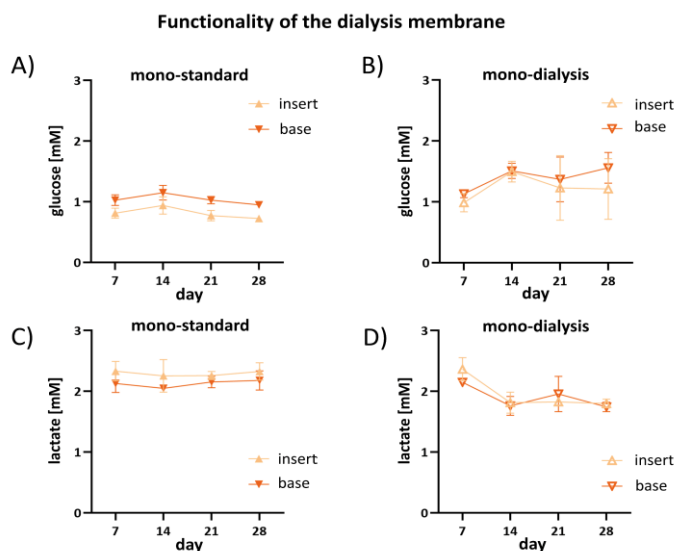


Figure 4.3 Functionality of the dialysis membrane. A, B) Glucose and C, D) lactate measurements on culture medium of the monoculture cell experiment over 28 days performed in our dialysis system (n = 3). Measurements were taken in both the insert and the base of the system. At each timepoint the difference between insert and base is nonsignificant ($p > 0.05$, Welch's t-tests).

4.3.2 Functionality of the dialysis membrane: cell metabolic activity

To ensure that no toxic components build up in the cell culture system, cell metabolic activity

was followed over the culture time. Cell metabolic activity was measured in both the mono- and coculture for the standard and dialysis groups. In the monoculture, the cell metabolic activity of the standard group compared to the dialysis group was similar for each timepoint with no significant differences (Figure 4.4A). In the coculture, dialysis seems to be beneficial compared to the standard as the cell metabolic activity of the dialysis group was significantly higher (co-standard vs. co-dialysis) on day 7, 21, 28 (Figure 4.4B). The results indicate that both in mono- and coculture, the cells were equally or at some timepoints more metabolically active in the dialysis group compared to the standard showing that the dialysis system could beneficially influence the cell metabolic activity.

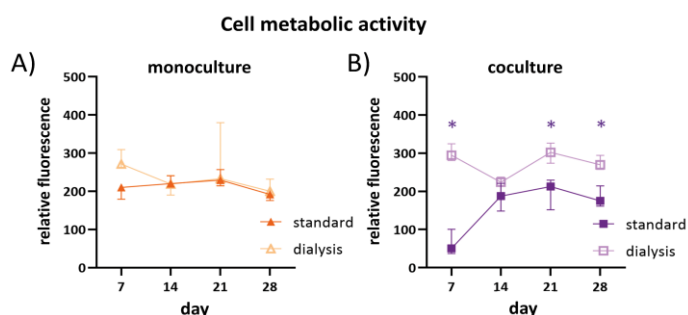


Figure 4.4 Cell metabolic activity (presto blue) of A) the monoculture and B) coculture measured during 28-day cell experiments shown as relative fluorescence versus medium control (n = 4). At each timepoint the difference between the control and dialysis samples was determined, with significant differences for $p < 0.5$ (Mann-Whitney tests) indicated with an asterisk.

4.3.2 Osteoblastic differentiation of MSCs in monoculture

ALP activity is a widely used marker for indirectly quantifying osteoblastic activity.¹⁶⁶ ALP activity on the cells' surface was determined weekly in the monoculture over a 28 day time period and normalized against the amount of DNA. The ALP activity was lowest in the negative control throughout all timepoints and was only slightly elevated at day 28. As expected, the ALP activity in the standard and dialysis groups was increased and this difference was significant compared to the negative control starting from day 14. There was a trend that the ALP activity was slightly higher in the dialysis group compared to the standard group with significant differences at day 14 and 21 (Figure 4.5A). These results indicate higher osteoblastic activity in the dialysis group compared to the standard group (Figure 4.5A).

To confirm extracellular matrix production and osteoblastic differentiation of the MSCs in the monoculture, samples were stained for collagen type-1, mineralization (Alizarin Red staining), RUNX-2 and osteopontin expression at the endpoint of the experiment (day 28). Collagen type 1 was present in all groups, but seemingly less and mostly located at the outer rim of the scaffold in the negative control compared to the standard and dialysis groups (Figure 4.5B). Mineralization was visible in the standard and dialysis groups while being absent in the negative control (Figure 4.5C). RUNX-2 expression was faintly present in the nucleus of

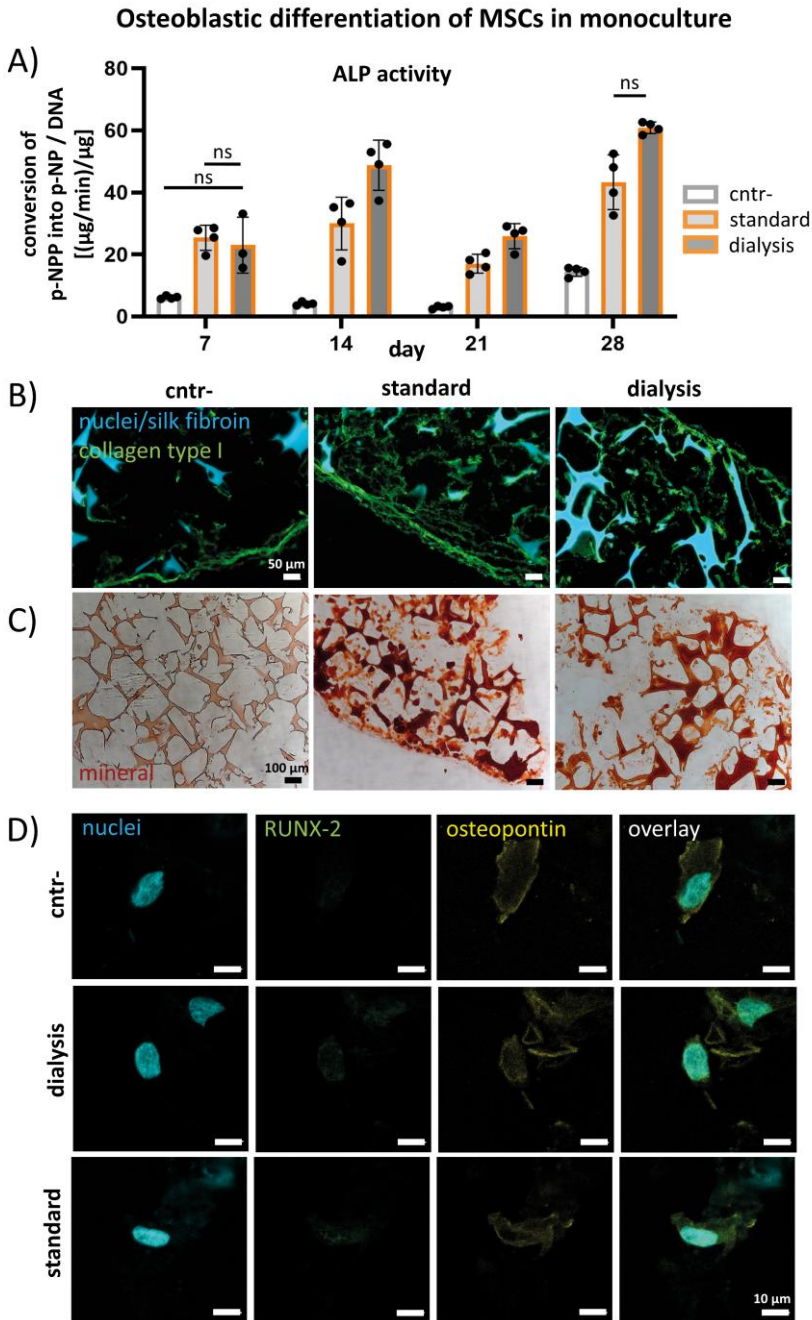


Figure 4.5 Osteoblastic differentiation of MSCs in monoculture. A) ALP activity divided by DNA ($n = 4$); significant differences are determined by two-way ANOVA with Tukey's post hoc test. All differences are significant ($p < 0.05$), unless indicated with "ns." B) Collagen type 1 production by the cells visualized by immunostaining at day 28. C) Mineralization shown by Alizarin Red staining at day 28. (d) RUNX-2 and osteopontin expression visualized by immunostaining at day 28.

the standard and dialysis groups while being absent in the negative control (Figure 4.5D). Osteopontin expression was visible in the body of cells in all groups (Figure 4.5D). The results confirm that the presence of the dialysis system allows for MSC to produce an ECM composed of collagen and mineral and for the cells to differentiate into osteoblasts.

4.3.3 Osteoclastic differentiation of MCs in coculture

TRAP activity is a widely used marker for indirectly quantifying osteoclastic activity.¹⁶⁶ TRAP activity was measured weekly in the coculture medium of both the base and the insert over a 28 day time period. Over time, TRAP activity in the base of both groups was stable and low (Figure 4.6A), most likely originating from the hPL.¹⁵⁸ In the insert TRAP activity increased over time with a significantly higher activity in the dialysis group compared to the standard at day 14 and 28 (Figure 4.6A). These results suggest retention of TRAP in the insert of the dialysis group leading to higher osteoclastic activity compared to the standard group, where the medium in the insert was replaced at every medium change (Figure 4.6A).

The coculture was investigated with SEM at day 14. In both the standard and dialysis group large (~25-40 μm) cells were visible that were attached to the surface (Figure 4.6B, in purple). These cells resemble osteoclast in morphology and size. Also, smaller (~5-10 μm) rounded cells were visible in both groups. These cells resemble monocytes in morphology and size and were expected to be present as monocytes had been seeded in abundance (Figure 4.6B, in blue). Further, an elongated cell was seen, resembling a towards osteoblast differentiated MSC in morphology and size (Figure 4.6B, in orange).

For the coculture, a different type of culture medium was used compared to the monoculture, as MSCs and MCs need different components to differentiate into osteoblasts and osteoclasts respectively. To confirm extracellular matrix production of the MSCs in the coculture medium, samples were stained for collagen type 1 and mineralization (Alizarin Red staining) at the endpoint of the experiment (day 28). In both coculture conditions, the standard and the dialysis, an ECM was produced with collagen type 1 and mineralization (Figure 4.6C).

4.4 Discussion

Regular culture medium exchange leads to loss of valuable auto- and paracrine factors produced by the cells. However, frequent renewal of culture medium is necessary to prevent waste product accumulation and to supply fresh nutrients and is therefore the gold standard in cell culture applications. The use of a cell culture compartment with a dialysis membrane could overcome the need for frequent cell culture medium renewal in the cell culture compartment as low MW molecules such as nutrients and waste products can easily pass the membrane, while high MW components such as growth factors are maintained. Here, a coculture system of human osteoblasts and osteoclasts was established in a dialysis system that seemed to allow for maintaining of the cells' secretome. Typical components of the ECM together with typical enzymatic activity of the cells (ALP and TRAP activity) were shown.

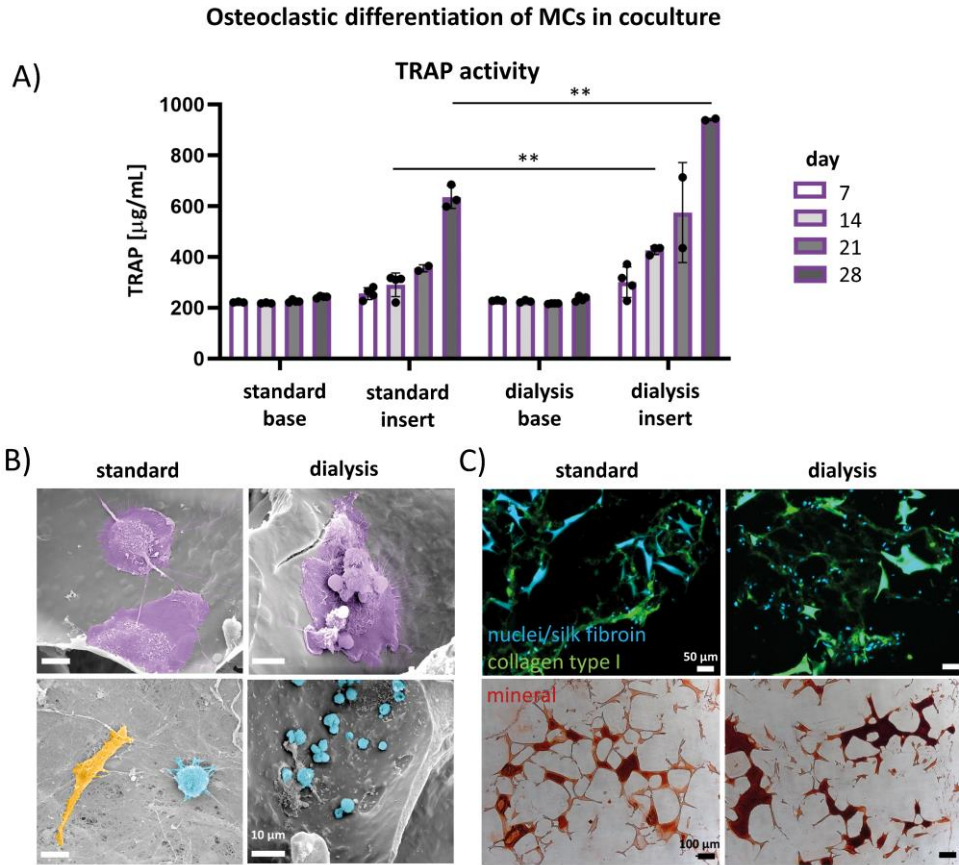


Figure 4.6 Osteoclastic differentiation of MCs in coculture. A) TRAP activity; significant differences ($p < 0.05$) are determined by comparing the inserts of the standard to the dialysis group for each timepoint using Welch's tests. B) Cell morphology visualized by SEM at day 14. Osteoclast-like cells are depicted in purple, osteoblast-like in orange and monocyte-like in blue. C) Collagen type 1 production of the cells visualized immunostaining at day 28. Mineralization shown by Alizarin Red staining at day 28.

In the present study, a simple cell culture system with a dialysis membrane was developed. For the use of a dialysis membrane in long-term cell culture applications, the characteristics of the membrane are important. Based on the sizes of the osteogenic cell culture medium components, a membrane with a MWCO of 20 kDa was chosen. The supplements of osteogenic monoculture medium are assumed to be able to pass this membrane: dexamethasone (390 Da), ascorbic acid (176 Da) and β -glycerophosphate (172 Da). However, the coculture supplements RANKL (20 kDa) and MCS-F (37 kDa) are not and are therefore only added in the beginning of the culture. No literature was found about the long-term half-life of these factors at 37°C, only that no degradation was detected within the first 48 hours.^{167,168} Although RANKL and MCS-F were only added in the beginning, evidence for the presence of osteoclasts was found. Thus, the supplements either stayed active or stimulated the coculture enough in the beginning. The possible cells' secretome consists of

high MW molecules that are assumed not to be able to pass the membrane such as ALP (86 kDa), RUNX-2 (57 kDa), osteopontin (55 kDa), TRAP (30-35 kDa) and extracellular vesicles (large range of MW).

Dialysis membranes are designed to be non-fouling. However, cell culture medium consists of nutritious liquids which are slightly viscous and sticky and could cause the membrane to clog over time.¹⁶⁹ Also, cell mediated mineral deposition on the cell side of the dialysis membrane has been reported.¹⁷⁰ However, it was not reported whether this deposition influenced the function of the dialysis membrane. Our system was functional over the culture period of 28 days. Small molecules such as glucose (180 Da) and lactate (90 Da) were able to pass the membrane continuously over the whole culture time. Large molecules such as TRAP (30-35 kDa) were maintained in the cell culture compartment. Moreover, the cells remained metabolically active, an indicator that the membrane still provided nutrients and removed waste products.

The dialysis culture system was used to study osteogenic differentiation of MSCs and MCs into osteoblasts and osteoclasts. It was hypothesized that the maintenance of auto- and paracrine factors in the culture medium would contribute to a more physiological microenvironment for the cells. The data reported here revealed higher osteoblastic and osteoclastic activity in the dialysis groups compared to the standard, shown by significantly higher ALP and TRAP activity respectively. Therefore, the dialysis system contributes to an excellent cell culture environment. Remarkably, this significant effect seen in the biochemical assays was not visible in the matrix production (collagen type 1 and mineralization). We hypothesize that this might be due to a difference in overall concentration of ascorbic acid and β -glycerophosphate. In the dialysis system, only the base medium is exchanged (500 μ L) while in the standard system both the insert and base media are exchanged (200+500 μ L), resulting in a lower overall concentration of these two factors. Ascorbic acid has been shown to increase the secretion of collagen type 1 and β -glycerophosphate is the phosphate source that is needed for mineralization.¹²⁰ It is recommended to study this effect in future experiments.

To analyze *in vitro* models over time, non-destructive methods including medium analysis are desired.⁷ A limitation of the current dialysis system is that the possibility to take medium samples from the insert is very limited. The principle of the system relies on the fact that the insert stays undisturbed. Also, the current design allows for only 200 μ L of cell culture medium in the insert. Taking medium samples would lead to a necessity for adding fresh medium. Therefore, at each timepoint samples were sacrificed to enable the performance of assays on the medium. Preferably we would have analyzed more markers, such as cathepsin K and carbonic anhydrase II to confirm OC differentiation.¹⁷¹ To overcome this limitation, non-invasive assays or sensors could be used such as for example biosensing by particle mobility (BPM)¹⁷² or aptamer based sensors.¹⁷³ Such sensors would allow for continuous monitoring of specific biomarkers without the need for medium sampling. A simpler solution could be the use of a larger volume culture medium in the insert. The amount of medium sampled should be very small relative to the total amount of medium in the insert, so that it would not

lead to disturbance of the microenvironment. However, making the volume too large, could lead to loss of the effect of the cells' secretome on the microenvironment due to dilution.¹⁴⁹

A crucial process of *in vitro* bone tissue formation is ECM production and mineralization. The data presented in this study, mainly in the coculture, indicate limited mineralization (alizarin red) in both the standard as the dialysis system. Furthermore, this mineralization occurs primarily in the scaffold material and not in the matrix produced by the cells. There are two possible explanations for this observation. Firstly, the presented experimental set-up cultures statically. It has been shown that for mineralized matrix production the cells prefer mechanical stimulation.¹⁷⁴ Here, the MSCs were initially stimulated by dynamic seeding,¹⁶³ but this effect was limited compared to what is usually seen in a dynamically loaded environment.¹⁷⁵ In future experiments, the use of a bioreactor that can apply for example fluid flow induced shear stress would be desired to improve the mineralization.¹⁷⁵ But implementing the dialysis system with its membrane will concomitantly affect the fluid flow. Secondly, it is still a major challenge to use the right type of coculture medium as both the MSCs and the MCs should be stimulated to differentiate into osteoblasts and osteoclasts respectively. Ideally, no exogenous osteogenic and osteoclastic factors need to be added and the cells interact with each other in homeostasis. The current setup is limited since it starts from OB and OC precursors that first need to differentiate into mature cells, but it has recently been shown that this differentiation process might also happen without exogenous supplementation.¹²⁴ The coculture medium used in our study may not have offered the ideal balance yet, probably resulting in a less mineralized matrix compared to the monoculture. MCs need a mineralized surface to attach to and to become osteoclasts. Recently, de Wildt *et al.* reported a pre-mineralized SF scaffold that acts as a bone-mimetic template.¹⁷⁶ They used poly aspartic acid and simulated body fluid to pre-mineralize silk fibroin scaffolds before cell seeding. The mineralized scaffolds supported both osteoclastic resorption and osteoblastic mineralization while in our study, the monocytes relied on MSCs first differentiating into osteoblasts and producing a mineralized matrix. Using the pre-mineralized template in combination with a dialysis culture system could lead to an even faster method to generate a physiological bone remodeling model.

The proposed dialysis culture system is not limited to bone and could be beneficial for a wide variety of cell culture applications. There is a huge variety of existing materials and MWCO options for the membrane, making it customizable for different needs. The MWCO can be chosen based on the cell culture medium ingredients and expected secretome. Caution however has to be taken to possible toxic elements in the manufactured dialysis membranes, such as glycerol, which has been shown to inhibit cell proliferation in several cell lines.^{177,178}

In conclusion, we have demonstrated the feasibility of a simple to use dialysis cell culture system for bone tissue engineering applications. The dialysis system enables retention of the cells' secretome and thereby omits the extra effort that the cells have to make to restore their communication after culture medium exchange. The system creates a stable microenvironment for the cells to differentiate into the osteogenic and osteoclastic lineage. This simple culture system has the potential to be applied in other TE fields and is recommended to be used for differentiation of various cell types.

Conflict of interest

The authors declare that the research was conducted in the absence of any commercial or financial relationships that could be construed as a potential conflict of interest.

Author contributions

MV, BW, KI and SH contributed to conception, methodology and design of the study. MV performed and analyzed the experiments. BW provided expertise on the practical experimental work, particularly the coculture experiments. MV wrote the original draft of the manuscript and prepared the figures. All authors contributed to manuscript revision and approved the submitted version. KI and SH contributed to the supervision. SH acquired funding for this research.

Funding

This work is part of the research program TTW with project number TTW 016.Vidi.188.021, which is (partly) financed by the Netherlands Organization for Scientific Research (NWO).

Acknowledgements

We thank Jurgen Bulsink for the design and fabrication of the 48-well plate holder. We thank the ICMS Animation Studio for creating the illustrations in Figure 4.1.

A fluorescence microscopy image showing a central, elongated, and somewhat irregularly shaped structure, likely a bone remodeling model. The structure is primarily red and green, with a dense, granular appearance. It is surrounded by a network of thin, branching structures, possibly representing blood vessels or other biological components, which are also stained with red and green. The background is dark, making the stained structures stand out. The text is overlaid on the central part of the image.

Part 2

Miniaturizing *in vitro* bone
remodeling models

Chapter 5

Towards bone-remodeling-on-a-chip: self-assembling 3D osteoblast-osteoclast coculture in a microfluidic chip

The contents of this chapter are based on:

Michelle A.M. Vis^a, Feihu Zhao^b, Esmee S.R. Bodelier^a, C. Marlous Bood^a, Jurgen Bolsink^a, Marina van Doeselaar^a, Hossein Eslami Amirabadi^c, Keita Ito^a, Sandra Hofmann^a (2023)
Submitted

^a *Department of Biomedical Engineering and Institute for Complex Molecular Systems (ICMS) Eindhoven University of Technology, Eindhoven*

^b *Department of Biomedical Engineering and Zienkiewicz Centre for Computational Engineering, Faculty of Science and Engineering, Swansea University, Swansea, United Kingdom*

^c *AZAR Innovations, Utrecht, Netherlands*

Abstract

Healthy bone is maintained by the process of bone remodeling. An unbalance in this process can lead to pathologies such as osteoporosis which are often studied with animal models. However, data from animals have limited power in predicting the results that will be obtained in human clinical trials. In search for alternatives to animal models, human *in vitro* models are emerging as they address the principle of reduction, refinement, and replacement of animal experiments (3Rs). At the moment, no complete *in vitro* model for bone-remodeling exists. Microfluidic chips offer great possibilities, particularly because of the dynamic culture options, which are crucial for *in vitro* bone formation. In this study, a scaffold free, fully human, 3D microfluidic coculture model of bone remodeling is presented. A bone-on-a-chip coculture system was developed in which human mesenchymal stromal cells differentiated into the osteoblastic lineage and self-assembled into scaffold free bone-like tissues with the shape and dimensions of human trabeculae. Human monocytes were able to attach to these tissues and to fuse into multinucleated osteoclast-like cells, establishing the coculture. Computational modeling was used to determine the fluid flow induced shear stress and strain in the formed tissue. Furthermore, a set-up was developed allowing for long-term (35 days) on-chip cell culture with benefits including continuous fluid-flow, low bubble formation risk, easy culture medium exchange inside the incubator and live cell imaging options. This on-chip coculture is a crucial advance towards developing *in vitro* bone remodeling models to facilitate drug testing.

5.1 Introduction

Bone is a dynamic tissue with multiple functions, i.e. allowing for movement, protecting organs, and storing essential minerals. Healthy bone is constantly maintained by the process of bone remodeling in which bone tissue is resorbed by osteoclasts and formed by osteoblasts. This process is regulated by osteocytes. Under homeostatic circumstances, the amount of bone matrix that is resorbed is equal to the amount that is formed, and thus bone mass is maintained.¹⁷⁹

In pathologies such as osteoporosis, the balance between formation and resorption is disturbed, leading to changes in the mechanical properties of the bone and their risk for failure. To study bone pathologies, animal models are often used. However, animal models are costly, time-consuming and ethically undesirable.³ Furthermore, data from animals frequently fail to predict the results obtained in human clinical trials.^{3,4} In search for alternatives to animal models, human *in vitro* models are emerging as they address the principle of reduction, refinement, and replacement of animal experiments (3Rs).¹⁴

Organ-on-chip devices represent one of the recent successes in the search for *in vitro* human models that can recapitulate organ-level and even organism-level functions.³ These organ-on-chip devices promise several advantages over traditional techniques such as integration of structural and dynamic cues, small amount of cells, samples and reagents leading to decreased costs and options for parallel and real-time analysis. Many successful studies have been published, showing the potential of organ-on-chip technologies.^{16,180} However, there are still challenges that need to be overcome.

One of the most important challenges is the formation of air bubbles within the device.¹⁸¹ Air bubbles can get trapped in the chip and thereby disturb its performance. When air bubbles flow over cells in culture, cell membranes damage can be caused due to dynamic air-liquid interfaces. This can result in cell death when the surface tension of these interfaces is high enough to rupture the cell membrane.¹⁸¹ In addition, bubbles can cause blockage of culture medium perfusion. This blockage could lead to pressure build-up that disturbs the stability of the system, can cause device failure and sudden mechanical stimulation of the cells.¹⁸²

Next to the bubble formation, the practical handling of the system may be challenging. Microfluidic technology often promises scale-up possibilities, but in practice this can be difficult to achieve.^{183,184} Setting up the cell culture, connecting the tubing, pumps and chips is usually a manual and complex task, limiting the number of samples that can be processed at the same time. In addition, researchers in the field advocate standardization.^{184,185} It is important that the design of the systems is intuitive and straightforward, while still enabling reliable and robust operation.

In this study, both bubble formation and ease-of-use were tackled by designing a practical experimental set-up for long-term (35 days) on-chip culture. The design requirements were: easy transportation between safety cabinet and incubator, short tubing length between medium reservoir and chip to reduce bubble formation risk, addition of live cell imaging,

quick culture medium exchange inside the incubator to reduce contamination risk and possibility to remove chips at different timepoints. In a second step, the set-up was used for running long-term (35 days) bone-remodeling-on-a-chip experiments.

Both osteoblasts and osteoclasts are essential to establish an *in vitro* bone remodeling model, as their interplay is important in the remodeling process.⁷ As scaffold integration into a microfluidic device can be challenging,¹⁸⁶ we relied on the cells' own matrix production and mineralization. In the present study, human mesenchymal stromal cells (MSCs) were differentiated on-chip into osteoblasts that produced their own mineralized extracellular matrix and self-assembled into three-dimensional (3D) bone tissues. Next, human monocytes (MCs) were added and differentiated on-chip into osteoclasts, establishing a direct osteoblast-osteoclast coculture. Computational modeling was used to determine the fluid flow induced shear stress and strain in the formed tissue.

5.2 Materials and Methods

5.2.1 General experimental set-up

The general approach and timeline for the bone-remodeling-on-a-chip included several steps (Figure 5.1). The materials and methods of each step are elaborately explained in the corresponding sections. Briefly, photolithography was employed as a fabrication method to create a silicon wafer mold, followed by soft lithography to create a polydimethylsiloxane (PDMS) layer in which the cell culture channels were located. The PDMS layer was bonded to a glass coverslip to complete the device. Before starting culturing cells in the device, the channels were coated with fibronectin to enhance cell adhesion. After the MSCs were well attached, osteogenic monoculture medium was perfused through the channels and culturing was continued for 21 days to allow for bone-like tissue formation. Next, MCs were added, and the medium was switched to coculture medium which was perfused through the channels for an additional 14 days.

5.2.2 Master mold fabrication and validation

A master mold for the patterned PDMS layer was produced with a silicon wafer by photolithography. The design of the photomask was drawn in AutoCAD (version 2021, Autodesk) and ordered at CAD/Art Services (Bandon, USA). First, a layer of negative photoresist (SU-8 2150, MicroChem, Newton, MA, USA) was spin-coated on top of a silicon wafer (\varnothing 100 mm, Si-Mat). To ensure a thickness of 200 μm , the spin-coater (model WS-650MZ-23NPPB, Laurell, North Wales, USA) was set to a rotating speed of 2000 rpm for 30 seconds. The wafer was soft-baked, and the photomask was placed on top of the wafer, followed by UV-light (model UV-EXP150S-SYS, Idonus, Hauterive, Switzerland) exposure with a dose of 315 mJ/cm^2 , initiating SU-8 crosslinking of the exposed parts of the photoresist. A post exposure bake was done to complete the crosslinking process, followed by submerging the wafer into a developer solution (mr-Dev 600, Micro Resist Technology GmbH, Berlin, Germany) for 15 to 18 minutes to remove uncured photoresist. Subsequently, hard baking was performed to stabilize the printed pattern. The height of the channel dimensions was validated using a Mitutoyo Mu-Checker electronic comparator (model M402 519-402, Mitutoyo America Corporation, Aurora, USA). Finally, the master mold was silanized using

1H,1H,2H,2H-perfluorooctyltriethoxysilane (Fluorochem Ltd, Hadfield, UK) under vacuum overnight.

Experimental set-up

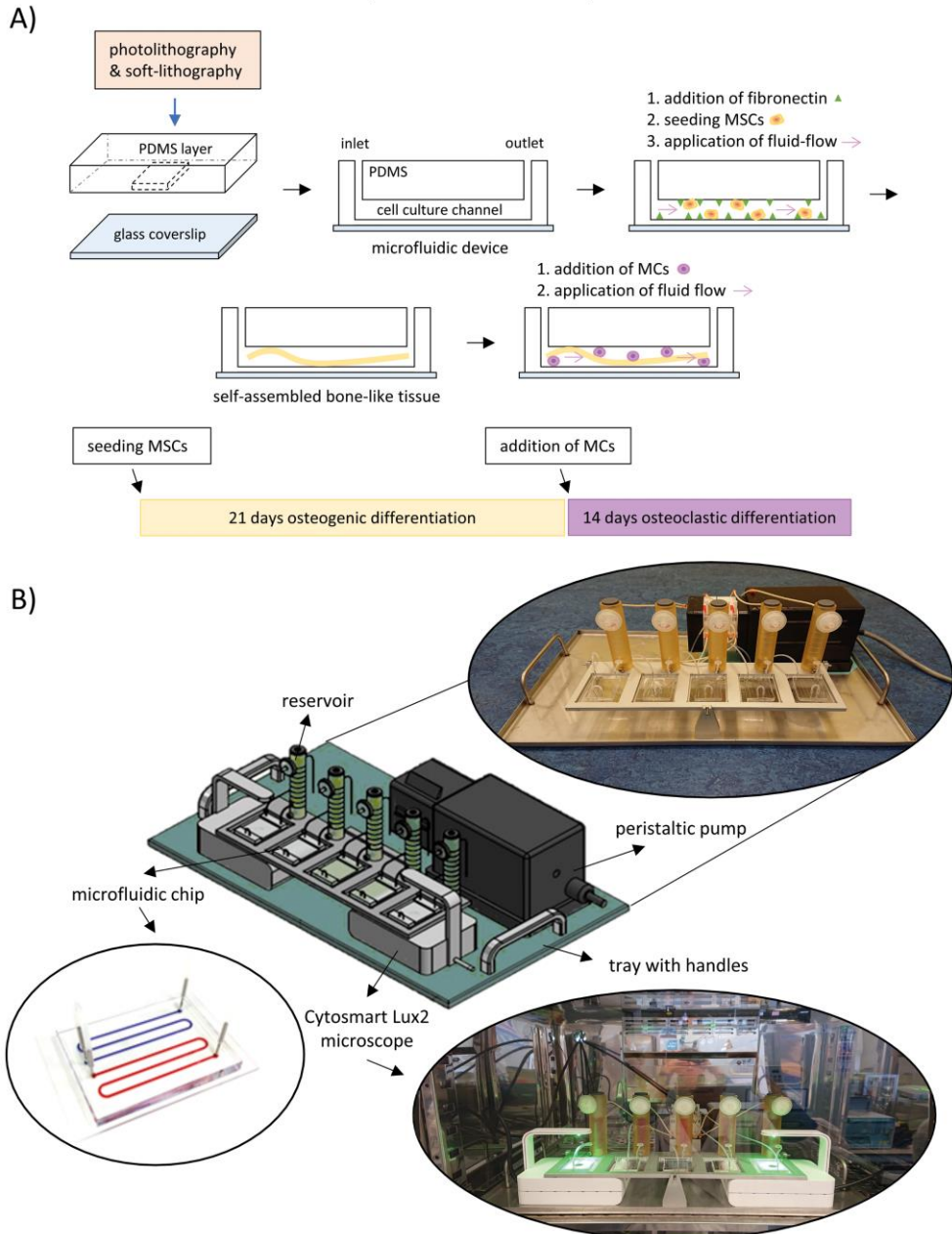


Figure 5.1 Outline of the experimental set-up. A) With the use of photo- and soft-lithography a PDMS microfluidic chip is created. The cell culture channel is coated with fibronectin 24 hours prior to seeding the MSCs. After 4 hours of attachment, culture medium fluid flow is applied for 21 days. The cells self-assemble into a bone-like tissue. After 21

days, MCs are seeded onto these tissues and allowed to attach for 24 hours. Next, fluid flow is applied, and the MCs are differentiated towards the osteoclastic lineage over an additional 14 days. B) The custom-made set-up comprises of a tray with handles on which a rack is fixed that holds five microfluidic chips and reservoirs. The peristaltic pump is placed behind this rack and Cytosmart Lux2 incubator microscopes are placed directly under two of the five chips.

5.2.3 Microfluidic chip fabrication

The microfluidic chips consisted of a PDMS part and a PDMS-coated glass coverslip and were made by standard soft lithography. The PDMS part contained two separate meandering channels with each a dimension of 200 μm height \times 800 μm width \times 134 mm length. PDMS base and curing agent (Sylgard 184 silicone elastomer kit, Dow Corning, Midland, MI, USA) were thoroughly mixed at a 10:1 ratio (w/w), degassed under vacuum, and poured onto the wafer mold. After curing the PDMS overnight at 65°C, the patterned PDMS layer containing the channels was released from the master mold. A glass coverslip with a size of 35 \times 64 mm and thickness of 0.17 mm was used to close off the microfluidic channels. To make sure the cells were exposed to the same substrate stiffness on the bottom surface as on the other walls of the channel, the coverslip was spin-coated with a thin layer of PDMS of approximately 130 μm in thickness. Rectangular PDMS pieces of 4 mm height \times 35 mm width \times 10 mm length were bonded at both ends of the PDMS chip to increase friction with the in- and outlet needles. Holes for the in- and outlets were punched with a \varnothing 1.2 mm biopsy punch (Harris Uni-Core, No. 7093508). To attach the rectangular pieces to the patterned PDMS layer, 20 watt oxygen plasma was applied for 30 seconds using the plasma asher (model K1050X, Emitech, Quorum technologies, UK). Next, the coverslip was plasma bonded to the PDMS chip. The microfluidic device was completed by baking it in an oven at 65°C for 2 hours.

5.2.4 Design and fabrication of the perfusion set-up

The set-up was designed and fabricated in-house according to requirements that were set to enable long-term on chip cell culture (Figure 5.1B). These requirements included: easy transportation between safety cabinet and incubator, short tubing length between reservoir and chip, addition of live cell imaging devices, easy culture medium exchange and possibility to collect chips at different timepoints. The set-up was designed in Autodesk Inventor 2022 (detailed drawing in Supplementary Information Figure S5.1). The base plate was made of stainless steel and functioned as carry tray. The chip holder was made of aluminum and received anodizing surface treatment to make them more chemically resistant. The reservoirs were made of polysulfone and contained grooves that indicated the medium volume in mL. Each reservoir could hold up to 8 mL of liquid.

5.2.5 Assembly of the set-up and preparation of the microfluidic chips for cell culture

A closed perfusion-based set-up was constructed (Figure 5.1B). The set-up composed of a peristaltic pump (model P-70, Harvard Apparatus, Holliston, USA) and five in-house made polysulfone medium reservoirs. Each reservoir was connected to a sterile syringe filter (syringe filter 0.2 μm , CA, Sartorius) for air exchange and was closed off with a self-healing rubber injection port (\varnothing 13 mm rubber bottle stoppers, SUCOHANS). Pump tubing (Ismatec pump tubing, 3-stop, PharMed BPT, 0.5 mm ID, yellow/orange) and silicon tubing (Ibidi GmbH, 0.5 mm ID) were connected to each other via metal tubes (Techcon, TE720050PK, 20G, 12.7 mm) and to the medium reservoirs via male luer connectors (Ibidi GmbH). Prior to assembling the set-up, the reservoirs and self-healing injection ports were sterilized with 70%

ethanol and flushed with distilled water, and if possible, subsequently autoclaved. One day prior to cell seeding, the set-up was assembled, the reservoirs were filled with 6 mL sterile phosphate buffered saline (PBS). The pump was set at a speed of 100 $\mu\text{L}/\text{min}$ to equilibrate the tubing and remove bubbles overnight. The set-up was placed in the incubator (37°C and 5% CO_2). The microfluidic chips were sterilized with 70% ethanol and flushed 3 times with sterile PBS. Next, the chips were coated with fibronectin (Human Plasma Fibronectin Purified Protein, Merck, Schiphol-Rijk, The Netherlands) in sterile PBS (100 $\mu\text{g}/\text{mL}$) and placed overnight in the incubator (37°C and 5% CO_2). At the day of cell seeding, the PBS was removed from the reservoirs, and they were filled with 6 mL cell culture medium each. The pump was set at a speed of 100 $\mu\text{L}/\text{min}$ for at least 4 hours before connecting the cell seeded microfluidic chips to remove bubbles. The chips were flushed with sterile PBS three times and filled with cell culture medium prior to cell seeding.

5.2.6 Monoculture: isolation, expansion and cultivation of MSCs

MSC isolation and characterization from human bone marrow (Lonza, Walkersville, MD, USA) was performed as previously described.¹⁶² MSCs were frozen at passage 3 with 1.25×10^6 cells/ml in freezing medium containing fetal bovine serum (FBS BCBV7611, Sigma-Aldrich) with 10% dimethylsulfoxide (DMSO, 1.02952.1000, VWR, Radnor, PA, USA) and stored in liquid nitrogen until use. Before experiments, MSCs were thawed and seeded at a density of 2.5×10^3 cells/ cm^2 in expansion medium containing DMEM (high glucose, 41966, Thermo Fisher Scientific), 10% FBS (BCBV7611, Sigma Aldrich), 1% Antibiotic Antimycotic (anti-anti, 15240, Thermo Fisher Scientific), 1% Non-Essential Amino Acids (11140, Thermo Fisher Scientific), and 1 ng/mL basic fibroblastic growth factor (bFGF, 100-18B, PeproTech, London, UK) at 37°C and 5% CO_2 . Upon 80% confluence, cells were detached using 0.25% trypsin-EDTA (25200, Thermo Fisher Scientific) and directly used for experiments at passage 4. Cells were resuspended at 1×10^6 cells/mL in osteogenic monoculture medium containing DMEM (low glucose, 22320, Thermo Scientific), 10% human platelet lysate¹⁵⁸ (hPL, PE20612, PL BioScience, Aachen, Germany), 1% Anti-Anti, 0.1 μM dexamethasone (D4902, Sigma-Aldrich), 50 $\mu\text{g}/\text{mL}$ ascorbic acid-2-phosphate (A8960, Sigma-Aldrich), 10 mM β -glycerophosphate (G9422, Sigma-Aldrich) and carefully pipetted into the channels of the chips. Each meandering channel contained $\sim 25 \mu\text{L}$ cell suspension and each chip had two meandering channels giving ~ 50.000 cells per chip. Next, the seeded chips were incubated at 37°C and 5% CO_2 for at least 4 hours before the pump was started to allow for cell attachment. Then the pump was set at a speed of 1 $\mu\text{L}/\text{min}$ and the chips remained in the incubator for 21 days. Medium was refreshed weekly by removing 3 mL of the total 6 mL and replacing it by 3 mL fresh osteogenic medium with double the concentration of dexamethasone, ascorbic acid and β -glycerophosphate. Medium refreshment took place inside the incubator via the self-healing injection ports.

5.2.7 Coculture: isolation of MCs and cultivation of MSCs and MCs

Human peripheral blood buffy coats from healthy volunteers under informed consent were obtained from the local blood donation center (agreement NVT0320.03, Sanquin, Eindhoven, the Netherlands). The buffy coats (~ 50 mL) were diluted to 200 mL in 0.6 % (w/v) sodium citrate in PBS adjusted to pH 7.2 at 4°C (citrate-PBS), after which the peripheral mononuclear

cell fraction was isolated by carefully layering 25 mL diluted buffy coat onto 13 mL Lymphoprep (07851, StemCell technologies, Cologne, Germany) in separate 50 mL centrifugal tubes, and centrifuging for 20 min with lowest brake and acceleration at $800\times g$ at room temperature. Human peripheral blood mononuclear cells (PBMCs) were collected, resuspended in citrate-PBS and washed 4 times in citrate-PBS supplemented with 0.01% bovine serum albumin (BSA, 10735086001, Sigma-Aldrich, Zwijndrecht, The Netherlands) to remove all Lymphoprep. PBMCs were frozen in freezing medium containing RPMI-1640 (RPMI, A10491, Thermo Fisher Scientific), 20% FBS (BCBV7611, Sigma-Aldrich) and 10% DMSO and stored in liquid nitrogen until further use. Prior to experiments, MCs were isolated from PBMCs using manual magnetic activated cell separation (MACS). PBMCs were thawed, collected in medium containing RPMI, 10% FBS (BCBV7611, Sigma-Aldrich) and 1% penicillin-streptomycin (p/s, 15070063, Thermo Fisher Scientific), and after centrifugation resuspended in isolation buffer (0.5% w/v BSA in 2mM EDTA-PBS). The Pan Monocyte Isolation Kit (130-096-537, Miltenyi Biotec, Leiden, The Netherlands) and LS columns (130-042-401, Miltenyi Biotec) were used according to the manufacturer's protocol. After magnetic separation, the cells were directly resuspended in osteogenic coculture medium containing α MEM (41061, Thermo Fisher Scientific), 5% hPL, 1% Anti-Anti supplemented with 0.1 μ M dexamethasone, 50 μ g/mL ascorbic acid-2-phosphate, 10 mM β -glycerophosphate) spiked with 50 ng/mL macrophage colony stimulating factor (M-CSF, 300-25, PeproTech). After 21 days of culturing the MSCs, the MCs were added to establish the coculture. To seed the MCs into the chips, the entire set-up was placed in a safety cabinet and the tubing was carefully removed from the chips. The MCs were counted, and a suspension of 5×10^6 cells/mL was carefully pipetted into the chips. Again, each meandering channel contained ~ 25 μ L cell suspension and each chip had two meandering channels giving ~ 250.000 cells per chip. The monoculture medium was completely removed from the reservoirs and tubing and replaced with coculture medium. The chips were reconnected, and the setup was placed back into the incubator where cells were allowed to attach for 24 hours before the fluid flow was run again at 1 μ L/min. After 2 days the coculture medium was replaced by coculture medium additionally containing 50 ng/mL receptor activator of NF κ -B ligand (RANKL, 310-01, PeproTech). Medium was changed weekly inside the incubator via the self-healing injection ports by removing 3 mL of the total 6 mL and replacing it by 3 mL fresh coculture medium with double the concentration of dexamethasone, ascorbic acid, β -glycerophosphate, M-CSF and RANKL. The culture was maintained for another 14 days, making a total of 35 days.

5.2.8 Brightfield time-lapse imaging

Brightfield images of the channels in the chip were taken to monitor cell morphology and assembly over time. One channel per chip and two chips per experiment were observed at 10x magnification with Lux2 microscopes (CytoSMART, Eindhoven, The Netherlands). Images were taken every three hours for the entire 35 days of culture.

5.2.9 Computational model for mechanical stimulation calculation

To quantify the mechanical stimulation in terms of fluid-induced wall shear stress and elastic strain on the cells, computational fluid dynamics (CFD) and fluid solid interaction (FSI)

models were used (Figure 2). Based on experimental observation, the cells are flatly attached to the bottom of the microfluidic channel at day 0, while at day 21, the cells have detached from the bottom and have formed into a long 3D bone-like tissue. It was observed that the tissue occupied approximately 1/3 of the microfluidic channel width (i.e., $1/3 \times 800 \mu\text{m} \approx 267 \mu\text{m}$), and the height was approximately $180 \mu\text{m}$. The computational model was based on these experimental observations. In the model, the tissue geometry was idealized into an elliptical cylinder. As the tissue orientation could be either along or across the microfluidic channel at day 21, these two orientations were proposed (Figure 2B), and the tissue geometries were constructed in ANSYS DesignModeler (ANSYS Inc., Pennsylvania, USA). In the computational model, a representative volume of the channel ($200 \mu\text{m H} \times 800 \mu\text{m W} \times 800 \mu\text{m L}$) was modelled (Figure 5.2).

For calculating the shear stress on cells at day 0, when the thin cell sheet was flatly attached on the channel bottom, the computational model was based on an empty channel by assuming that the shear stress on the channel bottom was equivalent to that on the cells. The calculation was based on the CFD model that follows the Navier-Stokes equation for incompressible flow:

$$\rho \left\{ \frac{\partial \mathbf{v}}{\partial t} + \rho \mathbf{v} \cdot \nabla \mathbf{v} = -\nabla p + \mu \nabla^2 \mathbf{v} \right. \quad (1)$$

where, ρ and μ are medium density and dynamic viscosity, respectively ($\mu = 0.93 \text{ mPa}\cdot\text{s}$, $\rho = 1009 \text{ kg/m}^3$)¹⁶⁹; \mathbf{v} is fluid velocity vector, p is pressure.

According to the pre-computation by ANSYS-CFX, the maximum Reynolds number was lower than 1. Therefore, the flow was defined as laminar flow. A flow rate of $1.0 \mu\text{L}/\text{min}$ used in experiment was prescribed at the inlet and outlet, respectively for mass conservation (Figure 2B). The channel walls were defined as non-slip boundaries (i.e., the fluid has zero velocity relative to the solid surfaces). The fluid domain was meshed by tetrahedral elements (global element size = $10 \mu\text{m}$) with a patch conforming algorithm as described in Zhao *et al.* (2020).¹⁸⁷ Moreover, the mesh for the cell/tissue region was refined with an element size of $4 \mu\text{m}$, which generated 1,255,967 elements in total. The CFD model was solved using finite volume (FV) method by ANSYS CFX solver under the convergence criteria of root mean square (RMS) residual of momentum and mass $< 1.0 \times 10^{-4}$.

For calculating the fluid-induced wall shear stress on cells at the surface and internal strain of the bone-like tissue at day 21, a FSI model was used. The fluid domain was meshed with the same strategy as above, which generated 1,203,992 tetrahedral elements. The solid domain (bone-like tissue) was modelled as a hyperelastic (Neo-Hookean) material with the strain density function as equation (2), and solved by finite element (FE) method in ANSYS:

$$W = C_1(\bar{I}_1 - 3) + \frac{1}{D_1}(\det(\mathbf{F}) - 1)^2 \quad (2)$$

where W and \mathbf{F} are the strain energy density and deformation gradient, respectively; \bar{I}_1 is the first invariant of the right Cauchy-Green deformation tensor, which is calculated as:

$$\bar{I}_1 = (\det(\mathbf{F}) - 1)^{-2/3} \bar{I}_1 = (\lambda_1 \lambda_2 \lambda_3)^{-2/3} (\lambda_1^2 + \lambda_2^2 + \lambda_3^2) \quad (3)$$

where λ_1 , λ_2 and λ_3 are the principal stretches.

In equation (2), C_1 and D_1 are material constants, which were calculated using shear modulus (G) and bulk modulus (K):

$$C_1 = \frac{G}{2} = \frac{E}{4(1+\nu)} \quad (4)$$

$$D_1 = \frac{2}{K} = \frac{6(1-2\nu)}{E} \quad (5)$$

where G , E and K are shear modulus, Young's modulus and bulk modulus, respectively; ν is the Poisson's ratio. The bone-like tissue (mixture of bone cells and extracellular matrix) was defined as an almost incompressible material with a Young's modulus E of 1.70 kPa and Poisson's ratio ν of 0.49, according to the experimental measurements in Taiai *et al.* (2005) and Titushkin and Cho (2007).^{188,189} So, the material parameters can be calculated as: $G = 0.57$ kPa, $K = 28.33$ kPa, $C_1 = 0.29$ kPa, $D_1 = 7.00 \times 10^{-5}$ Pa⁻¹.

In terms of boundary conditions of the FE model, one end of tissue was fixed, and the other end was defined as frictionless support (Figure 5.2B). The tissue surfaces formed the fluid-solid interface between the CFD and FE domains and this two-way FSI analysis followed a staggered iteration approach, which coupled the fluid force and solid deformation as described in Zhao *et al.* (2020).¹⁸⁷

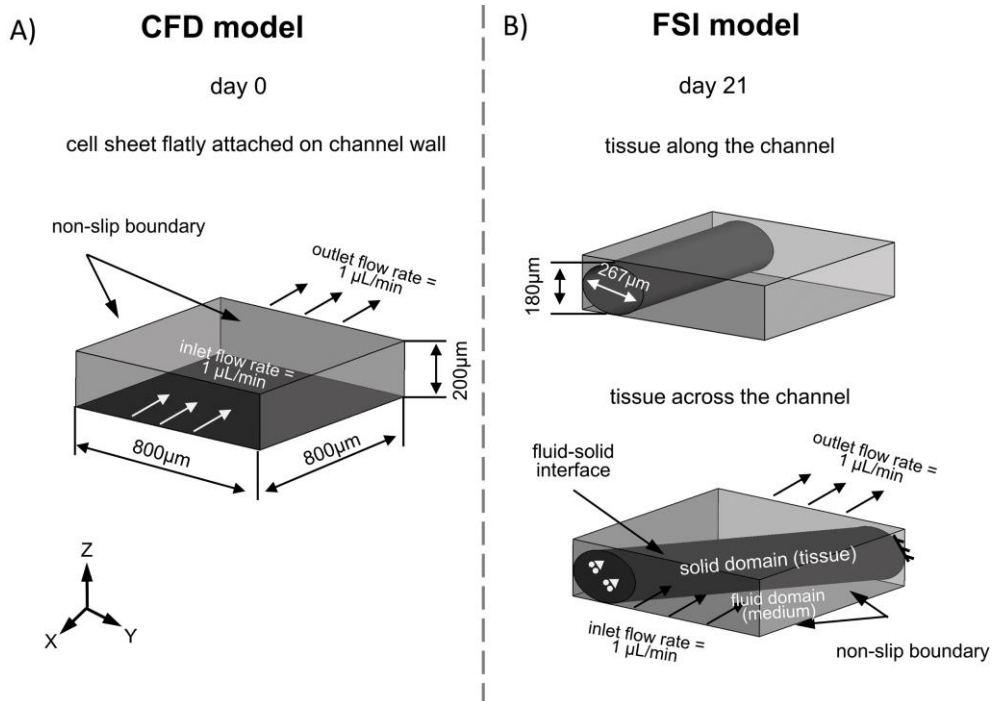


Figure 5.2 Determination of fluid shear stress. A) CFD model geometry and boundary conditions for calculating the shear stress on flat cell sheet at day 0. B) FSI model geometries and boundary conditions for calculating the shear stress on cells exposed to the medium and inside tissue at day 21.

5.2.10 Immunohistochemistry

At day 14, 21 and 35 chips were washed with PBS and fixed in 10% neutral-buffered formalin for 15 min. The chips were immunostained by washing with PBS-tween, permeabilizing in 0.5% Triton X-100 in PBS for 10 min and blocking in 10% normal goat serum in PBS for 30 min. Cells were incubated with DAPI, Phalloidin and immunostainings (Table 5.1) in PBS for 1 hour. Images were taken with either a fluorescent light microscope (Axio Observer 7, Zeiss, Oberkochen, Germany) (Figure 5.3B and 5.5A and B) or a confocal microscope (TCS SP5X, Leica Microsystems CMS GmbH, Mannheim, Germany) (Figure 5.5C).

Table 5.1 List of all dyes and antibodies used and their working concentrations/dilutions.

Antigen	Source	Catalogue No	Label	Species	Concentration/Dilution
DAPI	Sigma-Aldrich	D9542			0.1 µg/mL
Atto 647 conjugated Phalloidin	Sigma-Aldrich	65906			50 pmol
Collagen type-1	Abcam	Ab34710		Rabbit	1:200
RUNX-2	Abcam	Ab23981		Rabbit	1:500
Osteopontin	Thermo Fisher	14-9096-82		Mouse	1:200
TRAP	Abcam	Ab185716			1:200
Anti-rabbit (H+L)	Molecular Probes	A11008	Alexa 488	Goat	1:200
Anti-mouse IgG1 (H+L)	Molecular Probes	A21127	Alexa 555	Goat	1:200

5.2.11 Histology

Following the immunostaining the same samples of day 14 and 21 were overstained with Alizarin Red (2% in distilled water, A5533, Sigma-Aldrich) for 15 minutes to identify mineralization. Subsequently, channels were washed with distilled water until no further discoloration of the water occurred. Images were made using a brightfield microscope (Axio Observer Z1, Zeiss, Oberkochen, Germany).

5.2.12 Quantification of Ca²⁺ concentration in supernatant

The calcium concentration from the supernatant was measured to determine changes in calcium concentration in the medium, as an indicator for mineralized matrix deposition/resorption during osteogenic differentiation. A calcium assay (Stanbio, 0150-250, Block Scientific, Bellport, NY, USA) was performed according to the manufacturer's instructions (n=10). Briefly, 95 µl Cresolphthalein complexone reaction mixture was added to 5 µL sample and incubated at room temperature for 1 min. Absorbance was measured at 550 nm with a plate reader and absorbance values were converted to calcium concentrations using standard curve absorbance values.

5.2.13 Quantification of human pro-collagen 1 C-terminal propeptide

Human pro-collagen 1 C-terminal propeptide (PICP) as a product of collagen formation was quantified in cell supernatants of monocultured constructs at day 7, 14 and 21 using an enzyme-linked immunosorbent assay (ELISA, MBS2502579, MyBioSource, San Diego, CA, USA) according to the manufacturer's protocol ($n=2 \times 5$: two independent experiments with each 5 chips). 100 μL sample/standard was added to anti-human PICP coated microwells. After 90 min incubation at 37°C, samples were removed and replaced by 100 μL biotinylated antibody solution followed by 60 min incubation at 37°C. After thorough washing, 100 μL HRP-conjugate solution was added, and plates were incubated for 30 min at 37°C. Wells were again washed, and 90 μL substrate reagent was added followed by 15 min incubation in the dark at 37°C. To stop the reaction, 50 μL stop solution was added and absorbance was measured at 450 nm in a plate reader. Absorbance values were converted to PICP concentrations using standard curve absorbance values.

5.2.14 Gene expression by qPCR

To quantify gene expression levels, day 0 MSCs were pelleted by centrifuging 50.000 cells/pellet (230 rpm, 7 minutes), which is the same amount of cells as in the chips. Pellets were frozen and stored at -80°C. After 21 days of culturing in the chip, the self-assembled tissues were carefully taken out of the chips and also frozen and stored at -80°C. Frozen samples were crushed using a pestle to homogenize the samples, and subsequently lysed on ice using RLT lysis buffer. RNA was isolated using the Qiagen RNeasy kit (Qiagen, Hilden, Germany) following supplier instructions including a 15 minutes DNase incubation step (Qiagen; 74106) to remove genomic DNA contamination. After extraction, RNA quantity and purity were assessed with a spectrophotometer (NanoDrop™ One, Isogen Life Science, The Netherlands). cDNA was synthesized in a thermal cycler (protocol: 65°C (5 min), on ice (2 min) while adding the enzyme mixture, 37°C (2 min), 25°C (10 min), 37°C (50 min), and 70°C (15 min)) starting from a 20 μL reaction solution containing 200 ng of RNA, 1 μL dNTPs (10 mM, Invitrogen), 1 μL random primers (50 ng/ μL , Promega, C1181), 2 μL 0.1 M DTT, 4 μL 5x first strand buffer, 1 μL M-MLV Reverse Transcriptase (RT) (200 U/ μL , Invitrogen, 28025-013, Breda, the Netherlands) and supplemented with RNase-free ultra-pure water (ddH₂O). Genomic DNA contamination was checked with glyceraldehydes-3-phosphate dehydrogenase (GAPDH) primers, conventional PCR, and gel electrophoresis.

qPCR was executed to investigate the expression of genes related to osteogenic differentiation: COL-1, RUNX-2 and SPP1 (osteopontin), utilizing the primer sequences listed in Supplementary Information Table S1. Six reference genes were tested of which the two most stable ones were used (ATP5F1B and TOP1). Expression was investigated by adding 500 nM primer mix, 5 μL SYBR Green Supermix (Bio-Rad; 170-8886), and an additional 1.75 μL ddH₂O to 3 μL of diluted cDNA. C_t values were acquired by exposing the mixtures to the following thermal protocol: 95°C (3 min), 40 cycles of 95°C (20 s), 60°C (20 s), and 72°C (30 s), 95°C (1 min), and 65°C (1 min), concluded with a melting curve measurement. Differences in expression profiles were determined by normalizing the C_t values for the reference gene (only ATP5F1B shown, similar results to TOP1) (ΔC_t), correcting these values for the C_t value

of the control (day 0) ($\Delta\Delta C_t$) and applying the $2^{-\Delta\Delta C_t}$ formula to determine the fold changes in expression.

5.2.15 Quantification of tartrate-resistant acid phosphatase activity in the supernatant

Tartrate-resistant acid phosphatase (TRAP) concentration from the supernatant of the coculture was measured at day 23, 28 and 35 to determine the amount of secreted TRAP during osteoclastic differentiation (n=2+3: two independent experiments, one with 2 and one with 3 chips). 10 μ L of supernatant was placed in a 96-well plate and resuspended in 90 μ L assay buffer containing 3M NaAc, 10% Triton X-100, 1 mg/mL p-nitrophenyl phosphate (pNPP, Sigma Aldrich, 71768) (pH=5.5). Samples were incubated for 1.5 hours at 37°C. Finally, 100 μ L 0.3M NaOH solution was added to stop the reaction. The amount of TRAP was determined via the optical absorbance at 405 nm and absorbance values were converted to TRAP activity using standard curve absorbance values.

5.2.16 Quantification of human crosslinked C-telopeptide of collagen type 1

Human crosslinked C-telopeptide of collagen type 1 (CTX) as a collagen degradation product was quantified in cell supernatants of cocultured constructs at day 23, 28 and 35 using an ELISA (MBS162789, MyBioSource, San Diego, CA, USA) according to the manufacturer's protocol (n=2+3: two independent experiments, one with 2 and one with 3 chips). 50 μ L standard and 40 μ L sample were separately added to anti-human CTX coated microwells. 10 μ L Anti-CTX antibody was added to each sample well and 50 μ L streptavidin-HRP was added to all sample and standard wells and incubated for 60 min at 37°C. After thorough washing, 50 μ L substrate reagent A and 50 μ L substrate reagent B were added, followed by 10 min incubation in the dark at 37°C. To stop the reaction, 50 μ L stop solution was added and absorbance was measured at 450 nm in a plate reader. Absorbance values were converted to CTX concentrations using standard curve absorbance values.

5.2.17 Statistical analysis

Statistical analyses were performed, and graphs were prepared in GraphPad Prism (version 9.4.0, GraphPad, La Jolla, CA, USA) and R (version 4.0.2). Data was tested for normal distribution with Shapiro-Wilk tests. All data was normally distributed. One-way repeated measures ANOVA was performed for PICP, calcium, TRAP and CTX to compare consecutive timepoints. Post-hoc Tukey was applied to correct for multiple comparisons. qPCR data was tested for equal variances using Levene's test. As variances were not equal, Welch's t-test was performed for qPCR data to compare day 0 to day 21. All data is presented as mean plus/minus standard deviation.

5.3 Results

5.3.1 Experimental set-up enables long-term on-chip cell culture

A set-up was designed that successfully facilitated long-term (35 days) on-chip cell culture (Figure 5.1B). The set-up was quick to assemble. The carry tray with handles provided easy and safe transportation between safety cabinet and incubator. All components had a fixed position, refraining movement during transportation. The reservoir and chip were placed approximately at same height to reduce pressure difference, which has been described to prevent a distorted flow.¹⁸¹ Inside the incubator, the reservoirs were easily accessible for safe

and fast culture medium exchange through the self-healing rubber injection ports. The short tubing between reservoir and chip (2.5 cm) reduced the risk of air bubble formation, as long tubing length increases the assembly of small air bubbles into large ones. Compared to our previous set-up we were able to reduce the total tubing length by 46%, decreasing the bubble formation risk. Consequently, double the amount of cell seeded chips survived the 35-day culture period (detailed comparison with our previous set-up in Supplementary Information Table S5.2 and Figure S5.2).

5.3.2 Self-assembly of elongated 3D tissues containing of collagen type 1 and minerals

The morphology and behavior of cells was investigated using time-lapse live cell imaging (Figure 5.3A). The bright-field images showed that at day 0, the MSCs were spindle-shaped, which confirmed their attachment to the channel surfaces. At day 5, cells started to detach from the channel side walls. At day 10, cells self-assembled, thereby forming a string of connected cells in the middle part of the channel. The string compacted over time. At day 21, a dense 3D elongated construct was visible. Over the entire culture period, some cells remained attached to the channel walls to keep the formed tissue in place. This proved to be essential to withstand the shear stress created by the fluid flow. Non-attached cells and cell-assemblies were flushed out of the channels. At day 21, the self-assembled constructs were investigated for their composition. The extracellular matrix produced by the cells consisted of collagen type 1 (Figure 5.3B) and was highly mineralized as shown by Alizarin red staining (Figure 5.3C). The rate of collagen type 1 formation stayed constant over time shown by measuring PICP in the culture medium (Figure 5.3D). Collagen type 1 gene expression was significantly higher at the day 21 osteoblasts compared to day 0 MSCs (Figure 5.3E).

Quantification of calcium concentration in the cell culture supernatant showed that calcium was depleted from the supernatant during the first 21 days (Figure 5.3F). Significantly more calcium was depleted on day 14 and 21 compared to day 7. This observation together with the histological stainings implies that the produced collagenous extracellular matrix was mineralized with a calcium mineral and indicates the formation of a self-assembled 3D bone-like tissue.

5.3.3 Mechanical stimulation increased upon self-assembly of the tissues and is dependent on tissue orientation

Computational models (CFD and FSI) were used to quantify the mechanical stimulation in terms of shear stress and mechanical strain received by the cells in the chip. The fluid-induced shear stress on the monolayer of cells at day 0 was 3.66 mPa (Figure 5.4A). At day 21, the self-assembled cells on the surface received an average shear stress of 10.55 mPa and 45.30 mPa respectively for the tissue oriented along and across the channel (Figure 5.4A). Due to the deformation of the tissue under fluid flow, the cells embedded within the tissue could experience the mechanical strain. The average values of equivalent elastic strain within the tissue were 4.74×10^{-4} and 6.65×10^{-3} respectively for the tissue oriented along and across the channel (Figure 5.4B). These results show that the fluid flow shear stress on the cells both on the surface and within the tissue increased upon self-assembly and is highly dependent on the orientation of the self-assembled tissue.

Self-assembly of bone-like tissues

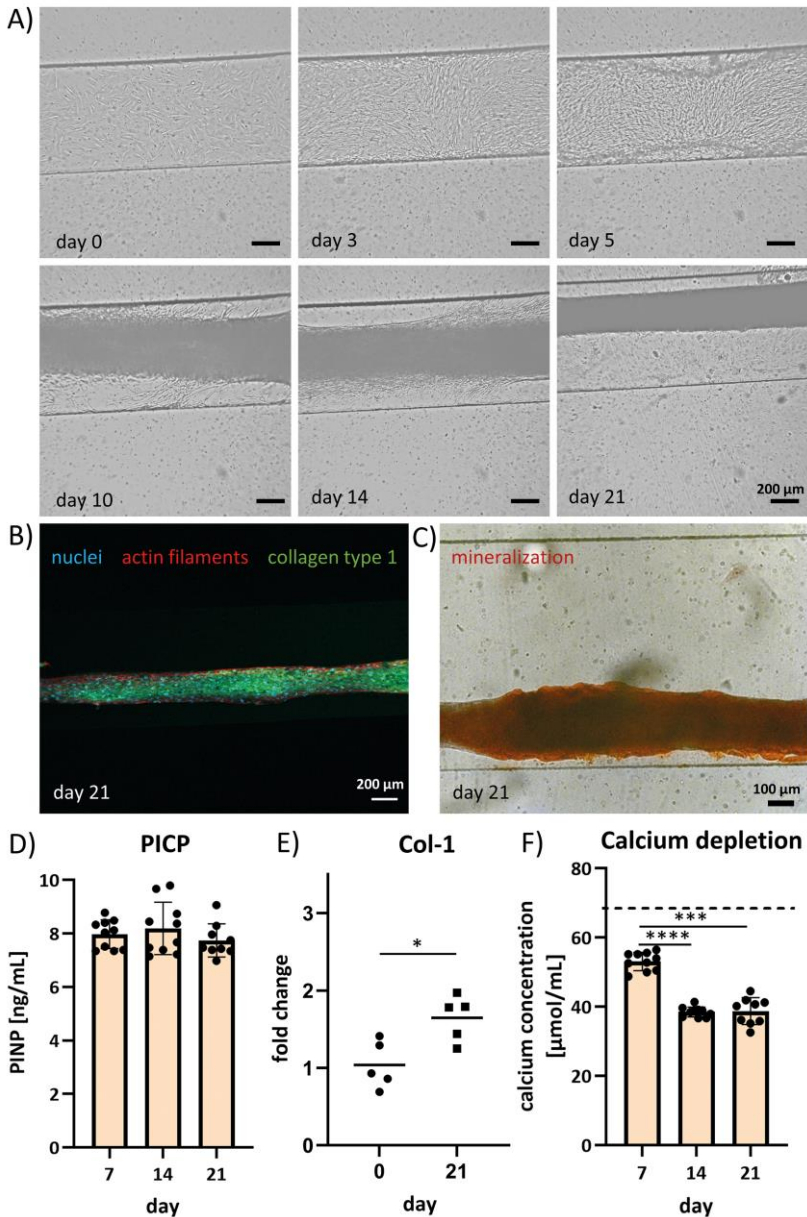


Figure 5.3 Self-assembly of 3D tissues. A) Time-lapse brightfield images of the 3D-self-assembly over time. At day 0, MSCs are seeded and attach to the channel in a monolayer. At day 3, the cells have spread over the bottom of the channel. At day 5, the cells start to detach from the channel walls. At day 10, the cells self-assemble into an elongated 3D tissue-like strut that becomes denser over the following days. B) The 3D tissue consists of collagen type 1 and C) is mineralized (Alizarin Red staining). D) PICP quantification as a measure for collagen formation (n=2x5). Differences are non-significant. E) Col-1 (n=5) gene expression measured before seeding in the chip (day 0) and after 21 days culturing in the chip (day 21). Values are displayed as $2^{\Delta\Delta Ct}$ to day 0. Significant differences are shown by * for $p < 0.05$. F) Calcium concentration in the culture medium showing calcium depletion (n=2x5). The dashed line represents the calcium concentration in fresh medium. Significant differences are shown by *** for $p < 0.001$ and **** for $p < 0.0001$.

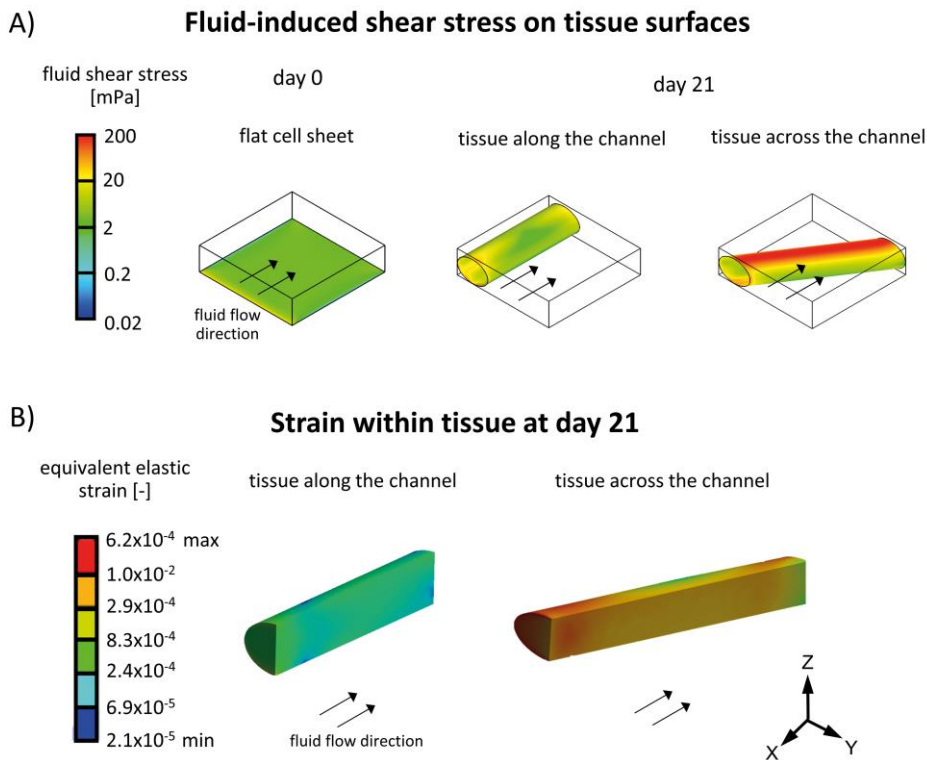


Figure 5.4 Shear stresses acting on the cells. A) Fluid-induced shear stress on cell/tissue surfaces at day 0 and 21. B) Sectional view of the strain within solid tissue (along and across the microfluidic channel) at day 21 due to the tissue deformation that is caused by fluid force.

5.3.4 Osteogenic differentiation of MSCs in a 21 day monoculture

To confirm osteoblastic differentiation of the MSCs in the first 21 days, samples were stained for RUNX-2 and osteopontin at day 14 and 21 and for DMP-1 at day 21. RUNX-2 was present in the nucleus and osteopontin in the body of the cells at day 14 and 21 (Figure 5.5A and B). DMP-1 was visible in the nucleus of the cells at day 21, indicating early signs of transition to osteocytes (Figure 5.5C). Although non-significant, RUNX-2 and osteopontin gene expression demonstrated an upward trend comparing day 21 to day 0 (Figure 5.5D and E). The immunostaining and gene expression results imply that the microfluidic chip allows for MSCs to differentiate into the osteoblastic lineage over time. It is to be noted that the density of the self-assembled 3D bone-like tissue complicated the imaging process, as the laser light was not able to penetrate through the thick matrix. Only cells on the surface of the tissues could be visualized.

Osteoblastic differentiation of MSCs

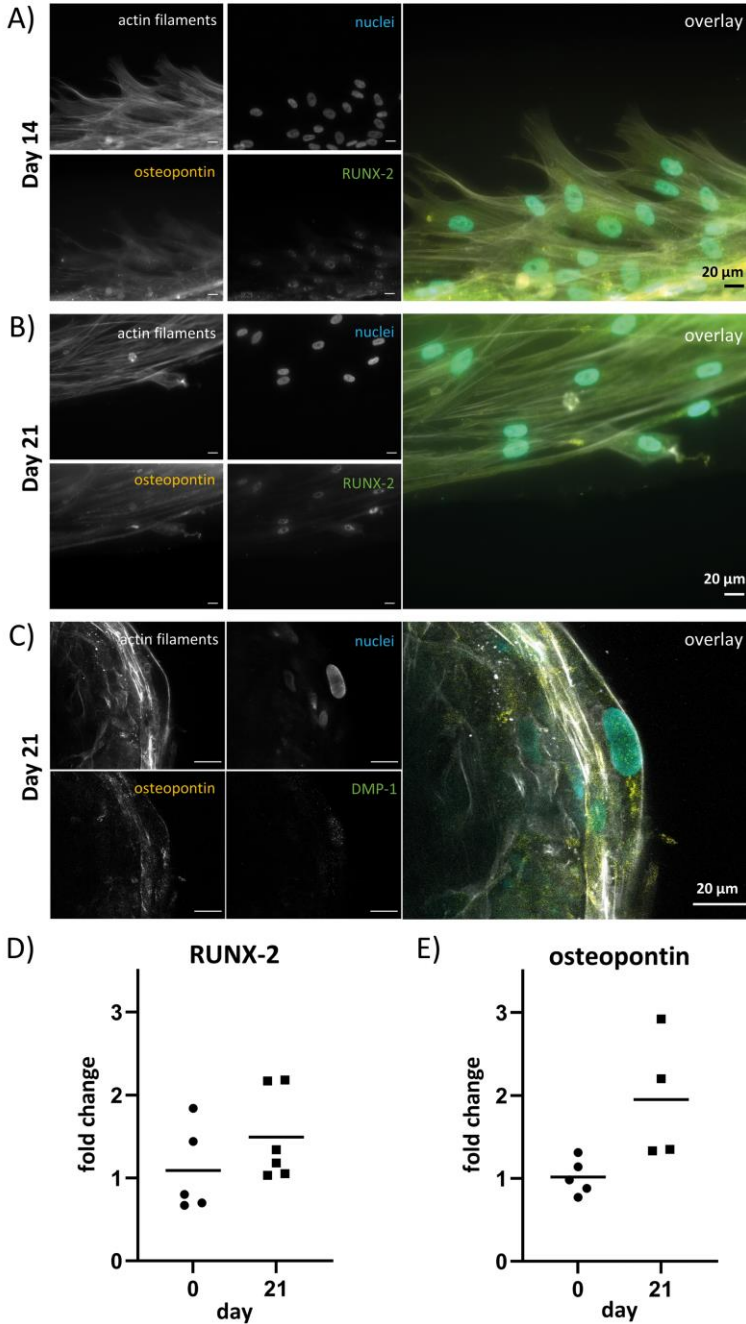


Figure 5.5 Osteogenic differentiation of MSCs: A) At day 14 and B) 21, osteopontin is expressed in the cells body and RUNX-2 in the nucleus. C) At day 21, DMP-1 expression is visible in the nucleus. All scale bars are 20 μ m. D) RUNX-2 (n=5 or 6) and E) osteopontin (n=4 or 5) gene expression measured before seeding in the chip (day 0) and after 21 days culturing in the chip (day 21). Values are displayed as $2^{\Delta\Delta Ct}$ to day 0. Differences are non-significant.

5.3.5 MCs fuse into multi-nucleated cells in 14-day coculture

After the 21-day tissue formation phase, MCs were added to the microfluidic chips and cultured for another 14 days (35 days in total). Monoculture medium was changed into coculture medium containing RANKL and M-CSF to induce osteoclastic differentiation of the MCs. At day 35, Z-stack images revealed the presence of mono- and multi-nucleated cells with different morphologies (Figure 5.6A and B). Elongated mononuclear cells with large ($\pm \text{Ø } 16 \text{ }\mu\text{m}$) oval shaped nuclei were identified as osteoblasts (Figure 5.6A, orange arrow). Round, multinucleated cells with smaller ($\pm \text{Ø } 12 \text{ }\mu\text{m}$) round nuclei were identified as fused monocytes/pre-osteoclasts (Figure 6A, purple arrow). An additional TRAP immunostaining revealed a multi-nucleated cell with a clear actin-ring and expression of TRAP in the cell body, found on the surface of the 3D bone-like tissue (Figure 5.6B). These results suggest that MCs were able to attach to the tissues upon cell seeding and could withstand the application of fluid flow within the chip. The MCs were stimulated towards the osteoclastic lineage shown by the formed multi-nucleated cells and TRAP staining.

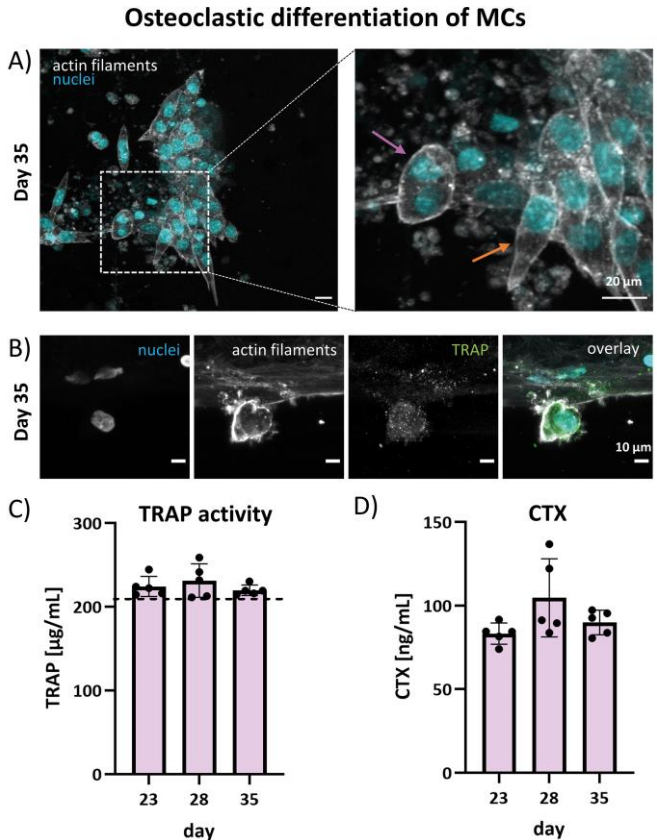


Figure 5.6 Osteoclastic differentiation of MCs within the coculture. A) At day 35, round multinucleated cells (purple arrow) and elongated mononuclear cells (orange arrow) are visible. B) On the surface of the bone-like tissue, a round, multinucleated cell is visible with a clear actin ring and TRAP expression in the cells body. This image is a maximum projection of z-stacks. C) TRAP activity (n=2+3); Dashed line represents the TRAP activity in fresh medium, containing TRAP originating from the hPL. Differences are non-significant. D) CTX quantification as a measure for collagen degradation (n=2+3). Differences are non-significant.

TRAP activity was measured in the coculture medium over time (Figure 5.6C). Differences between timepoints were non-significant. However, the TRAP activity measured in the samples showed a trend of being higher than the activity measured in fresh culture medium (Figure 5.6C, dashed line), indicating that there might be some contribution from the cells. The TRAP activity in fresh medium is most likely originating from the hPL.¹⁵⁸

By measuring CTX in the medium, collagen degradation by the cells was quantified. Collagen type 1 degradation was similar over time with non-significant differences between the timepoints (Figure 5.6D). A slight trend towards higher degradation at day 28 was seen.

5.4 Discussion

A bone-on-a-chip coculture system was developed in which human MSCs differentiated into the osteoblastic lineage and self-assembled into scaffold-free bone-like tissues with the shape and dimensions of human trabeculae (100–200 μm thick cylindrical rods).¹⁹⁰ Human MCs were able to attach to these tissues and to fuse into multinucleated osteoclast-like cells, establishing the coculture. The microfluidic chip and set-up were able to maintain the culture over a 35 day culture period. This on-chip coculture is a first step towards *in vitro* bone remodeling models for drug testing.

To date, bone-on-a-chip models have not been abundantly reported, probably because of the highly complex bone microenvironment and multicellularity.¹⁶ Coculturing osteoblasts and osteoclasts within the desired timeline is difficult given the differing differentiation timelines and cell culture medium compositions needed.^{149,183} Nonetheless, bone-on-a-chip systems have been reported for example for bone cell signaling,¹⁹¹ mechanical stimulation,¹⁹² and diseases.^{193,194} Most studies use cell lines and/or animal cells and do not incorporate a direct coculture of the different bone cells. Our specific *in vitro* bone remodeling model is fully human, having the advantage of no interspecies differences.^{195–198} We used primary cells, avoiding cell lines which are manipulated to enable continuous passaging, possibly affecting their outcomes.¹⁰

To our knowledge, only one other research group has reported a bone-on-a-chip design specifically for bone remodeling.^{10,199–201} Their lab-on-a-chip device comprises of three wells with each one of the three bone cell types. The osteoblasts (MC3T3-E1) are seeded on polystyrene discs, the osteoclasts (RAW 3264.7) are seeded on bone wafers, and osteocytes (MLO-Y4) on collagen type 1. The channels between the wells allow for exchange of conditioned medium. The chip allows for mechanical loading of the osteocytes by applying a static out of plane distention to stretch the cells.^{200,201} This platform allows for many different configurations and is planned to be used with direct cocultures and fluid flow. To date only indirect coculture and cell lines are used. While indirect cocultures allow cell-cell communication through soluble factors, the communication through their surface receptors and gap junctions is missing.¹⁴⁹ We show a direct coculture using primary cells and mechanical stimulation by fluid flow shear stress. Direct communication between osteoblasts and osteoclasts can be beneficial for the bone remodeling process as for example next to the soluble factors M-CSF and RANKL also their membrane bound variants play an important role in osteoclastogenesis.^{7,190}

Mechanical loading is a critical environmental factor during bone development and homeostasis. *In vivo*, bone shape, mass, and trabecular architecture change constantly in response to mechanical loading, a process called bone adaptation.²⁰² Shear stress and mechanical strain are both examples of mechanical loading that occurs in bone. Many types and magnitudes of shear stress and mechanical strain have been shown to have positive effects on bone cells. For example, fluid flow shear stress has been shown to enhance the osteogenic differentiation of MSCs.²⁰² A broad range of fluid flow shear stresses in microfluidic devices for bone tissue engineering has been reported from 0.01 mPa to 1.03 Pa.^{203–206} Our cells showed changes in spatial arrangement over time due to 3D self-assembly. Computational modeling provided us with insight into the associated changes in shear stress and strain. Our system falls into the reported range of fluid flow shear stresses with values of 3.66 mPa up to 45.30 mPa (Figure 5.4). The cells on the surface of the self-assembled 3D tissue are expected to feel shear stresses up to 45.30 mPa (Figure 5.4A). These cells are most likely the progenitor cells, osteoblasts, bone lining cells and osteoclasts. The embedded cells, the osteocytes, are expected to feel elastic strain up to 6.65×10^{-3} (Figure 5.4B). For comparison, during walking bones experience strains around 1×10^{-4} and *in vivo*, strain in the range of $1 \times 10^{-4} - 2 \times 10^{-3}$ is shown to be optimal for bone healing.²⁰⁷ It needs to be noted that our model used for the embedded cells, is based on a number of assumptions and did for example not take into account the hardening of the tissue when it mineralizes, which in turn might affect the load on the embedded cells. In future experiments it would be interesting to take a closer look to both the influence of tissue orientation (and thus altered mechanical stimulation) on cell differentiation and matrix production, and to the effects of mineralization on strain.

The analysis methods on chips and thus also in our chip can be challenging. At the moment, most methods are off-chip endpoint measurements, while non-destructive methods would be desired.^{7,16} Our system is still restricted in the number of samples we can generate, and the extended culture time reduces our ability to produce the desired number of samples necessary to carry out a complete analysis. Our set-up does offer the advantage of medium sampling thanks to the self-healing injection ports. In this way, assays on the culture medium can be performed at different timepoints. However, the dilution of secreted growth factors in a microfluidic chip using large media reservoirs in combination with the small amount of cells present in the chip is also a concern as it asks for sensitive assays.²⁰⁸ In the future, integration of biosensors into the chip could provide sensitive, non-invasive continuous monitoring of the experiment.¹⁶ For example, efforts in developing microfluidic based biosensing technologies for continuous and long-term measurement of glucose, lactate, pyruvate, dissolved oxygen, pH and reactive oxygen species have already been reported.²⁰⁹

In bone, the extracellular matrix produced by the cells is a very important microenvironment that is particularly essential for the differentiation of osteoblasts into osteocytes. To resemble physiological bone, the organic matrix should comprise a highly dense and aligned collagen network.⁶ Mineralization should occur inside and outside of the collagen fibrils.²¹⁰ In our system, collagen appears to orient in the fluid-flow direction (Figure 5.3B) and mineralization of the extracellular matrix was observed (Figure 5.3C). However, to ensure proper collagen

alignment and correct mineral location, advanced techniques such as transmission electron microscopy (TEM) and focused ion beam scanning electron microscopy (FIB-SEM) that allow for nanoscale sample investigation are needed.⁶ Future work is needed to elucidate the nanoscale properties of our matrix.

When the challenges of sample size and analytical methods have been overcome in the future, our bone-remodeling-on-a-chip is expected to provide a valuable platform for drug testing. In comparison to cell monocultures, direct coculture offers the opportunity to study the interaction between osteocytes, osteoblasts and osteoclasts under influence of different stimuli, such as drugs and altered mechanical loads in a 3D environment resembling bone trabeculae. We envision the potential to use both healthy donor cells and patient cells in the model to compare the effects of drugs. Furthermore, we would be able to take steps towards personalized medicine and accurately screen for the most suitable drugs for individual patients.

In conclusion, we have demonstrated a scaffold-free, fully based on primary human cells, 3D microfluidic coculture model. MSCs were differentiated on-chip into the osteoblastic lineage and self-assembled into bone-like tissues with the dimensions of human trabeculae. Next, MCs were added to these tissues and differentiated on-chip into osteoclast-like cells. Furthermore, a set-up was developed allowing for long-term (35 days) on-chip cell culture with benefits including mechanical stimulation through applied fluid-flow, low bubble formation risk, easy culture medium change inside the incubator and live-cell imaging options. This on-chip coculture is a crucial advance towards developing *in vitro* bone remodeling models to facilitate drug testing in the future.

Conflict of interest

The authors declare that the research was conducted in the absence of any commercial or financial relationships that could be construed as a potential conflict of interest.

Author contributions

MV, KI and SH contributed to conception, methodology and design of the study. MV, EB and MB performed the experiments. MV analyzed the results. FZ made and analyzed the computational model. JB, HEA, MV and MB designed the set-up. JB drew and built the set-up. MvD executed the RNA isolation, cDNA synthesis and qPCR and analyzed the gene expression results. MV wrote the original draft of the manuscript and prepared the figures. All authors contributed to manuscript revision and approved the submitted version. KI and SH contributed to the supervision. SH acquired funding for this research.

Funding

This work is part of the research program TTW with project number TTW 016.Vidi.188.021, which is (partly) financed by the Netherlands Organization for Scientific Research (NWO).

Acknowledgements

We thank dr. Bregje de Wildt for her expertise and help on the coculture experiments. We thank dr. Andreas Pollet for his expertise and help on the microfluidic cell culture.

Supplementary information

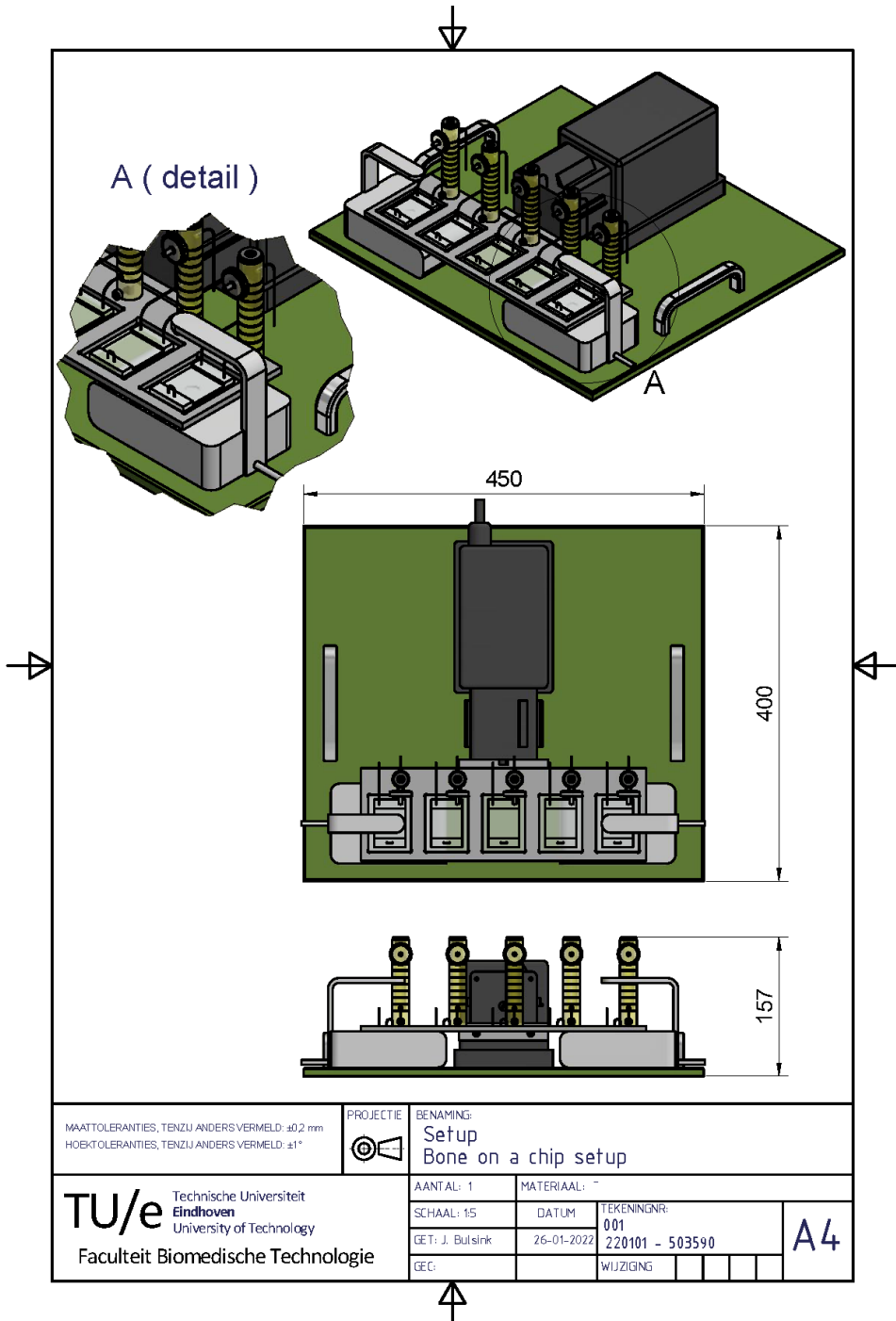


Figure S5.1 Detailed drawing of the optimized set-up. Measures are in millimeter.

Table S5.1 Primer sequences of analyzed genes

Gene	5' – 3'
COL1	F- AATCACCTGCGTACAGAACGG R- TCGTCACAGATCACGTCATCG
RUNX2	F- GTCATGGCGGGTAACGATGA R- GGGTTCCCGAGGTCCATCTA
SPP1	F- GCCGAGGTGATAGTGTGGTT R- AACGGGGATGGCCTTGTATG
ATP5F1B	F- CCAGCAGATTTTGGCAGGTGA R- AGACCCCTCACGATGAATGC

Table S5.2. Comparison of performance of initial and optimized set-ups.

Measured parameter	Initial set-up	Optimized set-up
Duration of assembling the setup inside biosafety cabinet	~1.5 - 2h	~45 min - 1h
Total tubing length	51 cm	23.5 cm
Tubing length between reservoir and chip	15 cm	2.5 cm
Number of connectors and valves	6	5
Duration of medium change	30 min	15 min
Chip cell survival after culture period	~44%	~90%

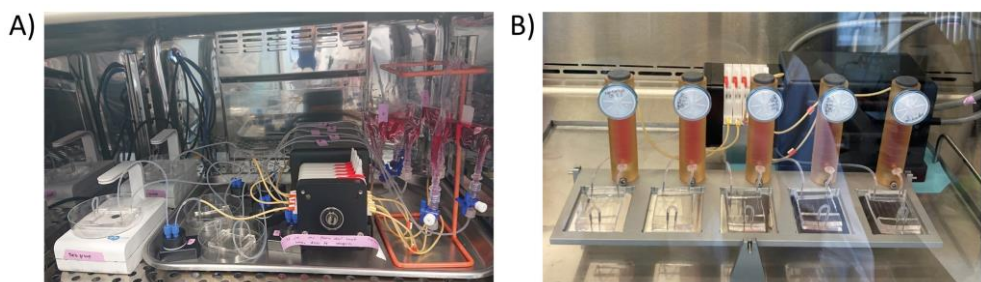


Figure S5.2 Photographic images of A) the initial set-up and B) the optimized set-up showing the difference in level of organization, tubing length and handleability.

Manual for setting up a coculture in the bone-remodeling-on-a chip

Protocol for preparing the experimental set-up

This protocol describes how to prepare the experimental set-up. A schematic overview of the set-up with perfusion flow through the microfluidic chips using the peristaltic pump is shown in **Figure S5.3**

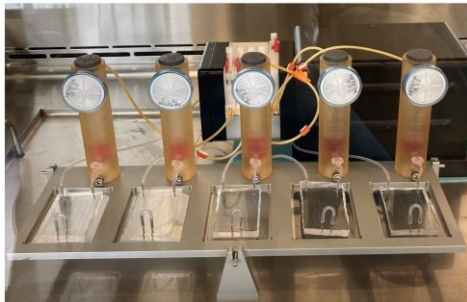


Figure S5.3 Image of the set-up inside the biosafety cabinet

Materials and Equipment

- Silicon tubing (ibidi GmbH, 0.5 mm ID) [Total length per chip = 23.5 cm]
- 3-Stop orange/yellow pump tubing (Darwin microfluidics, 3-stop PharMed BPT Pump tubing, IM-95714-18, LOT: 4090424, 0.51 mm ID) [5x]
- 20 gauge needle tips (Darwin Microfluidics, Stainless steel straight PDMS couplers, PB-STN-20G-20, 0.5 mm ID, 0.89 mm OD) [25x]
- Sterile filter (Sartorius Minisart, 16534-K, with male Luer lock of 28 mm diameter, 0.2 μm pore size) [5x]
- Male Luer lock connectors (ibidi GmbH) [10x]
- Self-healing injection ports, 20 mm (SUCOHANS, for 13 mm diameter opening) [5x]
- Medium reservoirs (polysulfone, 6 mL V), custom made (see **Figure S5.4A**) [5x]
- Metal tray (50 cm x 30 cm), custom made (see **Figure S5.4B**)
- Paper clips foldback [5x]
- Hex Key, 3 mm
- Syringe microneedle (20mm length) [5x]
- Syringe microneedle (80mm length) [5x]
- 70% ethanol (VWR chemicals)
- 1% SDS (VWR chemicals)
- Lux2 microscope (CytoSMART)
- Standard incubator (37°C, 5% CO₂)

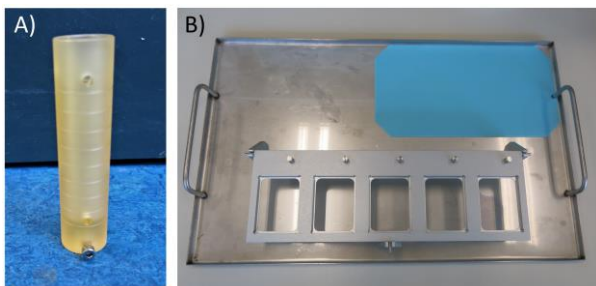


Figure S5.4 A) In-house made reservoir. B) In-house made tray

Procedure

Start the preparation of the experimental setup at least two days prior to the cell seeding in the devices.

STEP 1: Cut the tubing

NOTE: The amount of tubing described in this step accounts for one chip. The required amount of tubing depends on the number of microfluidic chips used for cell culture. In this study, a maximum of five chips can be connected to the peristaltic pump. Therefore, each tubing needs to be prepared five times.

A. Cut the tubing of a length of 15 cm. These pieces will be used for connecting the orange/yellow tubing to the outlet of the microfluidic chips and will be called "outlet tubing".

B. Cut the tubing of a length of 2.5 cm. These pieces will be used for connecting the reservoir to the inlet of the chips and will be called "inlet tubing".

C. Cut the tubing of a length of 3 cm. These pieces will be used for connecting the channels inside the chips to each other and will be called "connector tubing".

D. Cut two pieces of tubing of a length of 3 cm. These pieces will be used for attaching the tubing to the setup and will be called "complementary tubing".

STEP 2: Prepare the complete tubing

A. Prepare the connector tubing by inserting needle tips (**Figure S5.5B**) on both ends (**Figure S5.5C**).

B. Prepare the inlet tubing by connecting a male Luer lock (**Figure S5.5A**) on one end and a needle tip on the other end of the inlet tubing (**Figure S5.5D**).

C. Place the complementary tubing on both ends of the connector tubing (**Figure S5.5E**).

D. Insert a needle tip on one end of the orange/yellow tubing and a male Luer lock to the other end (**Figure S5.5F**).

E. Prepare the outlet tubing by inserting a needle tip on one end (**Figure S5.5G**).

G. Connect the inlet tubing to one complementary tubing (**Figure S5.5H**).

F. Connect the outlet tubing to the orange/yellow tubing via the needle tip of the orange/yellow tubing (**Figure S5.5I**).

H. Connect the outlet tubing to the other complementary tubing (**Figure S5.5J**)

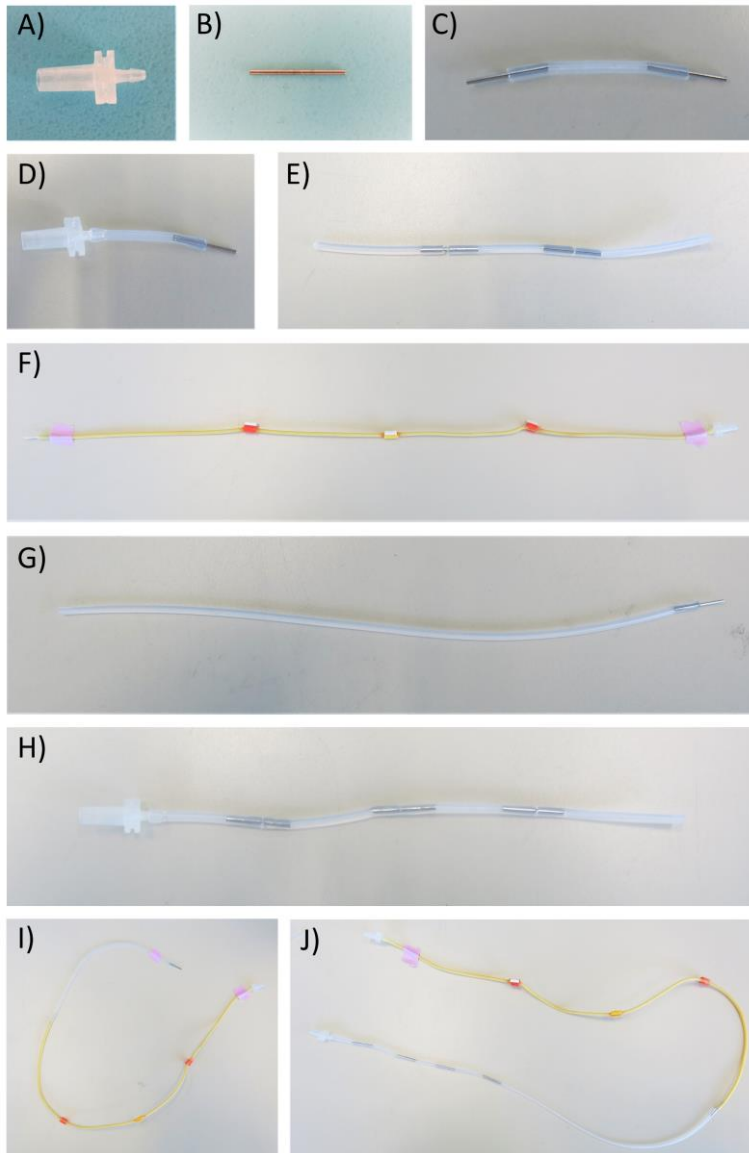
NOTE: The needed tubing length varies a bit between batches of chips. Always assemble the set-up before it is sterilized to check if the tubing length is appropriate. Sometimes, the outlet tubing needs to be a little longer.

STEP 3: Sterilize the components

A. Autoclave the medium reservoirs, including the injection ports.

B. Sterilize the tubing by flushing 2x with 1% SDS, then 2x with 70% ethanol and subsequently 2x with sterile PBS

NOTE: The tubing can be reused about 3x, but carefully check if it looks okay. After use, clean the tubing by flushing it 2x with water and dishwash soap and 2x with 70% ethanol. Push air through the tubing using an empty syringe to dry it. Store in a way that allows further drying



STEP 4: Build the set-up and equilibrate with PBS

This step should be prepared at least one day prior to cell seeding. All steps need to be performed inside a biosafety cabinet. Illustration of a step-by-step manual can be found in **Figure S5.6**.

A. Sterilize the metal tray and motor drive unit of the peristaltic pump with a tissue sprayed with ethanol and place these inside the biosafety cabinet. Place the peristaltic pump on the anti-slip matt.

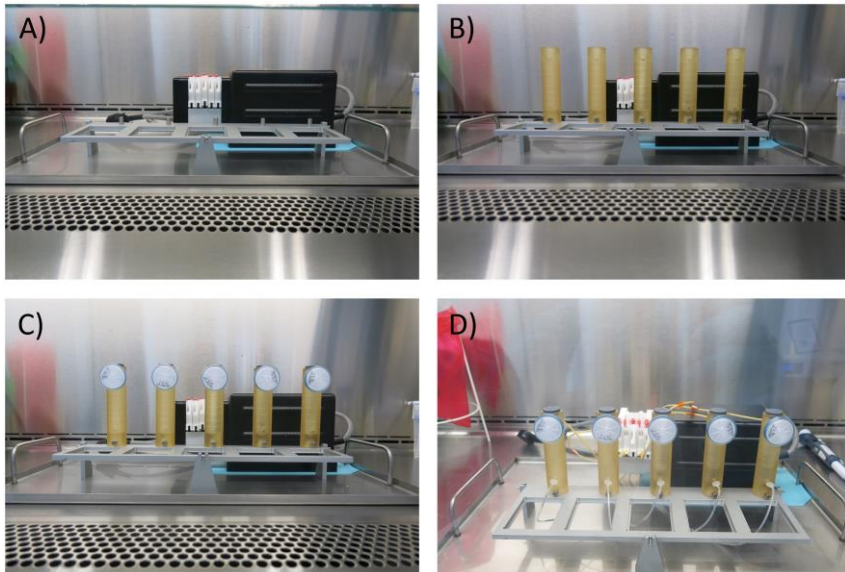


Figure S5.6 Step by step images of building the set-up

B. Prepare the medium reservoirs by screwing them with the Hex key to their specific location (**Figure S5.6B**). Add a fluid-tight filter to each medium reservoir at opening "A" (**Figure S5.7**) and place a self-healing injection port on top of the medium reservoirs (opening "B", **Figure S5.7**, **Figure S5.6C**).

C. Place the orange/yellow tubing in the tubing cassettes of the pump. Connect the male Luer lock connector to the medium reservoir at opening "C" (**Figure S5.7**). Place a clip at the other end of the outlet tubing. NOTE: connect each reservoir to the tubing one-by-one to avoid intertwined tubing (**Figure S5.6D**).

D. Fill the medium reservoirs via the injection port with sterile PBS using a syringe attached to a 20 mm microneedle.

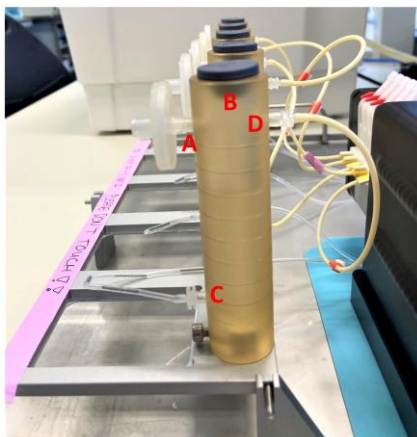


Figure S5.7 Side view of the medium reservoir

E. NOTE: perform this step reservoir by reservoir. Loosen the cassette and paper clip at the end of the orange/yellow tubing, and retrieve with a 200 μ L pipette the PBS until a blub is formed on the male Luer lock connector. Connect the male Luer lock to the reservoir at opening "D" (**Figure S5.7**). Fasten the cassette.

F. Put the experimental set-up in a standard incubator. Connect the cable of the peristaltic pump to the control unit that is placed on top of the incubator. Start the peristaltic pump for 24h with a flow of 100 μ L/min.

STEP 5: Equilibrate the set-up with osteogenic medium

This step should be performed at least the day of cell seeding into the microfluidic chips. All steps need to be performed inside a biosafety cabinet.

A. Pause the peristaltic pump and detach the cable. Take the set-up out of the incubator and spray with ethanol and place it inside the biosafety cabinet. Check if no PBS has leaked, otherwise fasten the male Luer lock connectors.

B. NOTE: perform the following steps reservoir by reservoir. Clean the injection ports with ethanol and retrieve the PBS from the medium reservoir with a syringe attached to a microneedle (80 mm). Detach the orange/yellow tubing with the male Luer lock and place a paper clip at this end. Loosen the cassette for the tubing and paper clip, and retrieve all PBS out of the tubing using a 200 μ L pipette (retrieve three times for all PBS). Place the paper clip back on the tubing.

C. Fill the reservoir with 6 mL of osteogenic medium using a syringe attached to a 20 mm microneedle. Again, take the paper clip of the tubing and retrieve the medium through the tubing with a 200 μ L pipette. Ensure there is a blob on top of the male Luer lock and attach this to the medium reservoir at point "D". Fasten the cassette of the pump.

D. Put the experimental set-up in a standard incubator. Connect the cable of the peristaltic pump to the control unit that is placed on top of the incubator. Start the peristaltic pump for 24h with a flow of 100 μ L/min.

Protocol for MSC seeding and culturing in the microfluidic chips

This section describes how to prepare the microfluidic chips for MSC seeding and how to seed the cells in the chips.

Materials and equipment

- Primary human bone marrow-derived MSCs
- Osteogenic culture medium
- Commercially available or fabricated microfluidic chips
- Human Plasma Fibronectin Purified Protein
- Phosphate buffered saline
- 70% ethanol
- Paper clips foldback [5x]
- Petri dish [1 per chip]
- Standard incubator (37°C, 5% CO₂)

Procedure

The expansion of MSCs derived from bone marrow needs to be started 7 to 10 days prior the day for cell seeding. The time it costs to become confluent varies per donor. All steps need to be performed in a biosafety cabinet.

STEP 1: Prepare the microfluidic devices

This step needs to be performed 24 hours prior to cell seeding into the microfluidic chips.

A. Label the microfluidic chips and channels A and B.

B. Pipette 3x 50 μ L 70% ethanol in each channel to sterilize the channels.

C. Expose the chips to UV-light for 10 minutes to sterilize the outside of the chips

D. Pipette 3x 50 μ L sterile PBS in each channel to remove the ethanol.

E. Coat the channels with fibronectin (100 μ g/mL in sterile PBS) to promote cell attachment to the channel bottom surface. The fibronectin stock solution has a concentration of 1 mg/mL, therefore it needs to be diluted 10x. Flush each channel 1x with 50 μ L diluted fibronectin.

F. Place the chips in petri dishes and incubate them overnight in a standard incubator. One chip can be put under the Lux 2 microscope in the incubator to monitor cell attachment. Use tape on the Lux to indicate the position of the chip in order to observe the same position in the future.

STEP 2: Seed MSCs into the microfluidic chips

This step needs to be performed the day after step 1. The estimated time is 1 hour for five chips.

A. Pipette 2x 50 μ L sterile PBS in each channel to remove the fibronectin solution.

B. Pipette 1x 50 μ L osteogenic medium.

C. Trypsinize, count, centrifuge at 270 rcf (*) for 7 minutes and resuspend the cells with a 1 mL pipette at a concentration of 1×10^6 cells in osteogenic medium.

D. Seed the MSCs in the chips by flushing each channel 1x with the cell suspension. Confirm under a light microscope each channel contains cells.

Optional: Place filter tips in all in- and outlets of the chips to prevent air entering the channels. Fill a filter tip with 30 μ L osteogenic medium, then drop the filter tip from the pipette and hold your finger on top of the filter tip to push out one drop of osteogenic medium. Next, place the filter tip at the in-/outlet.

E. Place the chips in petri dishes and incubate them without flow in a standard incubator, for at least 4h. Place one chip under the Lux 2 microscope to monitor if cells attach sufficiently.

Protocol for connecting the chips to the set-up and starting the dynamic culture

This step needs to be performed 4 hours after cell seeding. All steps need to be performed inside a biosafety cabinet.

Materials and Equipment

- Osteogenic culture medium
- Phosphate buffered saline
- 70% ethanol
- Paper clips foldback [5x]
- Petri dish
- Lux2 microscope (CytoSMART)
- Standard incubator (37°C, 5% CO₂)

Procedure

A. Take the set-up out of the incubator and spray with ethanol and place it inside the biosafety cabinet.

B. Check under a light microscope if cells are attached to the channel surface.

C. NOTE: perform the following steps chip by chip. Place two paper clips on both sides of the needle pin between the outlet and complementary tubing. Place two paper clips on both sides of the needle pin between the inlet and complementary tubing.

D. When air bubbles have formed in a channel, pipette 50 μ L osteogenic medium into the channel to flush them out. Do this very slowly to prevent cells detachment!

E. Place the chips on their specific location in the set-up. Disconnect the inlet tubing from the connector tubing, make sure the needle pin remains in the inlet tubing. Shortly open the paper clip of the inlet tubing to ensure there is liquid to liquid contact. Put the needle tip into the inlet of channel A of the microfluidic chip. If the PDMS chip lacks an extra PDMS layer on top of the in- and outlets, put the needle

down for 2/3 in the chip. If the PDMS chip contains these extra layers, put the needle down for 1/2 in the chip. Be careful not to break the glass coverslip!

F. Disconnect the end of the connector tubing closest to the inlet tubing from the complementary tubing, and make sure the needle pin remains in the connector tubing. Put the needle tip into the outlet of channel A of the microfluidic chip as described in the previous step.

G. Disconnect the other end of the connector tubing from the complementary tubing, and make sure the needle pin remains in the connector tubing. Put the needle tip into the inlet of channel B of the microfluidic chip as described in the previous step.

H. Disconnect the outlet tubing from the complementary tubing, and make sure the needle pin remains in the outlet tubing. Put the needle tip into the outlet of channel B of the microfluidic chip as described in the previous step.

I. Remove all paper clips from the tubing. Flush the complementary tubing with PBS and store these sterile in petri dishes until further use.

J. Put the experimental setup in a standard incubator. Connect the cable of the peristaltic pump to the control unit that is placed on top of the incubator. Place one chip under the Lux 2 microscope. Start the peristaltic pump with a flow of 1 $\mu\text{L}/\text{min}$. To be sure to prevent that the cable of the peristaltic pump opens the door of the incubator, use tape to close this door.

NOTE: How the cells behave in the first hours to first two nights after the flow has started, is telling for their cell viability over the next weeks. Therefore, regularly check whether air bubbles have formed inside the channels. The flow can be increased shortly (1-2 seconds) with the peristaltic pump to remove any non-attached air bubbles. When bubbles are attached, these must be removed manually. This can be done by taking out the set-up and placing it in the biosafety cabinet. A bubble in channel A requires removal of the inlet tubing, whereas a bubble in channel B requires removal of the connector tubing. Before detaching the needle pin of the tubing, place a paper clip on the tubing. Then, pipette very slowly 50 μL osteogenic medium through the channels to remove the bubble.

Protocol for medium change during cell culture

This protocol describes how to perform medium change inside the incubator. The medium needs to be prepared a day in advance to the scheduled medium change. Medium change poses a contamination risk, therefore ensure sterility when changing medium. Step 1 explains how to prepare the control medium. Step 2 describes the medium change of the optimized setup.

Materials and Equipment

- Cell culture flask, vented
- Cryovial (Sigma-Aldrich, 2 mL) [1x per chip]
- Sterile 50 mL Falcon tube (VWR)
- 70% ethanol
- Tissues
- Biosafety cabinet
- Freezer (-20°C)
- Fridge (4°C)
- Syringe (Norm-Ject, luer lock, 3 mL) [1x and 1 per chip]
- Sterile syringe microneedle 20 mm [1 per chip]
- Sterile syringe microneedle 80 mm (B.Braun Sterican Needles, 21G x 31/8 , 0.80 x 80 mm) [1 per chip]

Procedure

STEP 1: Prepare the control medium

The medium needs to be prepared the day before medium change is scheduled. This medium lacks growth factors and is defined as "control medium". The amount of medium is dependent on the number of chips. For a total medium volume per chip of 6 mL, needs to be prepared per chip.

This step needs to be performed inside a biosafety cabinet. The estimated time is 10 minutes.

- A. Prepare the right amount of control medium in a cell culture flask.
- B. Place the flask inside the incubator and open the vented cap. Incubate the medium for 24 hours to discard air bubbles.

STEP 2A: Change the medium in the incubator

Preparing the medium needs to be performed inside a biosafety cabinet, whereas the actual medium change is done in the incubator. The estimated time is 20 minutes.

- A. Take the flask out of the incubator to the biosafety cabinet. Add the right amount of growth factors to the medium. Transfer the medium to a 50 mL falcon tube. This medium is called "fresh medium".
- B. Label the cryovials with chip number and date.
- C. Pause the peristaltic pump.
- D. Put a 80 mm microneedle on top of the syringe and press the syringe to push out the air present in the syringe. Cover the syringe and microneedle with their packaging. NOTE: This syringe with microneedle is used for retrieving culture medium of the reservoirs. For five chips, five syringes and microneedles are required. These can be prepared prior to the following steps.

NOTE: steps E - I should be performed reservoir by reservoir, so repeat these steps five times. The syringe used for fresh medium retrieval can be reused, however the 20 mm microneedle can only be used for one reservoir.

- E. Put a 20 mm microneedle on top of the syringe and press the syringe to push out the air. Do not throw away the plastic packaging of both the syringe and microneedle. Retrieve 3 mL of fresh medium in the syringe. Cover the syringe and microneedle with their packaging. Be careful not to cut yourself!
- F. Go to the incubator with (1) 1 empty syringe, (2) 1 syringe with fresh medium, and (3) tissue and ethanol.
- G. Wipe the self-healing injection ports with a tissue sprayed with ethanol.
- H. Inject the 80 mm microneedle in the injection port and retrieve 3 mL of culture medium. Cover the needle and syringe again with their packaging. Next, inject the 20 mm microneedle and fill the reservoir to 6 mL with fresh medium. Go back to the biosafety cabinet.
- I. Go back to the safety cabinet and inject the culture medium in the correct labeled cryovial. Wait until the incubator is minimal 35°C before repeating steps E to I for each chip.
- J. Clean all injection ports with a tissue sprayed with ethanol. Resume the peristaltic pump.
- K. Store all cryovials in the freezer (-20°C) until further use.
- L. Discard the microneedles in the sharp waste bin and syringes at biochemical waste. Leftovers of the medium can be stored in the fridge (4°C) up to a week.

Protocol for monocyte seeding into the microfluidic chip

This section describes how to perform monocyte cell seeding into the microfluidic chips, thereby obtaining a MSC-MC co-culture. Monocyte isolation from buffy coats is required.

Materials and Equipment

- Human-derived isolated monocytes
- Co-culture medium
- Autoclaved or sterile complementary tubing [2 per chip]
- Syringe microneedle (20mm) [5x]
- Syringe microneedle (80mm) [5x]
- Disposable plastic syringe (Terumo, 10 mL) [5x]
- Cryovial 2 mL [1 per chip]
- Paper clips foldback
- PBS
- 70% ethanol

Procedure

STEP 1: Seed monocytes into the microfluidic devices

This step needs to be performed inside a biosafety cabinet.

A. Pause the peristaltic pump and detach the cable. Take the setup out of the incubator and spray with ethanol and place it inside the biosafety cabinet.

NOTE: perform step B to E chip by chip.

B. Place three paper clips on the inlet tubing, connector tubing, and outlet tubing that are inserted in the chip. Disconnect the needle pin of the inlet tubing and connector tubing of channel A from the chip and connect both using a complementary tubing. Then, disconnect the needle pin of the outlet tubing and connector tubing of channel B from the chip and connect both using a complementary tubing.

C. Place a microfluidic chip in a petri dish and observe under a microscope if struts have formed.

D. Seed the MCs in the chip by flushing each channel 1x with the cell suspension. Seed the cells very slowly to prevent rupture of any formed struts by the MSCs. Confirm under a light microscope each channel contains cells.

E. Place the microfluidic chip in a petri dish and incubate it for 24 hour without flow to promote cell attachment.

STEP 2: Equilibrate the microfluidic setup with co-culture medium

This step should be performed on the day of MC seeding. All steps need to be performed inside a biosafety cabinet.

A. NOTE: perform the following steps reservoir by reservoir. Clean the injection ports with ethanol and retrieve the supernatant from the medium reservoir with a syringe attached to a microneedle (80 mm) in correctly labeled cryovials. Store all cryovials in the freezer (-20°C) until further use.

B. Detach the orange/yellow tubing with the male Luer lock and place a paper clip at this end. Loosen the cassette for the tubing and paper clip, and retrieve all medium out of the tubing using a 200 μ L pipette. Place the paper clip back on the tubing.

C. Fill the reservoir with 6 mL of co-culture medium using a syringe attached to a 20 mm microneedle. Again, take the paper clip of the tubing and retrieve the medium through the tubing with a 200 μ L pipette. Ensure there is a blob on top of the male Luer lock and reattach this to the medium reservoir. Fasten the cassette of the pump.

D. Put the experimental setup in a standard incubator. Connect the cable of the peristaltic pump to the control unit that is placed on top of the incubator. Start the peristaltic pump for 24h with a flow of 1 μ L/min.

STEP 3: Connect chips to set-up

This step should be performed 24 hours after MC seeding in a biosafety cabinet.

A. Take the set-up out of the incubator and spray with ethanol and place it inside the biosafety cabinet.

B. NOTE: perform the following steps chip by chip. Place two paper clips on both sides of the needle pin between the outlet and complementary tubing. Place two paper clips on both sides of the needle pin between the inlet and complementary tubing.

C. Place the chips on their specific location in the setup. Disconnect the inlet tubing from the connector tubing, make sure the needle pin remains in the inlet tubing. Shortly open the paper clip of the inlet tubing to ensure there is liquid to liquid contact. Put the needle tip into the inlet of channel A of the microfluidic chip. If the PDMS chip lacks an extra PDMS layer on top of the in- and outlets, put the needle down for 2/3 in the chip. If the PDMS chip contains these extra layers, put the needle down for 1/2 in the chip. Be careful not to break the glass coverslip!

D. Disconnect the end of the connector tubing closest to the inlet tubing from the complementary tubing, and make sure the needle pin remains in the connector tubing. Put the needle tip into the outlet of channel A of the microfluidic chip as described in the previous step.

E. Disconnect the other end of the connector tubing from the complementary tubing, and make sure the needle pin remains in the connector tubing. Put the needle tip into the inlet of channel B of the microfluidic chip as described in the previous step.

F. Disconnect the outlet tubing from the complementary tubing, and make sure the needle pin remains in the outlet tubing. Put the needle tip into the outlet of channel B of the microfluidic chip as described in the previous step.

G. Remove all paper clips from the tubing.

H. Put the experimental setup in a standard incubator. Connect the cable of the peristaltic pump to the control unit that is placed on top of the incubator. Place one chip under the Lux 2 microscope. Start the peristaltic pump with a flow of 1 μ L/min. To be sure to prevent that the cable of the peristaltic pump opens the door of the incubator, use tape to close this door.

STEP 4: Medium change including RANKL

2 days after MC seeding, RANKL should be added. This can be done according to the medium change protocol.

Chapter 6

Osteogenic differentiation on a chip using pumpless bidirectional fluid flow

The contents of this chapter are based on:

Michelle A.M. Vis^a, Nils C.H. van Creijl^a, Andreas M.A.O. Pollet^b, Jaap M.J. den Toonder^b, Keita Ito^a, Sandra Hofmann^a (2023) *In preparation*

^a *Department of Biomedical Engineering and Institute for Complex Molecular Systems (ICMS) Eindhoven University of Technology, Eindhoven, the Netherlands*

^b *Microsystems, Department of Mechanical Engineering and Institute for Complex Molecular Systems (ICMS) Eindhoven University of Technology, Eindhoven, the Netherlands*

Abstract

Dynamic culturing has been shown to be advantageous in tissue engineering. In bone tissue engineering, researchers have been attempting to mimic the concept of mechanical loading by perfusion flow cultures, which are regarded as one of the most accurate representations of loading in bone. Most perfusion experiments require specialized pumps and tubing to create a unidirectional fluid flow which results in rather complex set-ups. Gravity-driven flow could offer an alternative as it is simpler. Furthermore, bidirectional flow can better recapitulate the multidirectional movement of the interstitial fluid within the native bone. In this study, human mesenchymal stromal cells were osteogenically differentiated in a microfluidic chip perfused by bidirectional gravity driven flow. Extracellular matrix production in terms of collagen type 1 and mineralization were visualized and compared between static and dynamic cultures. After 21 days of culturing, monocytes were added and differentiated toward osteoclasts in the coculture for another 14 days, making a total of 35 days. Our results once again demonstrate the benefit of mechanical loading over static culture for osteogenic differentiation, this time in a microfluidic chip device. Gravity driven flow systems are relatively easy and cost-effective to construct and maintain, and they offer an accessible solution towards higher throughput organ-on-chip models for potential drug testing.

6.1 Introduction

Interest in discovering alternatives to animal testing is growing as data from animal models often does not align with the results of clinical trials conducted on humans.^{3,4} The lack of human relevant preclinical models has resulted in a high rate of failure of therapeutics in the clinic, as well as an increase in healthcare costs.³ Human *in vitro* models can be used to address these difficulties. One of the recent successes in the pursuit to create human *in vitro* models is the use of organ-on-chip devices. These devices are lined with living cells cultured under fluid flow and can simulate organ-level physiology and pathophysiology with high fidelity.³ Organ-on-chip devices promise several advantages over traditional *in vitro* culture techniques such as integration of structural and dynamic cues, small volumes of cells, samples and reagents leading to decreased costs and options for parallel and real-time analysis.

Dynamic culturing has been shown to be advantageous when tissue engineering bone. Researchers in bone tissue engineering have been trying to mimic the concept of mechanical loading by perfusion flow cultures that are considered to represent one of the loading concepts in bone the closest.^{174,211} For example, when human mesenchymal stromal cells (MSCs) were dynamically stimulated during seeding into scaffolds, increased osteogenic differentiation and mineral deposition were observed compared to statically seeded cells.¹⁶³ Also, MSC behavior could be steered and even predicted based on the amount of applied mechanical stimulation by fluid flow, causing either enhanced cell proliferation or enhanced osteogenic differentiation.^{174,212-214} Bone-on-a-chip systems are able to provide perfusion flow, and are increasingly reported in literature.¹⁶

Most perfusion experiments require specialized pumps and tubing to create a fluid flow which results in rather complex set-ups. Gravity-driven fluid flow could offer a simpler alternative, requiring only a rocking plate which is readily available in most laboratories. The rocking motion enables a pumpless bidirectional flow inside the chip channel by means of gravity driven flow between two reservoirs. Such platforms are relatively easy and cost-effective to construct and maintain²¹⁵ and they have been used for a variety of organ-on-chip models, including skin,²¹⁶ liver,²¹⁷ and blood brain barrier.^{95,218} By integrating microchannels and reservoirs on the chip, these systems can be compact and stackable, making them suitable for high throughput applications.^{219,220}

The use of bidirectional flow has been introduced as an effective strategy to stimulate bone tissue engineered constructs by better recapitulating the multidirectional movement of the interstitial fluid within the native bone.²²¹⁻²²³ Bidirectional fluid flow was first used to improve cell seeding efficiency in perfusion bioreactors and later it was shown to promote osteogenic differentiation.²²⁴⁻²²⁷ The gravity-driven bidirectional flow could thus have beneficial effects compared to the unidirectional flow used in most bone-on-chip models.

In this study, we investigated the use of gravity-driven bidirectional fluid flow for bone-on-a-chip devices. We studied the effect of bidirectional fluid flow on osteogenic differentiation of human MSCs in a chip by comparing it with static cultures and our previous pump system with unidirectional flow (Chapter 5). It was hypothesized that bidirectional flow enhances

collagen type 1 deposition and mineralization compared to unidirectional flow and static cultures, as it mimics interstitial conditions.^{11,221} In addition, a coculture was established by adding human monocytes (MCs) to the chips after the 21-day osteogenic differentiation of the MSCs. The MCs were osteoclastogenically differentiated for an additional 14 days, making a total of 35 culture days.

6.2 Materials and Methods

6.2.1 General experimental set-up

The general approach for osteogenic differentiation of MSCs using bidirectional fluid flow included several steps (Figure 6.1). Briefly, photolithography was employed as fabrication method to create a mold of SU-8 photoresist on a silicon wafer, followed by soft lithography to create a polydimethylsiloxane (PDMS) layer in which the cell culture channels were located. The PDMS layer was bonded to a glass coverslip to complete the device. Before starting culturing in the device, the channels were coated with fibronectin to enhance cell adhesion (Figure 6.1A). After the MSCs were well attached, bidirectional flow was induced by rocking the chips on a rocking plate (Figure 6.1B). The channel was aligned along the rocking axis to induce a fluid flow. The plate was set at an angle of 7° and tilted every 3 minutes (Figure 6.1C). Culture medium was perfused through the channels and culturing was continued for 21 days to allow for bone-like tissue formation. Next, MCs were added, and the medium was switched to coculture medium which was perfused through the channels for an additional 14 days.

6.2.2 Master mold fabrication and validation

A master mold for the patterned PDMS layer was produced on a silicon wafer by photolithography. The design of the photomask was drawn in AutoCAD (version 2021, Autodesk) and ordered at CAD/Art Services (Bandon, USA). First, a layer of negative photoresist (SU-8 2150, MicroChem, Newton, MA, USA) was spin-coated on top of a silicon wafer (Ø100 mm, Si-Mat). To ensure a thickness of 200 µm, the spin-coater (model WS-650MZ-23NPPB, Laurell, North Wales, USA) was set to a rotating speed of 2,000 rpm for 30 seconds. The wafer was soft-baked, and the photomask was placed on top of the wafer, followed by UV-light exposure with a dose of 315 mJ/cm² (model UV-EXP150S-SYS, Idonus, Hauterive, Switzerland), initiating SU-8 crosslinking of the exposed parts of the photoresist. A post exposure bake was done to complete the crosslinking process, followed by submerging the wafer into a developer solution (mr-Dev 600, Micro Resist Technology GmbH, Berlin, Germany) for 15 to 18 minutes to remove uncured photoresist. Subsequently, hard baking was performed to stabilize the printed pattern. The height of the channel dimensions was validated using a Mitutoyo Mu-Checker electronic comparator (model M402 519-402, Mitutoyo America Corporation, Aurora, USA). Finally, the master mold was silanized using 1H,1H,2H,2H-perfluorooctyltriethoxysilane (Fluorochem Ltd, Hadfield, UK) under vacuum overnight.

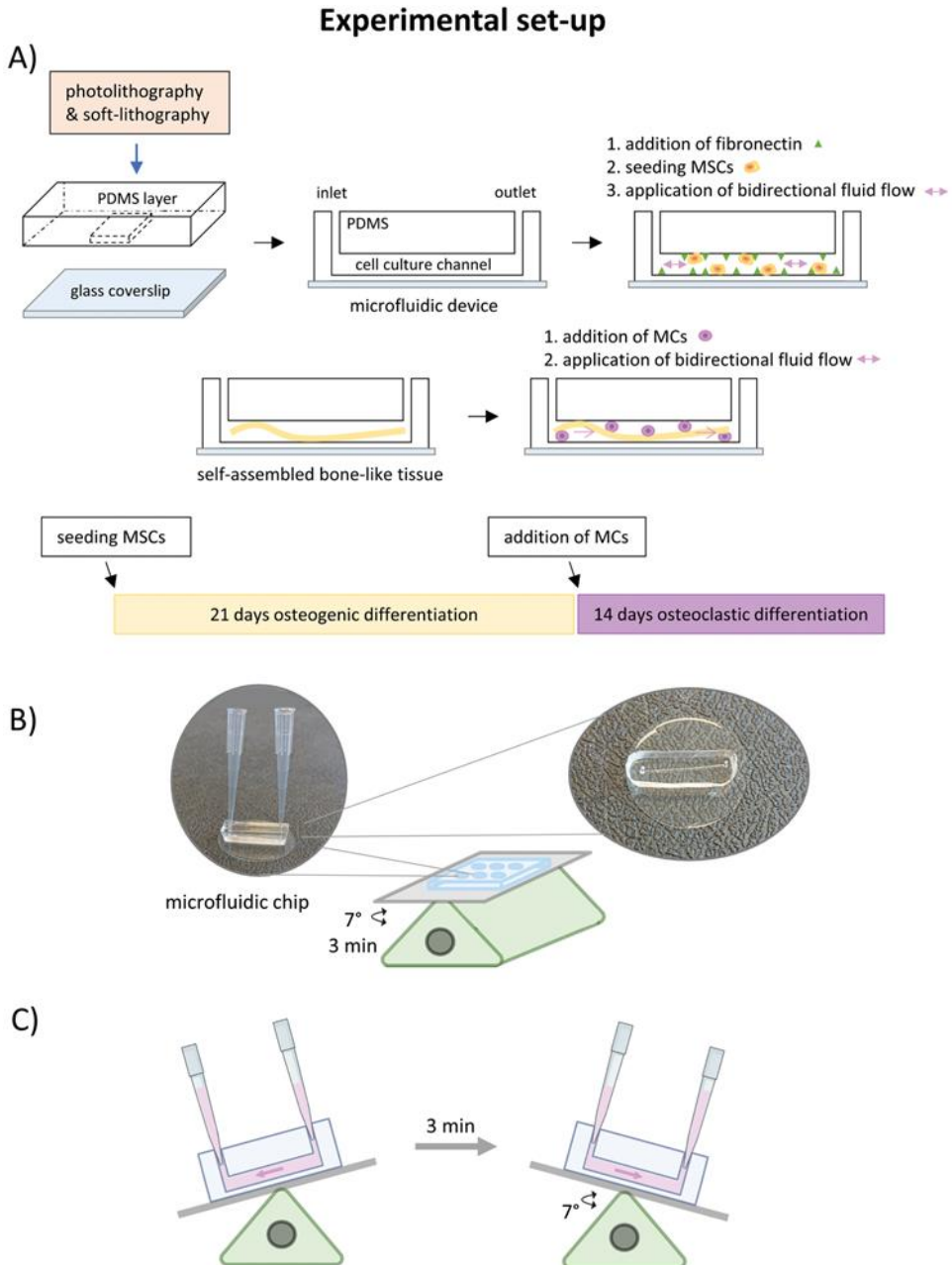


Figure 6.1 Outline of the experimental set-up. A) With the use of photo- and soft-lithography a PDMS microfluidic chip is created. The cell culture channel is coated with fibronectin 24 hours prior to seeding the MSCs. After 4 hours of attachment, culture medium bidirectional flow is applied for 21 days. After 21 days, MCs are seeded onto these tissues and allowed to attach for 24 hours. Next, bidirectional flow is applied, and the MCs are differentiated towards the osteoclastic lineage over an additional 14 days. B) The set-up comprises of a rocking plate with a 6 wells plate holding the chips. The chips have pipet tip reservoirs. C) The rocking plate is tilted 7° every 3 minutes to generate a bidirectional fluid flow

6.2.3 Microfluidic chip fabrication

The microfluidic chips consisted of a PDMS part and a PDMS-coated glass coverslip and were made by standard soft-lithography. The PDMS part contained one straight channel with dimensions of 200 μm height x 800 μm width x 23 mm length. PDMS base and curing agent (Sylgard 184 silicone elastomer kit, Dow Corning, Midland, MI, USA) were thoroughly mixed at a 10:1 ratio (w/w), degassed under vacuum, and poured onto the wafer mold. After curing the PDMS overnight at 65°C, the patterned PDMS layer containing the channels was released from the master mold. A round glass coverslip with a size of \varnothing 32 mm and thickness of 0.17 mm was used to close off the microfluidic channels. To make sure the cells were exposed to the same substrate stiffness on the bottom surface as on the other walls of the channel, the coverslip was spin-coated with a thin layer of PDMS of approximately 130 μm in thickness. Holes for the in- and outlets were punched with a \varnothing 1.2 mm biopsy punch (Harris Uni-Core, No. 7093508). To attach the patterned PDMS layer to the PDMS coated coverslip, 20-watt oxygen plasma was applied for 30 seconds using a plasma asher (model K1050X, Emitech, Quorum technologies, UK). The microfluidic device was completed by baking it in an oven at 65°C for 2 hours. Prior to cell seeding, the devices were sterilized with 70% ethanol and flushed 3 times with sterile PBS. Next, the devices were coated with fibronectin (Human Plasma Fibronectin Purified Protein, Merck, Schiphol-Rijk, The Netherlands) in sterile PBS (100 $\mu\text{g}/\text{mL}$) and placed overnight in the incubator (37°C and 5% CO_2).

6.2.4 Fluid-flow induced shear stress calculation

Gravity driven culture medium perfusion was used to provide the cells with a bidirectional fluid flow. To determine the pressure differences ΔP [Pa] that influence the desired medium flow rate Q [m^3/s] and the shear stress τ [Pa], the Bernoulli equation defined for time dependent height differences was used (Supplementary Information S1):

$$\Delta P = \rho g(HT(t) + HL(t - \Delta t) - HR(t - \Delta t)) \quad (1)$$

With fluid density $\rho = 1009 \text{ kg}/\text{m}^3$, gravitational constant $g = 9.81 \text{ m}/\text{s}^2$, tilting height HT [m], and the heights of the left (HL) and right (HR) reservoirs [m]. All heights were corrected by time t [s] and determined by the tilting angles and times of the rocking plate, in this case 7° tilting every 3 minutes. The height differences plotted against time were calculated using MATLAB software (version 2020a, The MathWorks, Inc.), resulting in the pressure difference (Figure 6.2A and B).

Using the obtained pressure differences, the medium flow rate was calculated at different time points of tilting²²⁸ :

$$Q = \frac{h^3 w \Delta P}{12 \mu l} \left(1 - 0.630 \frac{h}{w}\right) \quad (2)$$

With channel length $l = 2.3 \times 10^{-2} \text{ m}$, width $w = 8 \times 10^{-4} \text{ m}$, and height $h = 2 \times 10^{-4} \text{ m}$ and dynamic viscosity of the medium $\mu = 9.3 \times 10^{-4} \text{ Pa}\cdot\text{s}$ ¹⁶⁹.

Using the obtained values for Q (Figure 6.2C), the shear stress in the channels was calculated at the different time points of tilting²²⁹ :

$$\tau = \frac{6\mu Q}{h^2 w} \quad (3)$$

For clarification, the rocking plate fully tilts 7°, stays in this position for 3 minutes and then fully tilts to the other side.

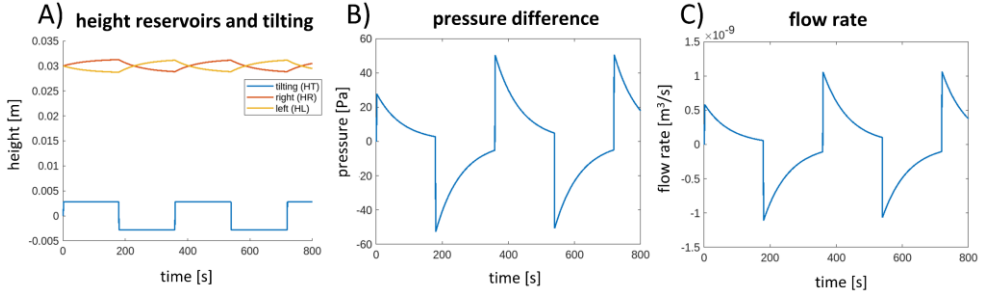


Figure 6.2 Graphs obtained via MATLAB using a rocking time of 3 minutes and angle of 7°. A) Height of the reservoirs and tilting [m] at different time points. B) Pressure difference [Pa] and C) Flow rates [m³/s] in one of the inlets over time during tilting. A negative pressure or flow rate means that the inlet is at its lowest position, resulting in a flow towards the inlet.

6.2.6 Isolation, expansion, and cultivation of MSCs

MSC isolation and characterization from human bone marrow (Lonza, Walkersville, MD, USA) was performed as previously described.¹⁶² MSCs were frozen at passage 3 with 1.25 × 10⁶ cells/ml in freezing medium containing FBS (BCBV7611, Sigma-Aldrich) with 10% dimethylsulfoxide (DMSO, 1.02952.1000, VWR, Radnor, PA, USA) and stored in liquid nitrogen until use. Before experiments, MSCs were thawed and seeded at a density of 2.5 × 10³ cells/cm² in expansion medium containing DMEM (high glucose, 41966, Thermo Fisher Scientific), 10% FBS (BCBV7611, Sigma Aldrich), 1% antibiotic antimycotic (anti-anti, 15240, Thermo Fisher Scientific), 1% non-essential amino acids (NEAA, 11140, Thermo Fisher Scientific), and 1 ng/mL basic fibroblastic growth factor (bFGF, 100-18B, PeproTech, London, UK) at 37 °C and 5% CO₂. Upon 80% confluence, cells were detached using 0.25% trypsin-EDTA (25200, Thermo Fisher Scientific) and directly used for experiments at passage 4. Cells were resuspended at 1 × 10⁶ cells/mL in osteogenic monoculture medium containing DMEM (low glucose, 22320, Thermo Scientific), 10% human platelet lysate¹⁵⁸ (hPL, PE20612, PL BioScience, Aachen, Germany), 1% anti-anti, 0.1 μM dexamethasone (D4902, Sigma-Aldrich), 0.05 mM ascorbic acid-2-phosphate (A8960, Sigma-Aldrich), 10 mM β-glycerophosphate (G9422, Sigma-Aldrich) and carefully pipetted into the channels of the chips. ~7 μL cell suspension per chip was used, resulting in ~7000 cells/chip. The chips were placed in 6 well plates and incubated at 37°C and 5% CO₂ for at least 4 hours to allow cell attachment. Thereafter, the pipet tip reservoirs (200 μL Saphire sterile filter tips, 775353, Greiner Bio-One, the Netherlands), filled with 100 μL osteogenic culture medium each were attached to the channels (two tips per chip). Next, the 6 well plates containing the chips were placed on the rocking plate (OrganoFlow® L, Mimetas, Leiden, the Netherlands) which was set at an angle of 7°, tilting every 3 minutes. Medium was refreshed 3x/week by removing the pipet tip reservoirs and replacing them with new pipet tips filled with 100 μL fresh osteogenic medium each. The chips were cultured for 21 days.

6.2.7 Coculture: isolation of monocytes and cultivation of MSCs + monocytes

Human peripheral blood buffy coats from healthy volunteers under informed consent were obtained from the local blood donation center (agreement NVT0320.03, Sanquin, Eindhoven, the Netherlands). The buffy coats (~ 50 mL) were diluted to 200 mL in 0.6 % (w/v) sodium citrate in PBS adjusted to pH 7.2 at 4°C (citrate-PBS), after which the peripheral mononuclear cell fraction was isolated by carefully layering 25 mL diluted buffy coat onto 13 mL Lymphoprep (07851, StemCell technologies, Cologne, Germany) in separate 50 mL centrifugal tubes, and centrifuging for 20 min with lowest brake and acceleration at 800×g at RT. Human peripheral blood mononuclear cells (PBMCs) were collected, resuspended in citrate-PBS and washed 4 times in citrate-PBS supplemented with 0.01% bovine serum albumin (BSA, 10735086001, Sigma-Aldrich, Zwijndrecht, The Netherlands) to remove all Lymphoprep. PBMCs were frozen in freezing medium containing RPMI-1640 (RPMI, A10491, Thermo Fisher Scientific), 20% FBS (BCBV7611, Sigma-Aldrich) and 10% DMSO and stored in liquid nitrogen until further use. Prior to experiments, monocytes (MCs) were isolated from PBMCs using manual magnetic activated cell separation (MACS). PBMCs were thawed, collected in medium containing RPMI, 10% FBS (BCBV7611, Sigma-Aldrich) and 1% penicillin-streptomycin (p/s, 15070063, Thermo Fisher Scientific), and after centrifugation resuspended in isolation buffer (0.5% w/v BSA in 2mM EDTA-PBS). The Pan Monocyte Isolation Kit (130-096-537, Miltenyi Biotec, Leiden, The Netherlands) and LS columns (130-042-401, Miltenyi Biotec) were used according to the manufacturer's protocol. After magnetic separation, the cells were directly resuspended in osteogenic coculture medium containing α MEM 41061, 5% hPL, 1% anti-anti supplemented with 0.1 μ M dexamethasone, 0.05 mM ascorbic acid-2-phosphate, 10 mM β -glycerophosphate) spiked with 50 ng/mL macrophage colony stimulating factor (M-CSF, 300-25, PeproTech). After 21 days of culturing the MSCs, the MCs were added to establish the coculture. To seed the MCs into the chips, the 6 well plates containing the chips were placed in a safety cabinet and the pipet tip reservoirs were removed from the chips. The MCs were counted, and a suspension of 5×10^6 /mL was carefully pipetted into the chips, ~7 μ L per chip, resulting in ~35,000 cells/chip. Pipet tip reservoirs filled with 100 μ L coculture medium each were placed on the in- and outlets. The chips were placed back into the incubator where cells were allowed to attach for 24 hours before the rocking motion was started again at an angle of 7°, tilting every 3 minutes. After 2 days the coculture medium was replaced by coculture medium additionally containing 50 ng/mL receptor activator of NF κ -B ligand (RANKL, 310-01, PeproTech). Medium was refreshed 3x/week by removing the pipet tip reservoirs and replacing them with new pipet tips filled with 100 μ L fresh coculture medium each. The culture was maintained for another 14 days, making a total of 35 days.

6.2.10 Immunohistochemistry

At day 14, 21 and 35, chips were washed with PBS and fixed in 10% neutral-buffered formalin for 15 min. The chips were immunostained by washing with PBS-tween, permeabilizing in 0.5% Triton X-100 in PBS for 10 min and blocking in 10% normal goat serum in PBS for 30 min. Cells were incubated with DAPI, Phalloidin and immunostainings (Table 6.1) in PBS for 1 hour. Images were taken with a fluorescent light microscope (Axio Observer 7, Zeiss, Oberkochen, Germany). Images showing the results of unidirectional flow (Figure 6.3D) were

from an earlier study, using the same (immuno)stainings. Details on the methods of how these samples were cultured can be found in Chapter 5.2.

Table 6.1 List of all dyes and antibodies used and their working concentrations/dilutions

Antigen	Source	Catalogue No	Label	Species	Concentration/Dilution
DAPI	Sigma-Aldrich	D9542			0.1 µg/mL
Atto 647 conjugated Phalloidin	Sigma-Aldrich	65906			50 pmol
Collagen type-1	Abcam	Ab34710		Rabbit	1:200
RUNX-2	Abcam	Ab23981		Rabbit	1:500
Osteopontin	Thermo Fisher	14-9096-82		Mouse	1:200
Anti-rabbit (H+L)	Molecular Probes	A11008	Alexa 488	Goat	1:200
Anti-mouse IgG1 (H+L)	Molecular Probes	A21127	Alexa 555	Goat	1:200

6.2.11 Histology

Following the immunostaining the same samples of day 14 and 21 were stained with Alizarin Red (2% in distilled water, A5533, Sigma-Aldrich) for 15 minutes to identify mineralization. Subsequently, channels were washed with distilled water until no further discoloration of the water occurred. Images were made using a brightfield microscope (Axio Observer Z1, Zeiss, Oberkochen, Germany). Images showing the results of unidirectional flow (Figure 6.3D) were from an earlier study, using the same staining. Details on the methods of how these samples were cultured can be found in Chapter 5.2.

6.3 Results

6.3.1 Shear stress in dynamic culture conditions

Numerical analysis was used to estimate the mechanical stimulation in terms of shear stress received by the cells in the chip. When using a tilting angle of 7° and rocking time of 3 minutes the flow rate fluctuates between $Q = 5.82 \times 10^{-11}$ and 1.01×10^{-9} m³/s depending on the timepoint after tilting (Figure 6.2A and C). This fluctuation occurs due to the bidirectional character and thus transient effect of the fluid flow. Using these fluid flow rates in equation 3, results in shear stresses between 10 and 180 mPa (Figure 6.3).

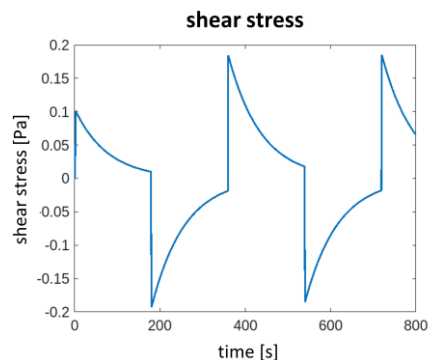


Figure 6.3 The expected shear stress when using a rocking time of 3 minutes and angle of 7°

6.3.2 Osteogenic medium and dynamic culturing are both essential for 3D mineralized matrix production

The cell cultures were investigated for their composition at day 14 and 21, comparing static and dynamic conditions. At day 21, also osteogenic medium versus control medium was compared. The cells in the static conditions were flatly spread over the channel bottom and remained two dimensional (2D), spread and spindle shaped over time (Figure 6.4A, B and C, left columns). In dynamic conditions, the cells self-assembled into layered, three dimensional (3D) structures (Figure 6.4A, B, C, and D, right columns, red arrows), indicating the need for mechanical cues to produce 3D structures.

Collagen type 1 (immunofluorescent antibody staining) was visible in the extracellular matrix (ECM) of all osteogenic groups (Figure 6.4A, B and D), but more prominently in the dynamically unidirectional cultured group at day 21 (Figure 6.4D). In the control medium group, both the static and dynamic culture, collagen type 1 was visible in the cell body, but not in the ECM (Figure 6.4C).

Mineralization (Alizarin red staining) occurred in all osteogenic groups (Figure 6.4A, B and D), but more prominently in the dynamically unidirectional cultured group (Figure 6.4D). Mineralization did not occur in control medium group (Figure 6.4C), indicating that osteogenic factors in the culture medium are essential for mineral deposition in the ECM in the present setup.

6.3.3 Osteogenic differentiation of MSCs

To confirm osteoblastic differentiation of the MSCs during the 21-day culture, samples were stained for RUNX-2 and osteopontin expression at day 14 and 21. RUNX-2 was present in the nucleus and osteopontin in the body of the cells at day 14 and 21 (Figure 6.5A and B). The cells changed in morphology from stellate toward more cuboidal from day 14 to 21. The results confirm that the microfluidic chip allows for MSCs to differentiate into osteoblast-like cells.

6.3.4 Osteoclastic differentiation of MCs

After the 21-day tissue formation phase, MCs were added to the microfluidic chips and cultured for another 14 days (35 days in total). Monoculture medium was changed into coculture medium containing RANKL and M-CSF to induce osteoclastic differentiation of the MCs. At day 35, mono- and multi-nucleated cells with different morphologies were present. Based on Figure 6.4, elongated mononuclear cells with large ($\pm \text{Ø } 16 \mu\text{m}$) oval shaped nuclei were identified as osteoblast-like cells (Figure 6.5A and B, white ovals). Round, multinucleated cells with smaller ($\pm \text{Ø } 12 \mu\text{m}$) round nuclei were identified as fused monocytes (Figure 6.6A, green circles) and pre-osteoclasts (Figure 6.6B, orange circle). These results suggest that MCs were able to attach to the mineralized tissues upon cell seeding and could withstand the dynamic conditions. The MCs were stimulated towards the osteoclastic lineage shown by the formed multi-nucleated cells, establishing a coculture on a chip.

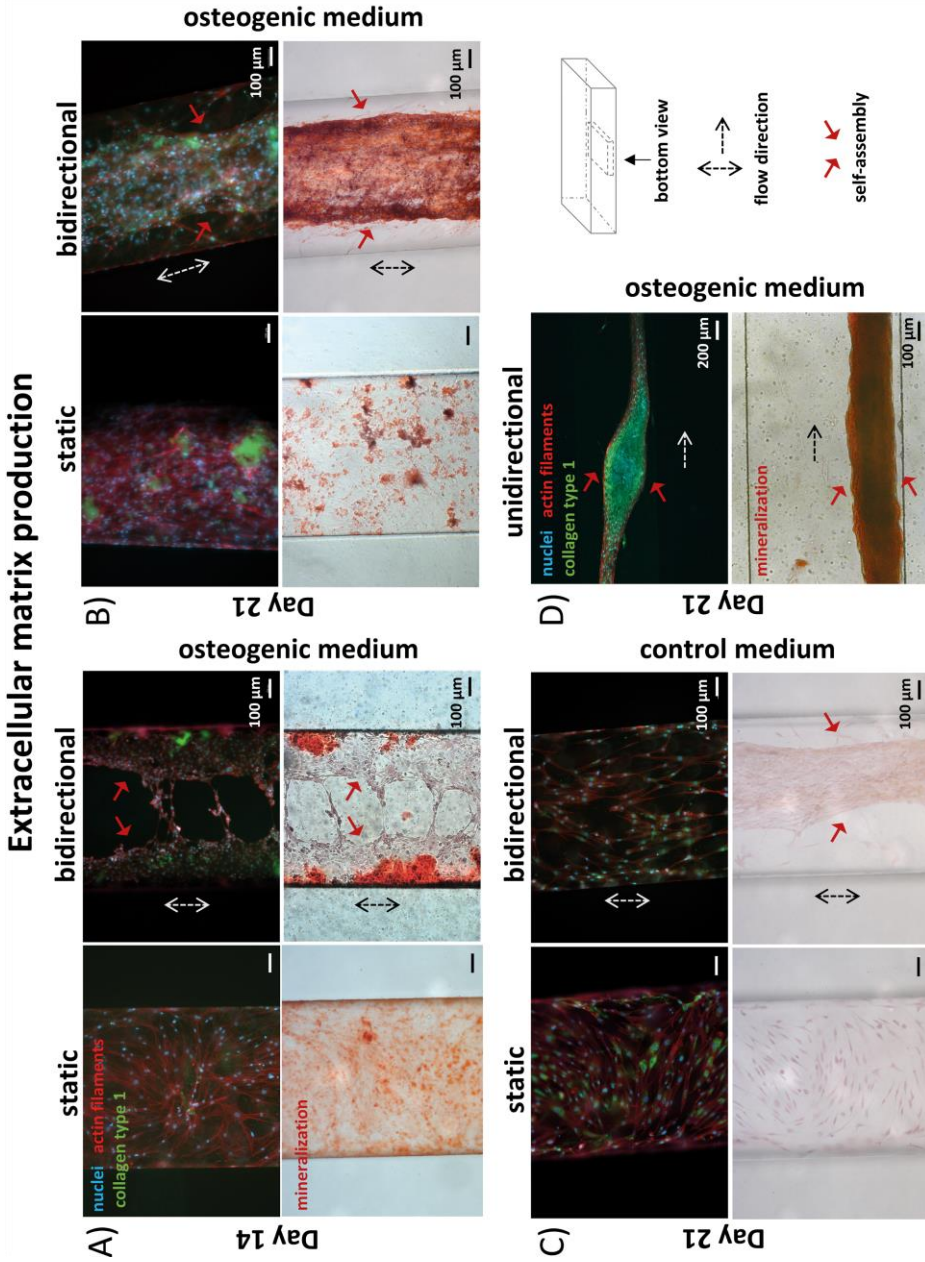


Figure 6.4 ECM production in terms of collagen type 1 (immunostaining) and mineralization (Alizarin Red). Cells cultured statically and dynamically with bidirectional flow in osteogenic culture medium A) at day 14, and B) at day 21. C) With bidirectional flow in control medium at day 21. D) Images from an earlier study using a pump system with unidirectional flow in osteogenic culture medium at day 21. Images were taken from the bottom of the chips. Flow direction is indicated with dotted arrows and self-assembly with red arrows.

Osteoblastic differentiation of MSCs

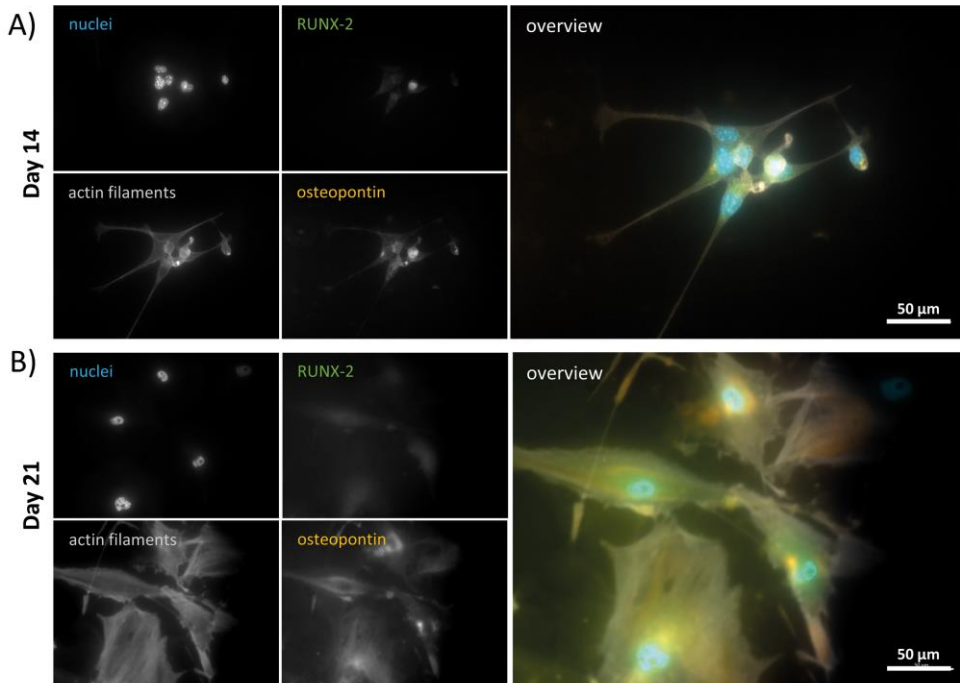


Figure 6.5 Osteogenic differentiation of MSCs: A) at day 14 and B) at day 21. Osteopontin is expressed in the cells body and RUNX-2 in the nucleus.

Osteoclastic differentiation of MCs

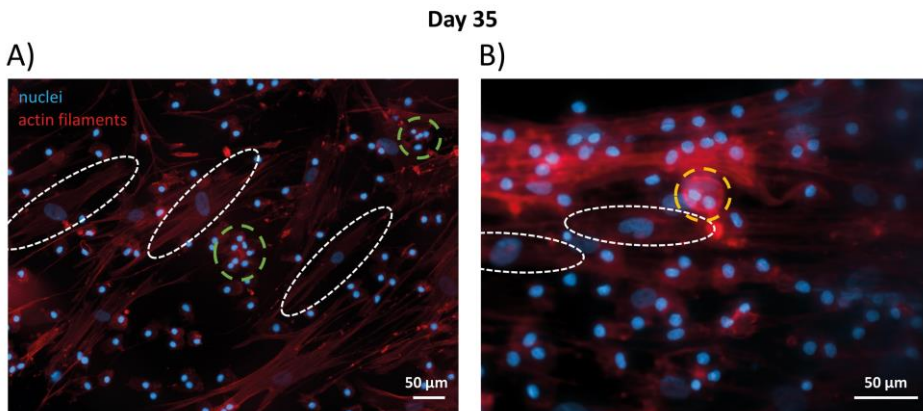


Figure 6.6 Coculture after 35 days. A) White ovals show osteoblasts, green circles show fusing monocytes. B) yellow circles show multinucleated pre-osteoclasts with clear actin ring.

6.3.5 Comparison of pump and gravity driven flow set-up

Comparing the previous unidirectional pump system (Chapter 5) with the bidirectional gravity driven flow system points out both practical (Table 6.2) and biological (Table 6.3)

(dis)advantages between the systems. The gravity driven flow system is easy and quick to set up, without any tubing. It allows for culturing four 6-well plates simultaneously, creating the possibility to culture 24 chips. Culture medium exchange remains a labor intensive and manual task as for each chip the pipet tip reservoirs need to be exchanged three times a week. The unidirectional pump system allows for easy and quick culture medium exchange thanks to the custom designed reservoirs (Chapter 5.2.4).

Table 6.2 Set-up parameters comparing pump set-up with gravity driven flow set-up.

Measured parameter	Pump set-up	Gravity driven flow set-up
Duration of assembling the setup inside biosafety cabinet	~45 min – 1 h	~10 min
Total tubing length	23.5 cm	0 cm
Duration of medium change	15 min	30 min
Sample size per experiment	≤5	≤24

Both set-ups allow for osteogenic differentiation of MSCs and enabled long-term coculturing of osteoblasts and osteoclast (35 days). However, some long-term cultured chips in the gravity driven flow set-up did not survive due to clogging of the in- and outlets leading to obstructed medium flow. Overall, the unidirectional pump set-up performs better in terms of matrix production and mineralization, creating more defined firm bone-like tissues (Figure 5.3 and 6.3).

Table 6.3 Outcome parameters comparing pump set-up with gravity driven flow set-up. Comparison is based on samples cultured in osteogenic differentiation medium under fluid flow. Used scale from best to worst performance: ++, +, +-, -, --

Measured parameter	Pump set-up	Gravity driven flow set-up
Fluid flow direction	unidirectional	bidirectional
Expected shear stress	3.7 - 446 mPa	47 - 150 mPa
Chip cell survival after culture period	~90%	~80%
Osteogenic differentiation (quantitative)	++	++
Collagen 1 production (quantitative)	++	+ -
Mineralization (quantitative)	++	++
3D self-assembly	100%	~85%
Appearance	clearly defined firm tissue	less distinctly defined looser tissue
Coculture and long term-culture (35 days)	++	+

6.4 Discussion

Human MSCs were osteogenically differentiated in a bone-on-a-chip, perfused by gravity driven bidirectional flow. Gravity driven flow offers a simple perfusion method, requiring only a rocking plate and no pumps and tubing. ECM production in terms of collagen type 1 and mineralization were visualized and compared between static and dynamic cultures. After 21 days of culturing MSCs, MCs were added and cocultured for another 14 days, making a total of 35 days, resulting in a coculture of the two cell types that are essential for bone remodeling.

Homeostasis in bone tissue is influenced by shear stress generated by interstitial fluid flow in the lacunar-canalicular network.¹¹ Osteocytes are occupying the lacunae, small spaces in mineralized bone tissue. They are connected via narrow channels, the canaliculi, through which interstitial fluid is squeezed under influence of mechanical loading, creating a bidirectional fluid flow. A numerical model by Weinbaum *et al.* (1994) estimated the induced fluid flow shear stress sensed by osteocytic processes within their canaliculi to range between 0.8 and 3 Pa.^{11,230} In our system, the cells are expected to experience shear stress in a considerably lower range of 10 – 180 mPa. These cells are however, probably not (yet) osteocytes but MSCs differentiating towards osteoblasts. To investigate whether osteocytes are present, specialized techniques such as 3D focused ion beam scanning electron microscopy (FIB-SEM) are needed.²³¹ Next to this physiological shear stress felt by the osteocytes, many studies have shown that *in vitro* osteogenic differentiation of MSCs is supported by shear stresses in a broad range of 0.1 mPa – 1.03 Pa in microfluidic devices.^{203–206} This type of stimulation is more important in our system, as the MCSs first have to differentiate into osteoblasts. The shear stress values in our system are within this reported range.

Our expected shear stress was calculated based on empty channels and thus does not take into account the volume of the cells and produced matrix. Therefore, the calculations do not describe the mechanical environment correctly once the matrix volume starts to occupy the channel. Our previous research using computational models has shown a broad range in shear stress depending on the matrix produced by the cells (Chapter 5.3.3). Monolayer cells were expected to feel a shear stress of 3.66 mPa, while cells on the surface of the 3D tissues (osteoblasts) got up to 45.30 mPa. In future research, simulations would be beneficial to gain a more realistic image of the shear stress in the bidirectional flow system seeded with matrix producing cells.

Fluid shear stress regulates cell function by stimulating multiple intracellular signaling pathways.²³² We hypothesized that bidirectional flow enhances collagen type 1 deposition and mineralization compared to unidirectional flow and static cultures, as it mimics interstitial conditions.^{11,221} Comparing static and dynamic conditions, presence of collagen type 1 and minerals was seen in both types of culture. Self-assembled 3D constructs only formed when shear stress was applied, while in static conditions, the matrix remained 2D. Osteogenic culture medium containing ascorbic acid, dexamethasone and β -glycerophosphate turned out to be essential for matrix deposition and mineralization, which was not observed in control medium cultures without these supplements. Other studies have shown that osteogenic

differentiation is possible without chemical induction by osteogenic medium, solely by mechanical stimulation in both 2D^{233,234} and 3D,²³⁵ even in 3D without osteoinductive scaffold material.²²¹ Again, a broad range of shear stresses were used in these studies (0.2 mPa – 2.2 Pa), indicating that the optimal magnitude and duration of mechanical stimulation are yet to be determined. This optimum might be species-specific and donor-specific, complicating the search.²³⁵

Comparing unidirectional and bidirectional flow, our results did not confirm beneficial effects of bidirectional flow on collagen type 1 production and mineralization compared to unidirectional flow. This might be caused by a suspected lower shear stress in the bidirectional flow system compared to the unidirectional one. We observed (partly) obstructed channels in the bidirectional flow system, which certainly influenced the shear stress. A study directly comparing unidirectional and bidirectional flow in a perfusion bioreactor observed better ECM deposition when using bidirectional flow.²²¹ However, alkaline phosphatase (ALP) activity was not significantly different between the two flow types.²²¹ Unfortunately, our study is limited by a lack of quantitative data due to the small number of cells present in each chip (~7000), leading to undetectable results, obscured by culture medium interference. For future research, more sensitive methods need to be explored to obtain accurate quantitative data.

Taking together we have seen that both the bidirectional rocking plate system and our previous unidirectional pump system have their advantages and disadvantages for dynamically culturing bone-on-a-chip devices. With this research, we provided two different methods for dynamic culturing of these devices, that can be selected based on the specific goals of the research project. For example, the unidirectional pump systems shows more defined 3D firm tissues, which could be important when studying bone remodeling as osteoclasts need firm matrix to attach to and become functional.²³⁶ The bidirectional system however, could be preferred to study comparison of multiple groups as more samples can be studied simultaneously.

In conclusion, we have demonstrated the benefit of dynamic culturing for osteogenic differentiation in bone-on-a-chip devices. Gravity driven bidirectional flow offers a simple and scalable way to induce the desired dynamic cues by fluid flow shear stress. We also showed the suitability of the set-up for long term (35 days) cell culturing and coculturing of MSCs and MCs. In the future, gravity driven systems could offer an accessible solution towards higher throughput organ-on-chip models for drug testing.

Conflict of interest

The authors declare that the research was conducted in the absence of any commercial or financial relationships that could be construed as a potential conflict of interest.

Author contributions

MV, KI and SH contributed to conception, methodology and design of the study. MV and NvC performed the experiments. AP wrote the MATLAB script. AP, MV and NvC did the calculations. MV analyzed the results. MV wrote the original draft of the manuscript and

prepared the figures. All authors contributed to manuscript revision and approved the submitted version. MV, JdT, KI and SH contributed to the supervision. SH acquired funding for this research.

Funding

This work is part of the research program TTW with project number TTW 016.Vidi.188.021, which is (partly) financed by the Netherlands Organization for Scientific Research (NWO).

Supplementary Information

S1 Fluid-flow induced shear stress calculation

The Bernoulli equation is defined for time dependent height differences as follows:

$$\Delta P = \rho g \Delta h \quad \text{Bernoulli derived for height difference}$$

with

$$\Delta h = \sin(\alpha) l \quad \text{Define height difference by using the tilting angle of the plate}$$

gives

$$HT(t) = \sin\left(\alpha \sin\frac{2\pi t}{tt}\right) l \quad \text{For the tilting}$$

and

$$\Delta P = \rho g (HT(t) + HL(t - \Delta t) - HR(t - \Delta t))$$

For the height reservoirs: HR (right reservoir) and HL (left reservoir)

$$HR = HR(t - \Delta t) \pm \frac{Q(t)}{\pi r^2} \quad \text{Calculate current reservoir level by taking previous level and correcting with the flow rate to get current reservoir level}$$

$$HL = HL(t - \Delta t) \pm \frac{Q(t)}{\pi r^2}$$

Chapter 7

General discussion

7.1 Rationale and main findings

Healthy bone is maintained by the process of bone remodeling. An unbalance in this process leads to pathologies such as osteoporosis. Animal models are often used to study bone pathologies. However, data from animals frequently fail to predict the results obtained in human clinical trials. Human *in vitro* models are emerging as alternatives as they address the principle of reduction, refinement, and replacement of animal experiments (3Rs). Osteoblast-osteoclast cocultures can be used to study bone physiology, bone diseases and drugs in these models. The emergence of organ-on-chip, which utilizes microfluidic technology to simulate the natural environment of tissues, has enabled scientists to miniaturize tissue engineered constructs. This technology has great potential to improve the accuracy and efficiency of bone tissue engineering, as well as to provide insights into the underlying mechanisms of healthy and diseased bone.

7.1.1 Creating a systematic osteoblast-osteoclast coculture database

The use of osteoblast-osteoclast cocultures is not always clearly mentioned in the title and abstract in literature, making it difficult to identify these studies. As a result, researchers are all developing their own methods, leading to many methodological differences and incomparable results. Therefore, we systematically identified all osteoblast-osteoclast coculture studies that have been published before the year 2020 in **Chapter 2**. Differences in methods were mapped systematically in an openly available database, giving comprehensive details on cells, culture conditions and analytical techniques for using and studying osteoblast-osteoclast co-cultures. In this way, researchers can quickly identify publications relevant to their specific needs and easily validate and compare their work with existing literature.

7.1.2 Culture medium dialysis improves the microenvironment for cell culture

The first part of this thesis focused on ways to advance the microenvironment for *in vitro* bone remodeling models. Coculturing of cells in *in vitro* tissue models is widely used to study how they interact with each other. This asks for a highly specific environment, meeting the requirements of all involved cell types and therefore requires a great deal of optimization. We provided steps that can guide optimization of culture medium composition and volume in cocultures with a particular focus on cell communication via the cells' secretome in **Chapter 3**. The effect of medium exchange on cells is often an overlooked topic but particularly important for this type of cell communication. Medium exchange leads to loss of valuable auto- and paracrine factors produced by the cells but is necessary for nutrient supply and to prevent waste product accumulation. Thus, it remains the gold standard in cell culture applications. We proposed a method based on dialysis to reduce loss of the cells' secretome during culture medium exchange in **Chapter 4**. With our custom-made dialysis culture system, human mesenchymal stromal cells (MSCs) were differentiated into osteoblasts and monocytes (MCs) into osteoclasts while the secretome was maintained via dialysis. We showed an increased osteoblastic and osteoclastic activity in the dialysis groups compared to the standard non-dialysis groups. This culture system showed the potential to create a more efficient microenvironment compared to standard culture methods, allowing for cell

interactions via secreted factors in mono- and cocultures. In addition, this system could be applied for many other tissue types.

7.1.3 Bone-remodeling-on-a-chip with an osteoblast-osteoclast coculture

The second part of this thesis explored methods to miniaturize our *in vitro* bone remodeling models. At the moment, no complete *in vitro* model for bone-remodeling exists. Microfluidic chips offer great possibilities, particularly because of the dynamic culture options, which are crucial for *in vitro* bone formation. We developed a bone-on-a-chip coculture system in which human MSCs were differentiated into osteoblasts and self-assembled into scaffold free bone-like tissues with the shape and dimensions of human trabeculae in **Chapter 5**. Human MCs were able to attach to these tissues and to fuse into multinucleated osteoclast-like cells, establishing the coculture. Furthermore, a set-up was developed allowing for long-term (35 days) on-chip cell culture with benefits including continuous fluid-flow, low bubble formation risk, easy culture medium exchange inside the incubator and live-cell imaging options. In **Chapter 6**, we investigated the use of gravity-driven bidirectional flow for bone-on-a-chip devices. Perfusion set-ups require specialized pumps and tubing and can be rather complex. Gravity-driven flow could offer an alternative as it is simpler, requiring only a rocking plate which is readily available in most laboratories. The rocking motion enables a bidirectional flow inside the chip channel. We studied the effect of bidirectional flow on osteogenic differentiation of MSCs by comparing it with static cultures and our previous pump system with unidirectional flow. A clear benefit of flow compared to static cultures was seen in terms of extracellular matrix production and mineralization by the cells. With Chapter 5 and 6 we provided two different methods for dynamic culturing of bone-on-a-chip devices, of which each has its own advantages and can be selected based on the specific goals of the research project.

7.2 Challenges and perspectives for our bone-remodeling-on-a-chip

7.2.1 Combining culture medium dialysis and bone-remodeling-on-a-chip

In this thesis, two distinct objectives were achieved. First, the cell culture microenvironment was advanced by using a dialysis culture system (Chapter 4). Second, the bone remodeling model was miniaturized by using organ-on-chip technology (Chapter 5). The logical next step is then to combine this work. For this, a specialized medium reservoir has been designed, incorporating the dialysis membrane (Chapter 4), which can then be used with the bone-on-chip set-up (Chapter 5). The set-up with specialized reservoir can also be combined with any type of organ-on-chip, keeping it versatile in use. The standard reservoir (Chapter 5, Figure 5.1B) has been adjusted so that two compartments are separated by a dialysis membrane that is kept in place by a rubber O-ring (Figure 7.1A and B). The lower compartment is looped to the chip via tubing, creating an undisturbed cell culture microenvironment (Figure 7.1C). The upper compartment allows for culture medium change. Nutrients and waste products will diffuse through the dialysis membrane, while the cell' secretome remains in the lower cell culture compartment. Two rubber injection ports provide access to the two compartments, one for medium sampling (lower compartment) and one for medium change (upper compartment). The study is currently ongoing. Hopefully this set-up will allow for an enhanced microenvironment for cell communication in our bone-remodeling-

on-a-chip which is particularly important for cell communication in the osteoblast-osteoclast coculture as shown in Chapter 4.

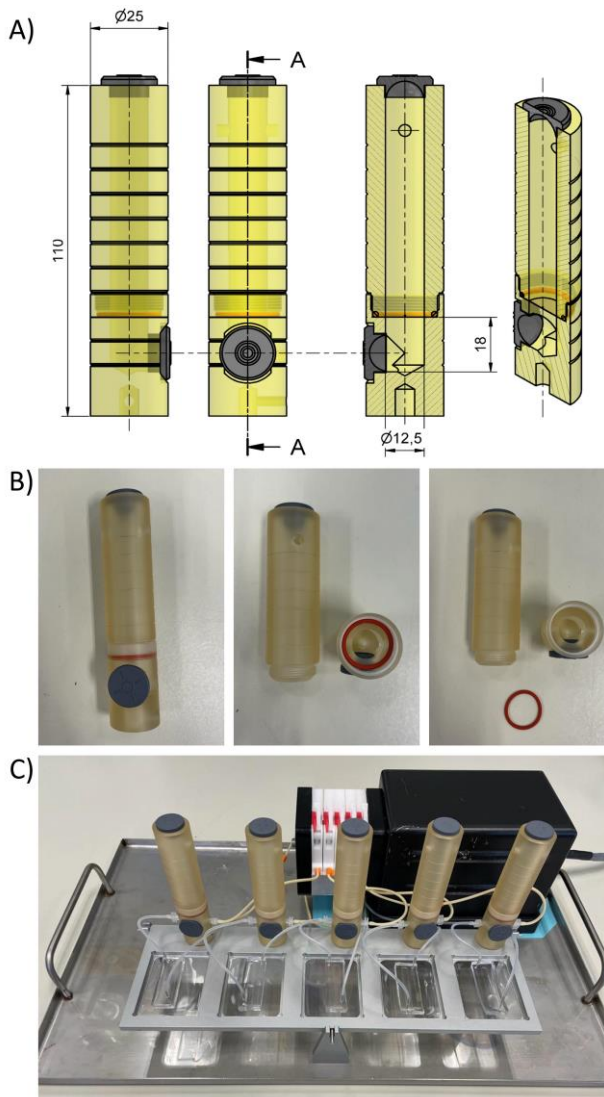


Figure 7.1 Design of the specialized reservoir for incorporating a dialysis membrane in the bone-remodeling-on-a-chip cell culture set-up. A) Detailed drawing of the reservoir. Measures are in millimeter. B) Photograph of the reservoir with two compartments, separated by a dialysis membrane that is hold in place with use of a rubber O-ring (red). The reservoirs are made of out of polysulfone and have rubber self-healing injection ports (grey). C) The total cell culture set-up with a peristaltic pump and five reservoirs connected to five chips.

7.2.2 Demonstration of bone remodeling

Our current work shows MSCs that differentiate into osteoblast and produce a bone-like tissue and MCs that differentiate into osteoclasts (Chapter 5). We did not yet show actual bone remodeling which requires demonstration of both formation and resorption events. To

demonstrate this, micro computed tomography (μ CT) or even nano CT could be used.^{175,237,238} By registering consecutive CT images it is possible to reveal both formation and resorption within a sample over time.²³⁷ CT is a non-destructive method and is therefore well suited to monitor mineralized volume change within the same samples over a longer period of time.

Supernatant analysis can be performed to detect analytes as a measure for bone formation and resorption, for example an enzyme-linked immuno sorbent assay (ELISA) of collagen type 1 propeptide for formation and telopeptide for resorption. We did use this method in Chapter 5 but were not able to show significant differences. This is probably due to dilution of secreted growth factors as we used large media reservoirs in combination with a small number of cells. With the combined dialysis and chip set-up (combining Chapter 4 and 5) we hope to overcome this limitation by maintaining the cell' secretome over the culture period.

In future research, compression can be introduced to the chip. In this way it is possible to study if our formed bone tissue will adapt in response to mechanical loading as is known from *in vivo*.²³⁹ Our model can also be developed further by investigating whether osteocytes are present. Osteocytes are considered to be the regulators of bone remodeling and are thus important to incorporate in the *in vitro* model. To investigate the presence of osteocytes, immunostainings such as early osteocyte markers dentin matrix protein-1 (DMP-1) and podoplanin, and late marker sclerostin can be investigated.²³¹ We did stain for DMP-1, which was visible in the nucleus (Chapter 5, Figure 5.5). However, to indicate early differentiation into osteocytes, the protein should be exported to the extracellular matrix, where it orchestrates mineralized matrix formation.²⁴⁰ Furthermore, osteocytes are embedded within the matrix of the tissue, making them invisible from the outside. We attempted to slice through the tissues by means of cryosectioning, but were unsuccessful due to the small dimensions of the tissues. In the future, specialized techniques such as 3D focused ion beam scanning electron microscopy (FIB-SEM) can be used to investigate whether osteocytes are present within the tissues.²³¹

7.3 Challenges and perspectives for the organ-on-chip field

7.3.1 Integration of biosensors

Integration of biosensors into tissue culture systems enables long-term monitoring of the microenvironments in these systems.¹⁴⁶ Biosensors should be able to detect biophysical parameters such as osmolarity, pH, and oxygen concentration as well as biochemical parameters such as biomarkers, cytokines and drug molecules.¹⁴⁶ An ideal cell culture system contains sensors that frequently evaluate developmental and functional parameters in a cell culture without the need for manual sample collection.¹⁴⁷

Organ-on-chip systems are often mentioned to have the benefit of integrating sensors. However, currently most analyses still take place off-chip and as endpoint measurements.¹⁶ Integrating biosensors could provide noninvasive, continuous monitoring of the experiment. In- and online biosensors show potential for providing real-time information regarding media composition.^{145,147,241} Multiplexed sensing, recording, and processing of real-time data could

provide novel insights into the optimal nutrients and culture conditions needed to maintain cell viability and to grow cells for up to weeks.¹⁴⁷ Furthermore, real-time data analytics can be used to respond to changes in culture conditions, adjusting inputs to obtain desired results.¹⁴⁷ For example, media composition can be tracked as a cell differentiates to determine how differentiation is progressing and accordingly growth factors can be removed or added to encourage or slow down further differentiation.¹⁴⁷

In the future, organ-on-chip research is heading towards automated and self-contained systems, which is necessary to enable cost effective high throughput drug screening. With the upcoming development of artificial intelligence algorithms, these systems are likely to become capable of autonomous decision-making. For example, in automated bone-remodeling-on-a-chip, biosensors could be used to accommodate for the differences in differentiation timelines between donors. When MSCs have differentiated into osteoblasts, automated monocyte seeding and culture medium change is triggered. After the monocytes have differentiated into osteoclasts, drugs are added and the response is monitored. Data will be collected automatically and sent to the researchers, allowing for high throughput screening and even personalized medicine.

7.3.2 Multidisciplinarity is key, complexity a pitfall

Organ-on-chip asks for biological, mechanical, mathematical, biochemical and engineering knowledge. In the organ-on-chip field, the necessity of multidisciplinarity is a recurring theme. Due to the complexities of the culture systems, interdisciplinary collaboration is essential.^{10,16} Many separate building blocks such as coculture techniques, complex microfluidic chip designs, integrated sensors and predictive models exist. However, to date, the combining efforts usually excel in one aspect but still lack complexity in the others, which can only be solved through a collective effort from multiple disciplines.

In addition, openness in sharing protocols and challenges is an essential part of the development of organ-on-chip systems. By openly sharing protocols and challenges, researchers are able to leverage the collective knowledge in the field and avoid the time and effort spent on reinventing the wheel. It is important to share not only the results, but also clear information on the methods and set-up of experiments. To provide a more comprehensive overview of the process, it is recommended to include data on the percentage of successful experiments in comparison to non-successful ones, as well as behind-the-scenes photographs of set-up in the incubator as shown in Chapter 5 (Supplementary Information S5.2).

The introduction of high-end organ-on-chip systems through multidisciplinary collaborations is a promising development. Nonetheless, the tradeoff between complexity and usability must carefully be considered. Researchers often try to replicate *in vivo* as close as possible, but that might not always be needed. More complex experiments are less easy to execute, leading to reproducibility issues and high costs. The level of complexity is therefore inversely correlated to the clinical translation.²⁴² To get to functional and usable organ-on-chips, parameters such as reproducibility, handling and costs need to be considered during the design phase.

7.3.3 Towards replacing animal models

In order to achieve a high level of success in creating *in vitro* on-chip alternatives to animal models, several steps have to be taken. Up until now, a few organ-on-chip models have reached the market, but the commercialization and application of the technology still lags behind high-profile academic research.²⁴³ This is largely because innovative organ-on-chip models have not yet been independently standardized, valorized, and qualified, making the value for end-users unclear.²⁴³ For this, an overarching consortium between academia, industry and regulators is necessary. Fortunately, this large consortium has already been founded.

In 2017, an European project called Organ-on-Chip In Development (ORCHID) started with the goal of creating a roadmap for organ-on-chip technology and of building a network of academic, research, industrial and regulatory institutions to move organ-on-chip devices from laboratories into industry.^{184,244} Experts were asked to share their views on the state-of-the-art, unmet needs, challenges and barriers of the field.¹⁸⁴ The major challenges for the acceptance of these organ-on-chips are: standardization, qualification, production and upscaling. It was strongly emphasized that there is an urgent need for an infrastructure that will be used for testing, qualification and standardization, to generate data and methodology accessible to end users and the research community.²⁴⁵

Different research groups generally use different protocols and only a relatively small number of samples/chips. This makes validation of the chip models more complicated. True validation will require large-scale evaluation, involving hundreds of devices of the same design carried out using the same protocols.³ Thus, it is unlikely that true validation will be achieved by academic researchers.³ Instead, it will probably be handled by the commercial market, which is now possible given that an increasing number of companies are manufacturing organ-on-chip devices as well as automated control systems to run them.³

In order to validate organ-on-chip devices, compounds and drugs that already demonstrated to be toxic or effective in animals or patients should show similar effects in organ-on-chip models.²⁴⁴ First, these comparison tests need to be run parallel to animal experiments or clinical trials. For comparing animal experiments, organ-on-chip devices using animal cells could be used. Eventually, the ultimate benchmark for success should be the replication of existing *in vivo* human clinical data.³

A recent organ-on chip study shows an example of how to deal with validation. In this study, 870 liver chips were analyzed to determine their ability to predict drug-induced liver injury caused by small molecules identified as benchmarks by a consortium of multiple pharmaceutical and biotechnological companies.¹⁴ The liver chip met the qualification guidelines across a blinded set of 27 known hepatotoxic and non-toxic drugs with a sensitivity of 87% and a specificity of 100%.^{3,246} With this, the chip demonstrated a major improvement in performance relative to hepatic spheroids (sensitivity of 42% and specificity of 67%)^{247,248} and animal models, in which eight of the tested components were approved for clinical use after which liver toxicity was identified in humans.

Eventually the combined efforts of these extensive consortia will hopefully provide us with validated organ-on-chip devices. The process of acceptance will probably happen gradually with replacement of one animal model at a time, but the first steps have been taken.³

7.4 General conclusion

To conclude, this thesis provides strategies for the microenvironmental advancement and miniaturization of human *in vitro* bone remodeling models. We are the first to show a fully human 3D direct osteoblast-osteoclast coculture on a chip. The systems we developed are not only of interest for bone tissue engineering applications but could also be used with many other tissue types. First, the dialysis system could be used for the proliferation and differentiation of different cell types. Particularly in cocultures it could enhance the cell communication through retainment of soluble factors. Second, the microfluidic chip set-up could be combined with any type of microfluidic chip and used for dynamic fluid flow cultures. With this thesis we aimed to hand out tools for improvement of *in vitro* models with the ultimate goal of replacing, reducing, and refining the use of animal models. We believe that *in vitro* models will provide reliable and predictive alternatives to animal testing in the future.

Bibliography

1. Clarke B. Normal Bone Anatomy and Physiology. *Clin J Am Soc Nephrol CJASN*. 2008;3(Suppl 3):S131-S139. doi:10.2215/CJN.04151206
2. Willem Lems, Agnes Offenbergh, Peter van den Berg, Joop van den Bergh, Natasha Appleman, Gijs de Klerk. Solutions for Fracture Prevention in the Netherlands. Published online January 2023. Accessed February 3, 2023. https://www.osteoporosis.foundation/sites/fofbonehealth/files/2023-01/2022_country_profile_ned_25.01.pdf
3. Ingber DE. Human organs-on-chips for disease modelling, drug development and personalized medicine. *Nat Rev Genet*. 2022;23(8):467-491. doi:10.1038/s41576-022-00466-9
4. Wong CH, Siah KW, Lo AW. Estimation of clinical trial success rates and related parameters. *Biostat Oxf Engl*. 2019;20(2):273-286. doi:10.1093/biostatistics/kxx069
5. Stranding S. *Gray's Anatomy - 42nd Edition*. Accessed January 23, 2023. <https://www.elsevier.com/books/gray's-anatomy/978-0-7020-7705-0>
6. de Wildt BWM, Ansari S, Sommerdijk NAJM, Ito K, Akiva A, Hofmann S. From bone regeneration to three-dimensional in vitro models: tissue engineering of organized bone extracellular matrix. *Curr Opin Biomed Eng*. 2019;10:107-115. doi:10.1016/j.cobme.2019.05.005
7. Owen R, Reilly GC. In vitro Models of Bone Remodelling and Associated Disorders. *Front Bioeng Biotechnol*. 2018;6. doi:10.3389/fbioe.2018.00134
8. Marieb EN, Hoehn K. *Human Anatomy And Physiology*. 9th ed. Pearson; 2012.
9. Tresguerres FGF, Torres J, López-Quiles J, Hernández G, Vega JA, Tresguerres IF. The osteocyte: A multifunctional cell within the bone. *Ann Anat - Anat Anz*. 2020;227:151422. doi:10.1016/j.aanat.2019.151422
10. Truesdell SL, Saunders MM. Bone remodeling platforms: Understanding the need for multicellular lab-on-a-chip systems and predictive agent-based models. *Math Biosci Eng MBE*. 2019;17(2):1233-1252. doi:10.3934/mbe.2020063
11. Wittkowske C, Reilly GC, Lacroix D, Perrault CM. In Vitro Bone Cell Models: Impact of Fluid Shear Stress on Bone Formation. *Front Bioeng Biotechnol*. 2016;4:87. doi:10.3389/fbioe.2016.00087
12. Kolb FO. Clinical Essentials of Calcium and Skeletal Disorders. *Ann Intern Med*. 1999;131(8):635. doi:10.7326/0003-4819-131-8-199910190-00033
13. Langer R, Vacanti JP. Tissue engineering. *Science*. 1993;260(5110):920-926. doi:10.1126/science.8493529
14. Russell WMS, Burch RL. *The Principles of Humane Experimental Technique*. Methuen & Co.; 1959.
15. Sung JH, Wang YI, Sriram NN, et al. Recent advances in body-on-a-chip systems. *Anal Chem*. 2019;91(1):330-351. doi:10.1021/acs.analchem.8b05293
16. Zhang Y, Yu T, Ding J, Li Z. Bone-on-a-chip platforms and integrated biosensors: Towards advanced in vitro bone models with real-time biosensing. *Biosens Bioelectron*. 2023;219:114798. doi:10.1016/j.bios.2022.114798
17. Mizoguchi T, Ono N. The diverse origin of bone-forming osteoblasts. *J Bone Miner Res*. 2021;36(8):1432-1447. doi:10.1002/jbmr.4410
18. Marks SC, Seifert MF. The lifespan of osteoclasts: Experimental studies using the giant granule cytoplasmic marker characteristic of beige mice. *Bone*. 1985;6(6):451-455. doi:10.1016/8756-3282(85)90223-6
19. Jilka RL, O'Brien CA. The Role of Osteocytes in Age-Related Bone Loss. *Curr Osteoporos Rep*. 2016;14(1):16-25. doi:10.1007/s11914-016-0297-0
20. Buenzli PR, Pivonka P, Smith DW. Spatio-temporal structure of cell distribution in cortical Bone Multicellular Units: A mathematical model. *Bone*. 2011;48(4):918-926. doi:10.1016/j.bone.2010.12.009
21. Feng X, McDonald JM. Disorders of Bone Remodeling. *Annu Rev Pathol*. 2011;6:121-145. doi:10.1146/annurev-pathol-011110-130203
22. Burkhardt AM, Zlotnik A. Translating translational research: mouse models of human disease. *Cell Mol Immunol*. 2013;10(5):373-374. doi:10.1038/cmi.2013.19
23. Contopoulos-Ioannidis DG, Ntzani E, Ioannidis JPA. Translation of highly promising basic science research into clinical applications. *Am J Med*. 2003;114(6):477-484.

24. Montagutelli X. Animal models are essential to biological research: issues and perspectives. *Future Sci OA*. 2015;1(4). doi:10.4155/FSO.15.63
25. Thomas DW, Burns J, Audette J, Adam Carroll, Dow-Hygelund C, Hay M. *Clinical Development Success Rates 2006-2015*.; 2016.
26. Owen R, Reilly GC. In vitro Models of Bone Remodelling and Associated Disorders. *Front Bioeng Biotechnol*. 2018;6:134. doi:10.3389/FBIOE.2018.00134
27. Holmes A, Brown R, Shakesheff K. Engineering tissue alternatives to animals: applying tissue engineering to basic research and safety testing. *Regen Med*. 2009;4(4):579-592. doi:10.2217/rme.09.26
28. Chambers TJ. Osteoblasts release osteoclasts from calcitonin-induced quiescence. *J Cell Sci*. 1982;57:247-260.
29. Takahashi N, Akatsu T, Udagawa N, et al. Osteoblastic cells are involved in osteoclast formation. *Endocrinology*. 1988;123(5):2600-2602. doi:10.1210/endo-123-5-2600
30. Simonet WS, Lacey DL, Dunstan CR, et al. Osteoprotegerin: A novel secreted protein involved in the regulation of bone density. *Cell*. 1997;89(2):309-319. doi:10.1016/S0092-8674(00)80209-3
31. Udagawa N, Takahashi N, Akatsu T, et al. Origin of osteoclasts: mature monocytes and macrophages are capable of differentiating into osteoclasts under a suitable microenvironment prepared by bone marrow-derived stromal cells. *Proc Natl Acad Sci U S A*. 1990;87(18):7260-7264. doi:10.1073/pnas.87.18.7260
32. Teitelbaum SL. Bone resorption by osteoclasts. *Science*. 2000;289(5484):1504-1508.
33. Suda T, Takahashi N, Udagawa N, Jimi E, Gillespie MT, Martin TJ. Modulation of Osteoclast Differentiation and Function by the New Members of the Tumor Necrosis Factor Receptor and Ligand Families. *Endocr Rev*. 1999;20(3):345-357. doi:10.1210/edrv.20.3.0367
34. de Vries RBM, Hooijmans CR, Langendam MW, et al. A protocol format for the preparation, registration and publication of systematic reviews of animal intervention studies. *Evid-Based Preclin Med*. 2015;2(1):e00007. doi:10.1002/ebm2.7
35. Remmers SJA, Wildt BWM, Vis MVA, et al. Osteoblast-osteoclast co-culture models of bone-remodelling: A systematic review protocol. doi:10.5281/ZENODO.3969441
36. Ouzzani M, Hammady H, Fedorowicz Z, Elmagarmid A. Rayyan-a web and mobile app for systematic reviews. *Syst Rev*. 2016;5(1):210. doi:10.1186/s13643-016-0384-4
37. Jemnitz K, Veres Z, Monostory K, Kóbori L, Vereczkey L. Interspecies differences in acetaminophen sensitivity of human, rat, and mouse primary hepatocytes. *Toxicol In Vitro*. 2008;22(4):961-967. doi:10.1016/j.tiv.2008.02.001
38. Bitar M, Brown RA, Salih V, Kidane AG, Knowles JC, Nazhat SN. Effect of cell density on osteoblastic differentiation and matrix degradation of biomimetic dense collagen scaffolds. *Biomacromolecules*. 2008;9(1):129-135. doi:10.1021/bm701112w
39. Jolly JJ, Chin KY, Farhana MFN, et al. Optimization of the Static Human Osteoblast/Osteoclast Co-culture System. *Iran J Med Sci*. 2018;43(2):208-213.
40. Jones GL, Motta A, Marshall MJ, El Haj AJ, Cartmell SH. Osteoblast: osteoclast co-cultures on silk fibroin, chitosan and PLLA films. *Biomaterials*. 2009;30(29):5376-5384.
41. De Vries TJ, Schoenmaker T, Aerts D, et al. M-CSF priming of osteoclast precursors can cause osteoclastogenesis-insensitivity, which can be prevented and overcome on bone. *J Cell Physiol*. 2015;230(1):210-225. doi:10.1002/jcp.24702
42. Kyllönen L, Haimi S, Mannerström B, et al. Effects of different serum conditions on osteogenic differentiation of human adipose stem cells in vitro. *Stem Cell Res Ther*. 2013;4(1):17. doi:10.1186/scri165
43. Suda T, Takahashi N, Udagawa N, Jimi E, Gillespie MT, Martin TJ. Modulation of osteoclast differentiation and function by the new members of the tumor necrosis factor receptor and ligand families. *Endocr Rev*. 1999;20(3):345-357. doi:10.1210/edrv.20.3.0367
44. Lindner U, Kramer J, Rohwedel J, Schlenke P. Mesenchymal stem or stromal cells: Toward a better understanding of their biology? *Transfus Med Hemotherapy*. 2010;37(2):75-83. doi:10.1159/000290897
45. Clarke MSF, Sundaresan A, Vanderburg CR, Banigan MG, Pellis NR. A three-dimensional tissue culture model of bone formation utilizing rotational co-culture of human adult osteoblasts and osteoclasts. *Acta Biomater*. 2013;9(8):7908-7916. doi:10.1016/j.actbio.2013.04.051

46. Kadow-Romacker A, Duda GN, Bormann N, Schmidmaier G, Wildemann B. Slight changes in the mechanical stimulation affects osteoblast- and osteoclast-like cells in co-culture. *Transfus Med Hemother*. 2013;40(6):441-447. doi:10.1159/000356284
47. Hammerl A, Diaz Cano CE, De-Juan-Pardo EM, van Griensven M, Poh PSP. A Growth Factor-Free Co-Culture System of Osteoblasts and Peripheral Blood Mononuclear Cells for the Evaluation of the Osteogenesis Potential of Melt-Electrowritten Polycaprolactone Scaffolds. *Int J Mol Sci*. 2019;20(5).
48. Bongio M, Lopa S, Gilardi M, Bersini S, Moretti M. A 3D vascularized bone remodeling model combining osteoblasts and osteoclasts in a CaP nanoparticle-enriched matrix. *Nanomed*. 2016;11(9):1073-1091. doi:10.2217/nnm-2015-0021
49. Domaschke H, Gelinsky M, Burmeister B, et al. In vitro ossification and remodeling of mineralized collagen I scaffolds. *Tissue Eng*. 2006;12(4):949-958. doi:10.1089/ten.2006.12.949
50. Schroder HC, Wang XH, Wiens M, et al. Silicate modulates the cross-talk between osteoblasts (SaOS-2) and osteoclasts (RAW 264.7 cells): inhibition of osteoclast growth and differentiation. *J Cell Biochem*. 2012;113(10):3197-3206.
51. Domaschke H, Gelinsky M, Burmeister B, et al. In vitro ossification and remodeling of mineralized collagen I scaffolds. *Tissue Eng*. 2006;12(4):949-958.
52. Hagenmüller H, Hofmann S, Kohler T, et al. Non-invasive time-lapsed monitoring and quantification of engineered bone-like tissue. *Ann Biomed Eng*. 2007;35(10):1657-1667. doi:10.1007/s10439-007-9338-2
53. Rossi E, Mracsco E, Papadimitropoulos A, et al. An In Vitro Bone Model to Investigate the Role of Triggering Receptor Expressed on Myeloid Cells-2 in Bone Homeostasis. *Tissue Eng Part C Methods*. 2018;24(7):391-398.
54. Krishnan V, Vogler EA, Sosnoski DM, Mastro AM. In vitro mimics of bone remodeling and the vicious cycle of cancer in bone. *J Cell Physiol*. 2014;229(4):453-462.
55. Boanini E, Torricelli P, Sima F, et al. Strontium and zoledronate hydroxyapatites graded composite coatings for bone prostheses. *J Colloid Interface Sci*. 2015;448:1-7.
56. Melke J, Zhao F, van Rietbergen B, Ito K, Hofmann S. Localisation of mineralised tissue in a complex spinner flask environment correlates with predicted wall shear stress level localisation. *Eur Cell Mater*. 2018;36:57-68. doi:10.22203/eCM.v036a05
57. Remmers S, Mayer D, Melke J, Ito K, Hofmann S. Measuring mineralised tissue formation and resorption in a human 3d osteoblast-osteoclast co-culture model. *Eur Cell Mater*. 2020;40:189-202. doi:10.22203/eCM.v040a12
58. Shetty S, Kapoor N, Bondu J, Thomas N, Paul T. Bone turnover markers: Emerging tool in the management of osteoporosis. *Indian J Endocrinol Metab*. 2016;20(6):846-852. doi:10.4103/2230-8210.192914
59. Golub EE, Boesze-Battaglia K. The role of alkaline phosphatase in mineralization. *Curr Opin Orthop*. 2007;18(5):444-448. doi:10.1097/BCO.0b013e3282630851
60. Sheu TJ, Schwarz EM, Martinez DA, et al. A phage display technique identifies a novel regulator of cell differentiation. *J Biol Chem*. 2003;278(1):438-443. doi:10.1074/jbc.M208292200
61. Kim YH, Yoon DS, Kim HO, Lee JW. Characterization of different subpopulations from bone marrow-derived mesenchymal stromal cells by alkaline phosphatase expression. *Stem Cells Dev*. 2012;21(16):2958-2968. doi:10.1089/scd.2011.0349
62. Vaughan A, Guilbault GG, Hackney D. Fluorometric methods for analysis of acid and alkaline phosphatase. *Anal Chem*. 1971;43(6):721-724. doi:10.1021/ac60301a001
63. Jancikla AJ, Takahashi K, Sun SZ, Yam LT. Naphthol-ASBI phosphate as a preferred substrate for tartrate-resistant acid phosphatase isoform 5b. *J Bone Miner Res*. 2001;16(4):788-793. doi:10.1359/jbmr.2001.16.4.788
64. Engvall E, Perlmann P. Enzyme-linked immunosorbent assay (ELISA) quantitative assay of immunoglobulin G. *Immunochemistry*. 1971;8(9):871-874. doi:10.1016/0019-2791(71)90454-X
65. Halleen JM, Tiitinen SL, Ylipahkala H, Fagerlund KM, Väänänen HK. Tartrate-resistant acid phosphatase 5b (TRACP 5b) as a marker of bone resorption. *Clin Lab*. 2006;52(9-10):499-509.
66. Halleen JM, Ylipahkala H, Alatalo SL, et al. Serum tartrate-resistant acid phosphatase 5b, but not 5a, correlates with other markers of bone turnover and bone mineral density. *Calcif Tissue Int*. 2002;71(1):20-25. doi:10.1007/s00223-001-2122-7

67. Young PS, Tsimbouri PM, Gadegaard N, Meek R, Dalby MJ. Osteoclastogenesis/osteoblastogenesis using human bone marrow-derived cocultures on nanotopographical polymer surfaces. *Nanomed*. 2015;10(6):949-957. doi:10.2217/nnm.14.146
68. Hikita A, Iimura T, Oshima Y, Saitou T, Yamamoto S, Imamura T. Analyses of bone modeling and remodeling using in vitro reconstitution system with two-photon microscopy. *Bone*. 2015;76:5-17.
69. Parfitt AM. Osteonal and hemi-osteonal remodeling: The spatial and temporal framework for signal traffic in adult human bone. *J Cell Biochem*. 1994;55(3):273-286. doi:10.1002/jcb.240550303
70. Manolagas SC. Birth and death of bone cells: basic regulatory mechanisms and implications for the pathogenesis and treatment of osteoporosis. *Endocr Rev*. 2000;21(2):115-137. doi:10.1210/edrv.21.2.0395
71. Susa M, Luong-Nguyen NH, Cappellen D, Zamurovic N, Gamse R. Human primary osteoclasts: in vitro generation and applications as pharmacological and clinical assay. *J Transl Med*. 2004;2(1):6. doi:10.1186/1479-5876-2-6
72. Yang J, Qiao M, Li Y, et al. Expansion of a population of large monocytes (atypical monocytes) in peripheral blood of patients with acute exacerbations of chronic obstructive pulmonary diseases. *Mediators Inflamm*. 2018;2018:1-13. doi:10.1155/2018/9031452
73. Pittenger MF, Mackay AM, Beck SC, et al. Multilineage potential of adult human mesenchymal stem cells. *Science*. 1999;284(5411):143-147.
74. Vis MAM, Ito K, Hofmann S. Impact of Culture Medium on Cellular Interactions in in vitro Co-culture Systems. *Front Bioeng Biotechnol*. 2020;8:911. doi:10.3389/fbioe.2020.00911
75. van der Valk J, Bieback K, Buta C, et al. Fetal Bovine Serum (FBS): Past - Present - Future. *ALTEX*. 2018;35(1):99-118. doi:10.14573/altex.1705101
76. Langenbach F, Handschel J. Effects of dexamethasone, ascorbic acid and β -glycerophosphate on the osteogenic differentiation of stem cells in vitro. *Stem Cell Res Ther*. 2013;4(5):117. doi:10.1186/scrt328
77. Wiedmann-Al-Ahmad M, Gutwald R, Lauer G, Hübner U, Schmelzeisen R. How to optimize seeding and culturing of human osteoblast-like cells on various biomaterials. *Biomaterials*. 2002;23(16):3319-3328. doi:10.1016/S0142-9612(02)00019-4
78. Motiur Rahman M, Takeshita S, Matsuoka K, et al. Proliferation-coupled osteoclast differentiation by RANKL: Cell density as a determinant of osteoclast formation. *Bone*. 2015;81:392-399. doi:10.1016/j.bone.2015.08.008
79. Gruber HE, Ivey JL, Thompson ER, Chesnut CH, Baylink DJ. Osteoblast and osteoclast cell number and cell activity in postmenopausal osteoporosis. *Miner Electrolyte Metab*. 1986;12(4):246-254.
80. Holmes A, Brown R, Shakesheff K. Engineering tissue alternatives to animals: applying tissue engineering to basic research and safety testing. *Regen Med*. 2009;4(4):579-592. doi:10.2217/rme.09.26
81. Thomson JA, Itskovitz-Eldor J, Shapiro SS, et al. Embryonic Stem Cell Lines Derived from Human Blastocysts. *Science*. 1998;282(5391):1145-1147. doi:10.1126/science.282.5391.1145
82. Holloway EM, Capeling MM, Spence JR. Biologically inspired approaches to enhance human organoid complexity. *Dev Camb Engl*. 2019;146(8). doi:10.1242/dev.166173
83. Esch MB, Smith AST, Prot JM, Oleaga C, Hickman JJ, Shuler ML. How multi-organ microdevices can help foster drug development. *Adv Drug Deliv Rev*. 2014;69-70:158-169. doi:10.1016/j.addr.2013.12.003
84. Fu J, Fernandez D, Ferrer M, Titus SA, Buehler E, Lal-Nag MA. RNAi High-Throughput Screening of Single- and Multi-Cell-Type Tumor Spheroids: A Comprehensive Analysis in Two and Three Dimensions. *SLAS Discov Adv Life Sci RD*. 2017;22(5):525-536. doi:10.1177/2472555217696796
85. Zhang C, Bakker AD, Klein-Nulend J, Bravenboer N. Studies on Osteocytes in Their 3D Native Matrix Versus 2D In Vitro Models. *Curr Osteoporos Rep*. 2019;17(4):207-216. doi:10.1007/s11914-019-00521-1
86. Caddeo S, Boffito M, Sartori S. Tissue Engineering Approaches in the Design of Healthy and Pathological In Vitro Tissue Models. *Front Bioeng Biotechnol*. 2017;5. doi:10.3389/fbioe.2017.00040
87. Robin M, Almeida C, Azais T, et al. Involvement of 3D osteoblast migration and bone apatite during in vitro early osteocytogenesis. *Bone*. 2016;88:146-156. doi:10.1016/j.bone.2016.04.031

88. Rossi E, Mracsko E, Papadimitropoulos A, et al. An In Vitro Bone Model to Investigate the Role of Triggering Receptor Expressed on Myeloid Cells-2 in Bone Homeostasis. *Tissue Eng Part C Methods*. 2018;24(7):391-398. doi:10.1089/ten.TEC.2018.0061
89. Guzmán R, Nardecchia S, Gutiérrez MC, et al. Chitosan scaffolds containing calcium phosphate salts and rhBMP-2: in vitro and in vivo testing for bone tissue regeneration. *PLoS One*. 2014;9(2):e87149. doi:10.1371/journal.pone.0087149
90. Salamanna F, Borsari V, Brogini S, et al. An in vitro 3D bone metastasis model by using a human bone tissue culture and human sex-related cancer cells. *Oncotarget*. 2016;7(47):76966-76983. doi:10.18632/oncotarget.12763
91. Goers L, Freemont P, Polizzi KM. Co-culture systems and technologies: taking synthetic biology to the next level. *J R Soc Interface*. 2014;11(96). doi:10.1098/rsif.2014.0065
92. Jessup CM, Kassen R, Forde SE, et al. Big questions, small worlds: microbial model systems in ecology. *Trends Ecol Evol*. 2004;19(4):189-197. doi:10.1016/j.tree.2004.01.008
93. Liu Y, Chan JKY, Teoh SH. Review of vascularised bone tissue-engineering strategies with a focus on co-culture systems. *J Tissue Eng Regen Med*. 2015;9(2):85-105. doi:10.1002/term.1617
94. Paschos NK, Brown WE, Eswaramoorthy R, Hu JC, Athanasiou KA. Advances in tissue engineering through stem cell-based co-culture. *J Tissue Eng Regen Med*. 2015;9(5):488-503. doi:10.1002/term.1870
95. Wang YI, Abaci HE, Shuler ML. Microfluidic blood-brain barrier model provides in vivo-like barrier properties for drug permeability screening. *Biotechnol Bioeng*. 2017;114(1):184-194. doi:10.1002/bit.26045
96. Strikoudis A, Cieślak A, Loffredo L, et al. Modeling of Fibrotic Lung Disease Using 3D Organoids Derived from Human Pluripotent Stem Cells. *Cell Rep*. 2019;27(12):3709-3723.e5. doi:10.1016/j.celrep.2019.05.077
97. Jalili-Firoozinezhad S, Gazzaniga FS, Calamari EL, et al. A complex human gut microbiome cultured in an anaerobic intestine-on-a-chip. *Nat Biomed Eng*. 2019;3(7):520-531. doi:10.1038/s41551-019-0397-0
98. Takasato M, Little MH. Making a Kidney Organoid Using the Directed Differentiation of Human Pluripotent Stem Cells. *Methods Mol Biol Clifton NJ*. 2017;1597:195-206. doi:10.1007/978-1-4939-6949-4_14
99. Saadeldin IM, Kim SJ, Choi YB, Lee BC. Improvement of cloned embryos development by co-culturing with parthenotes: a possible role of exosomes/microvesicles for embryos paracrine communication. *Cell Reprogramming*. 2014;16(3):223-234. doi:10.1089/cell.2014.0003
100. Saadeldin IM, Elsayed A, Kim SJ, Moon JH, Lee BC. A spatial model showing differences between juxtacrine and paracrine mutual oocyte-granulosa cells interactions. *Indian J Exp Biol*. 2015;53(2):75-81.
101. Skaper SD, Facci L. Central Nervous System Neuron-Glia co-Culture Models and Application to Neuroprotective Agents. *Methods Mol Biol Clifton NJ*. 2018;1727:63-80. doi:10.1007/978-1-4939-7571-6_5
102. Coll M, Perea L, Boon R, et al. Generation of Hepatic Stellate Cells from Human Pluripotent Stem Cells Enables In Vitro Modeling of Liver Fibrosis. *Cell Stem Cell*. 2018;23(1):101-113.e7. doi:10.1016/j.stem.2018.05.027
103. Venter C, Niesler C. A triple co-culture method to investigate the effect of macrophages and fibroblasts on myoblast proliferation and migration. *BioTechniques*. 2018;64(2):52-58. doi:10.2144/btn-2017-0100
104. Churm R, Dunseath GJ, Prior SL, Thomas RL, Banerjee S, Owens DR. Development and characterization of an in vitro system of the human retina using cultured cell lines. *Clin Experiment Ophthalmol*. Published online June 29, 2019. doi:10.1111/ceo.13578
105. Lin Y, Huang S, Zou R, et al. Calcium phosphate cement scaffold with stem cell co-culture and prevascularization for dental and craniofacial bone tissue engineering. *Dent Mater Off Publ Acad Dent Mater*. 2019;35(7):1031-1041. doi:10.1016/j.dental.2019.04.009
106. Zhang C, Zhao Z, Abdul Rahim NA, van Noort D, Yu H. Towards a human-on-chip: culturing multiple cell types on a chip with compartmentalized microenvironments. *Lab Chip*. 2009;9(22):3185-3192. doi:10.1039/b915147h

107. DesRochers TM, Holmes L, O'Donnell L, et al. Macrophage incorporation into a 3D perfusion tri-culture model of human breast cancer. *J Immunother Cancer*. 2015;3(2):P401. doi:10.1186/2051-1426-3-S2-P401
108. Katagiri W, Sakaguchi K, Kawai T, Wakayama Y, Osugi M, Hibi H. A defined mix of cytokines mimics conditioned medium from cultures of bone marrow-derived mesenchymal stem cells and elicits bone regeneration. *Cell Prolif*. 2017;50(3). doi:10.1111/cpr.12333
109. Marolt Presen D, Traweger A, Gimona M, Redl H. Mesenchymal Stromal Cell-Based Bone Regeneration Therapies: From Cell Transplantation and Tissue Engineering to Therapeutic Secretomes and Extracellular Vesicles. *Front Bioeng Biotechnol*. 2019;7. doi:10.3389/fbioe.2019.00352
110. Martins M, Ribeiro D, Martins A, Reis RL, Neves NM. Extracellular Vesicles Derived from Osteogenically Induced Human Bone Marrow Mesenchymal Stem Cells Can Modulate Lineage Commitment. *Stem Cell Rep*. 2016;6(3):284-291. doi:10.1016/j.stemcr.2016.01.001
111. Lotvall J, Valadi H. Cell to Cell Signalling via Exosomes Through esRNA. *Cell Adhes Migr*. 2007;1(3):156-158.
112. Valadi H, Ekström K, Bossios A, Sjöstrand M, Lee JJ, Lötvall JO. Exosome-mediated transfer of mRNAs and microRNAs is a novel mechanism of genetic exchange between cells. *Nat Cell Biol*. 2007;9(6):654-659. doi:10.1038/ncb1596
113. van Niel G, D'Angelo G, Raposo G. Shedding light on the cell biology of extracellular vesicles. *Nat Rev Mol Cell Biol*. 2018;19(4):213-228. doi:10.1038/nrm.2017.125
114. Lee YXF, Johansson H, Wood MJA, El Andaloussi S. Considerations and Implications in the Purification of Extracellular Vesicles - A Cautionary Tale. *Front Neurosci*. 2019;13:1067. doi:10.3389/fnins.2019.01067
115. Eagle H. Amino Acid Metabolism in Mammalian Cell Cultures. *Science*. 1959;130(3373):432-437. doi:10.1126/science.130.3373.432
116. Gstraunthaler G. Alternatives to the use of fetal bovine serum: serum-free cell culture. *ALTEX*. 2003;20(4):275-281.
117. van der Valk J, Bieback K, Buta C, et al. Fetal Bovine Serum (FBS): Past - Present - Future. *ALTEX*. 2018;35(1):99-118. doi:10.14573/altex.1705101
118. Haynesworth SE, Baber MA, Caplan AL. Cytokine expression by human marrow-derived mesenchymal progenitor cells in vitro: effects of dexamethasone and IL-1 alpha. *J Cell Physiol*. 1996;166(3):585-592. doi:10.1002/(SICI)1097-4652(199603)166:3<585::AID-JCP13>3.0.CO;2-6
119. Takeyama S, Yoshimura Y, Deyama Y, Sugawara Y, Fukuda H, Matsumoto A. Phosphate decreases osteoclastogenesis in coculture of osteoblast and bone marrow. *Biochem Biophys Res Commun*. 2001;282(3):798-802. doi:10.1006/bbrc.2001.4652
120. Langenbach F, Handschel J. Effects of dexamethasone, ascorbic acid and β -glycerophosphate on the osteogenic differentiation of stem cells in vitro. *Stem Cell Res Ther*. 2013;4(5):117. doi:10.1186/scrt328
121. Zhu S, Ehnert S, Rouß M, et al. From the Clinical Problem to the Basic Research—Co-Culture Models of Osteoblasts and Osteoclasts. *Int J Mol Sci*. 2018;19(8). doi:10.3390/ijms19082284
122. Robertson G, J. Bushell T, Zagnoni M. Chemically induced synaptic activity between mixed primary hippocampal co-cultures in a microfluidic system. *Integr Biol*. 2014;6(6):636-644. doi:10.1039/C3IB40221E
123. Boyce BF, Xing L. The RANKL/RANK/OPG pathway. *Curr Osteoporos Rep*. 2007;5(3):98-104. doi:10.1007/s11914-007-0024-y
124. Schulze S, Wehrum D, Dieter P, Hempel U. A supplement-free osteoclast-osteoblast co-culture for pre-clinical application. *J Cell Physiol*. 2018;233(6):4391-4400. doi:10.1002/jcp.26076
125. Sasaki H, Enomoto J, Ikeda Y, Honda H, Fukuda J, Kato R. Comparisons of cell culture medium using distribution of morphological features in microdevice. *J Biosci Bioeng*. 2016;121(1):117-123. doi:10.1016/j.jbiosc.2015.05.011
126. Yoshimura Y, Kikuri T, Hasegawa T, et al. How much medium do you use for cell culture? Medium volume influences mineralization and osteoclastogenesis in vitro. *Mol Med Rep*. 2017;16(1):429-434. doi:10.3892/mmr.2017.6611
127. Shimomura A, Iizuka-Kogo A, Yamamoto N, Nomura R. A lower volume culture method for obtaining a larger yield of neuron-like cells from mesenchymal stem cells. *Med Mol Morphol*. 2016;49(2):119-126. doi:10.1007/s00795-015-0131-2

128. Simão VA, Evangelista-Ribeiro CP, Brand H, et al. Metabolic and proliferation evaluation of human adipose-derived mesenchymal stromal cells (ASC) in different culture medium volumes: standardization of static culture. *Biologicals*. 2019;62:93-101. doi:10.1016/j.biologicals.2019.08.006
129. Oze H, Hirao M, Ebina K, et al. Impact of medium volume and oxygen concentration in the incubator on pericellular oxygen concentration and differentiation of murine chondrogenic cell culture. *In Vitro Cell Dev Biol Anim*. 2012;48(2):123-130. doi:10.1007/s11626-011-9479-3
130. Place TL, Domann FE, Case AJ. Limitations of oxygen delivery to cells in culture: An underappreciated problem in basic and translational research. *Free Radic Biol Med*. 2017;113:311-322. doi:10.1016/j.freeradbiomed.2017.10.003
131. Ozturk SS, Jorjani P, Taticek R, et al. Kinetics of Glucose Metabolism and Utilization of Lactate in Mammalian Cell Cultures. In: Carrondo MJT, Griffiths B, Moreira JLP, eds. *Animal Cell Technology: From Vaccines to Genetic Medicine*. Springer Netherlands; 1997:355-360. doi:10.1007/978-94-011-5404-8_56
132. Paul J. *Cell and Tissue Culture*. 5th edition. Churchill Livingstone; 1975.
133. Zielke HR, Sumbilla CM, Sevdalian DA, Hawkins RL, Ozand PT. Lactate: a major product of glutamine metabolism by human diploid fibroblasts. *J Cell Physiol*. 1980;104(3):433-441. doi:10.1002/jcp.1041040316
134. Glacken MW, Fleischaker RJ, Sinskey AJ. Reduction of waste product excretion via nutrient control: Possible strategies for maximizing product and cell yields on serum in cultures of mammalian cells. *Biotechnol Bioeng*. 1986;28(9):1376-1389. doi:10.1002/bit.260280912
135. Ozturk SS, Riley MR, Palsson BO. Effects of ammonia and lactate on hybridoma growth, metabolism, and antibody production. *Biotechnol Bioeng*. 1992;39(4):418-431. doi:10.1002/bit.260390408
136. Slivac I, Blajić V, Radošević K, Kniewald Z, Gaurina Srček V. Influence of different ammonium, lactate and glutamine concentrations on CCO cell growth. *Cytotechnology*. 2010;62(6):585-594. doi:10.1007/s10616-010-9312-y
137. Krüger-Genge A, Fuhrmann R, Jung F, Franke RP. Morphology of primary human venous endothelial cell cultures before and after culture medium exchange. *Clin Hemorheol Microcirc*. 2015;61(2):151-156. doi:10.3233/CH-151992
138. Mizrahi A, Avihoo A. Growth medium utilization and its re-use for animal cell cultures. *J Biol Stand*. 1977;5(1):31-37. doi:10.1016/0092-1157(77)90016-6
139. Adamson SR, Fitzpatrick SL, Behie LA, Gaucher GM, Lesser BH. In vitro production of high titre monoclonal antibody by hybridoma cells in dialysis culture. *Biotechnol Lett*. 1983;5(9):573-578. doi:10.1007/BF00130835
140. Büntemeyer H, Wallerius C, Lehmann J. Optimal medium use for continuous high density perfusion processes. *Cytotechnology*. 1992;9(1):59-67. doi:10.1007/BF02521732
141. Chen G, Gulbranson DR, Hou Z, et al. Chemically defined conditions for human iPSC derivation and culture. *Nat Methods*. 2011;8(5):424-429. doi:10.1038/nmeth.1593
142. Nath SC, Nagamori E, Horie M, Kino-Oka M. Culture medium refinement by dialysis for the expansion of human induced pluripotent stem cells in suspension culture. *Bioprocess Biosyst Eng*. 2017;40(1):123-131. doi:10.1007/s00449-016-1680-z
143. Shinohara M, Choi H, Ibuki M, et al. Endodermal differentiation of human induced pluripotent stem cells using simple dialysis culture system in suspension culture. *Regen Ther*. Published online May 30, 2019:14-19. doi:10.1016/j.reth.2019.05.004
144. Côme J, Nissan X, Aubry L, et al. Improvement of Culture Conditions of Human Embryoid Bodies Using a Controlled Perfused and Dialyzed Bioreactor System. *Tissue Eng Part C Methods*. 2008;14(4):289-298. doi:10.1089/ten.tec.2008.0029
145. Pereira Rodrigues N, Sakai Y, Fujii T. Cell-based microfluidic biochip for the electrochemical real-time monitoring of glucose and oxygen. *Sens Actuators B Chem*. 2008;132(2):608-613. doi:10.1016/j.snb.2007.12.025
146. Modarres HP, Janmaleki M, Novin M, et al. In vitro models and systems for evaluating the dynamics of drug delivery to the healthy and diseased brain. *J Controlled Release*. 2018;273:108-130. doi:10.1016/j.jconrel.2018.01.024

Bibliography

147. Young AT, Rivera KR, Erb PD, Daniele MA. Monitoring of Microphysiological Systems: Integrating Sensors and Real-Time Data Analysis toward Autonomous Decision-Making. *ACS Sens.* 2019;4(6):1454-1464. doi:10.1021/acssensors.8b01549
148. Deshpande RR, Wittmann C, Heinzle E. Microplates with integrated oxygen sensing for medium optimization in animal cell culture. *Cytotechnology.* 2004;46(1):1-8. doi:10.1007/s10616-004-6401-9
149. Vis MAM, Ito K, Hofmann S. Impact of Culture Medium on Cellular Interactions in in vitro Co-culture Systems. *Front Bioeng Biotechnol.* 2020;8. doi:10.3389/fbioe.2020.00911
150. Rose GG, Pomerat CM, Shindler TO, Trunnell JB. A Cellophane-Strip Technique for Culturing Tissue in Multipurpose Culture Chambers. *J Biophys Biochem Cytol.* 1958;4(6):761-764. doi:10.1083/jcb.4.6.761
151. Rose GG. Cytopathophysiology of tissue cultures growing under cellophane membranes. *Int Rev Exp Pathol.* 1966;5:111-178.
152. Rose GG. The circumfusion system for multipurpose culture chambers. I. Introduction to the mechanics, techniques, and basic results of a 12-chamber (in vitro) closed circulatory system. *J Cell Biol.* 1967;32(1):89-112. doi:10.1083/jcb.32.1.89
153. Vogler EA. A Compartmentalized Device for the Culture of Animal Cells. *Biomater Artif Cells Artif Organs.* 1989;17(5):597-610. doi:10.3109/10731198909117639
154. Dhurjati R, Liu X, Gay CV, Mastro AM, Vogler EA. Extended-Term Culture of Bone Cells in a Compartmentalized Bioreactor. *Tissue Eng.* 2006;12(11):3045-3054. doi:10.1089/ten.2006.12.3045
155. Mastro AM, Vogler EA. A three-dimensional osteogenic tissue model for the study of metastatic tumor cell interactions with bone. *Cancer Res.* 2009;69(10):4097-4100. doi:10.1158/0008-5472.CAN-08-4437
156. Krishnan V, Shuman LA, Sosnoski DM, Dhurjati R, Vogler EA, Mastro AM. Dynamic interaction between breast cancer cells and osteoblastic tissue: comparison of two- and three-dimensional cultures. *J Cell Physiol.* 2011;226(8):2150-2158. doi:10.1002/jcp.22550
157. Krishnan V, Vogler EA, Mastro AM. Three-Dimensional in Vitro Model to Study Osteobiology and Osteopathology. *J Cell Biochem.* 2015;116(12):2715-2723. doi:10.1002/jcb.25250
158. de Wildt BWM, Ito K, Hofmann S. Human Platelet Lysate as Alternative of Fetal Bovine Serum for Enhanced Human In Vitro Bone Resorption and Remodeling. *Front Immunol.* 2022;13. doi:https://doi.org/10.3389/fimmu.2022.915277
159. Meinel L, Fajardo R, Hofmann S, et al. Silk implants for the healing of critical size bone defects. *Bone.* 2005;37(5):688-698. doi:10.1016/j.bone.2005.06.010
160. Nazarov R, Jin HJ, Kaplan DL. Porous 3-D Scaffolds from Regenerated Silk Fibroin. *Biomacromolecules.* 2004;5(3):718-726. doi:10.1021/bm034327e
161. Tsukada M, Gotoh Y, Nagura M, Minoura N, Kasai N, Freddi G. Structural changes of silk fibroin membranes induced by immersion in methanol aqueous solutions. *J Polym Sci Part B Polym Phys.* 1994;32(5):961-968. doi:10.1002/polb.1994.090320519
162. Hofmann S, Hagenmüller H, Koch AM, et al. Control of in vitro tissue-engineered bone-like structures using human mesenchymal stem cells and porous silk scaffolds. *Biomaterials.* 2007;28(6):1152-1162. doi:10.1016/j.biomaterials.2006.10.019
163. Melke J, Zhao F, Ito K, Hofmann S. Orbital seeding of mesenchymal stromal cells increases osteogenic differentiation and bone-like tissue formation. *J Orthop Res.* 2020;38(6):1228-1237. doi:10.1002/jor.24583
164. Hulme CH, Westwood M, Myers JE, Heazell AEP. A high-throughput colorimetric-assay for monitoring glucose consumption by cultured trophoblast cells and placental tissue. *Placenta.* 2012;33(11):949-951. doi:10.1016/j.placenta.2012.08.001
165. Salvatierra JC, Yuan TY, Fernando H, et al. Difference in Energy Metabolism of Annulus Fibrosus and Nucleus Pulposus Cells of the Intervertebral Disc. *Cell Mol Bioeng.* 2011;4(2):302-310. doi:10.1007/s12195-011-0164-0
166. Remmers SJA, Wildt BWM de, Vis MAM, et al. Osteoblast-osteoclast co-cultures: A systematic review and map of available literature. *PLOS ONE.* 2021;16(11):e0257724. doi:10.1371/journal.pone.0257724
167. Cloud-Clone Corp. Monoclonal Antibody to Receptor Activator Of Nuclear Factor Kappa B Ligand (RANKL). Accessed July 27, 2022. <http://www.cloud-clone.com/products/MAA855Hu22.html>

168. Cloud-Clone Corp. Active Colony Stimulating Factor 1, Macrophage (MCSF). Accessed July 27, 2022. <http://www.cloud-clone.com/products/APA090Hu01.html>
169. Poon C. Measuring the density and viscosity of culture media for optimized computational fluid dynamics analysis of in vitro devices. *J Mech Behav Biomed Mater.* 2022;126:105024. doi:10.1016/j.jmbbm.2021.105024
170. Krishnan V, Dhurjati R, Vogler EA, Mastro AM. Osteogenesis in vitro: from pre-osteoblasts to osteocytes. *Vitro Cell Dev Biol - Anim.* 2010;46(1):28-35. doi:10.1007/s11626-009-9238-x
171. Bernhardt A, Koperski K, Schumacher M, Gelinsky M. Relevance of osteoclast-specific enzyme activities in cell-based in vitro resorption assays. *Eur Cell Mater.* 2017;33:28-42. doi:10.22203/eCM.v033a03
172. Yan J, van Smeden L, Merckx M, Zijlstra P, Prins MWJ. Continuous Small-Molecule Monitoring with a Digital Single-Particle Switch. *ACS Sens.* 2020;5(4):1168-1176. doi:10.1021/acssensors.0c00220
173. Xiao Y, Lai RY, Plaxco KW. Preparation of electrode-immobilized, redox-modified oligonucleotides for electrochemical DNA and aptamer-based sensing. *Nat Protoc.* 2007;2(11):2875-2880. doi:10.1038/nprot.2007.413
174. Vetsch JR, Betts DC, Müller R, Hofmann S. Flow velocity-driven differentiation of human mesenchymal stromal cells in silk fibroin scaffolds: A combined experimental and computational approach. *PLoS ONE.* 2017;12(7):e0180781. doi:10.1371/journal.pone.0180781
175. Melke J, Zhao F, van Rietbergen B, Ito K, Hofmann S. Localisation of mineralised tissue in a complex spinner flask environment correlates with predicted wall shear stress level localisation. *Eur Cell Mater.* 2018;36:57-68. doi:10.22203/eCM.v036a05
176. de Wildt BWM, van der Meijden R, Bartels PAA, et al. Bioinspired Silk Fibroin Mineralization for Advanced In Vitro Bone Remodeling Models. *Adv Funct Mater.*:2206992. doi:10.1002/adfm.202206992
177. Thermo Scientific. High performance dialysis guide. Published online 2013. Accessed June 1, 2022. <https://tools.thermofisher.com/content/sfs/brochures/1602457-High-Performance-Dialysis-Guide.pdf>
178. Wiebe JP, Dinsdale CJ. Inhibition of cell proliferation by glycerol. *Life Sci.* 1991;48(16):1511-1517. doi:10.1016/0024-3205(91)90275-g
179. Sieberath A, Della Bella E, Ferreira AM, Gentile P, Eglin D, Dalgarno K. A Comparison of Osteoblast and Osteoclast In Vitro Co-Culture Models and Their Translation for Preclinical Drug Testing Applications. *Int J Mol Sci.* 2020;21(3):912. doi:10.3390/ijms21030912
180. Zhang B, Korolj A, Lai BFL, Radisic M. Advances in organ-on-a-chip engineering. *Nat Rev Mater.* 2018;3(8):257-278. doi:10.1038/s41578-018-0034-7
181. Wang Y, Lee D, Zhang L, et al. Systematic prevention of bubble formation and accumulation for long-term culture of pancreatic islet cells in microfluidic device. *Biomed Microdevices.* 2012;14(2):419-426. doi:10.1007/s10544-011-9618-3
182. Williams MJ, Lee NK, Mylott JA, Mazzola N, Ahmed A, Abhyankar VV. A Low-Cost, Rapidly Integrated Debubbler (RID) Module for Microfluidic Cell Culture Applications. *Micromachines.* 2019;10(6):360. doi:10.3390/mi10060360
183. Probst C, Schneider S, Loskill P. High-throughput organ-on-a-chip systems: Current status and remaining challenges. *Curr Opin Biomed Eng.* 2018;6:33-41. doi:10.1016/j.cobme.2018.02.004
184. Mastrangeli M, Millet S, Partners TO, Raaij J van den E van. Organ-on-chip in development: Towards a roadmap for organs-on-chip. *ALTEX - Altern Anim Exp.* 2019;36(4):650-668. doi:10.14573/altex.1908271
185. Marx U, Akabane T, Andersson TB, et al. Biology-inspired microphysiological systems to advance patient benefit and animal welfare in drug development. *ALTEX - Altern Anim Exp.* 2020;37(3):365-394. doi:10.14573/altex.2001241
186. Mansoorifar A, Gordon R, Bergan RC, Bertassoni LE. Bone-on-a-Chip: Microfluidic Technologies and Microphysiologic Models of Bone Tissue. *Adv Funct Mater.* 2021;31(6):2006796. doi:10.1002/adfm.202006796
187. Zhao F, van Rietbergen B, Ito K, Hofmann S. Fluid flow-induced cell stimulation in bone tissue engineering changes due to interstitial tissue formation in vitro. *Int J Numer Methods Biomed Eng.* 2020;36(6):e3342. doi:10.1002/cnm.3342

Bibliography

188. Takai E, Costa KD, Shaheen A, Hung CT, Guo XE. Osteoblast Elastic Modulus Measured by Atomic Force Microscopy Is Substrate Dependent. *Ann Biomed Eng.* 2005;33(7):963-971. doi:10.1007/s10439-005-3555-3
189. Titushkin I, Cho M. Modulation of Cellular Mechanics during Osteogenic Differentiation of Human Mesenchymal Stem Cells. *Biophys J.* 2007;93(10):3693-3702. doi:10.1529/biophysj.107.107797
190. Zhao S, Zhang YKY, Harris S, Ahuja SS, Bonewald LF. MLO-Y4 osteocyte-like cells support osteoclast formation and activation. *J Bone Miner Res Off J Am Soc Bone Miner Res.* 2002;17(11):2068-2079. doi:10.1359/jbmr.2002.17.11.2068
191. Middleton K, Kondiboyina A, Borrett M, Cui Y, Mei X, You L. Microfluidics approach to investigate the role of dynamic similitude in osteocyte mechanobiology. *J Orthop Res.* 2018;36(2):663-671. doi:10.1002/jor.23773
192. Babaliari E, Petekidis G, Chatzinikolaidou M. A Precisely Flow-Controlled Microfluidic System for Enhanced Pre-Osteoblastic Cell Response for Bone Tissue Engineering. *Bioeng Basel Switz.* 2018;5(3):66. doi:10.3390/bioengineering5030066
193. George EL, Truesdell SL, Magyar AL, Saunders MM. The effects of mechanically loaded osteocytes and inflammation on bone remodeling in a bisphosphonate-induced environment. *Bone.* 2019;127:460-473. doi:10.1016/j.bone.2019.07.008
194. Paek K, Kim S, Tak S, et al. A high-throughput biomimetic bone-on-a-chip platform with artificial intelligence-assisted image analysis for osteoporosis drug testing. *Bioeng Transl Med.* n/a(n/a):e10313. doi:10.1002/btm2.10313
195. Fritsche E, Haarmann-Stemann T, Kapr J, et al. Stem Cells for Next Level Toxicity Testing in the 21st Century. *Small.* 2021;17(15):2006252. doi:10.1002/sml.202006252
196. Barré-Sinoussi F, Montagutelli X. Animal models are essential to biological research: issues and perspectives. *Future Sci OA.* 2015;1(4):FSO63. doi:10.4155/fso.15.63
197. Tanner MR, Beeton C. Differences in ion channel phenotype and function between humans and animal models. *Front Biosci Landmark Ed.* 2018;23(1):43-64. doi:10.2741/4581
198. Bracken MB. Why animal studies are often poor predictors of human reactions to exposure. *J R Soc Med.* 2009;102(3):120-122. doi:10.1258/jrsm.2008.08k033
199. George EL, Truesdell SL, York SL, Saunders MM. Lab-on-a-chip platforms for quantification of multicellular interactions in bone remodeling. *Exp Cell Res.* 2018;365(1):106-118. doi:10.1016/j.yexcr.2018.02.027
200. Truesdell SL, George EL, Seno CE, Saunders MM. 3D Printed Loading Device for Inducing Cellular Mechanotransduction via Matrix Deformation. *Exp Mech.* 2019;59(8):1223-1232. doi:10.1007/s11340-019-00531-1
201. SL Truesdell, EL George, CC Van Vranken, MM Saunders. A Lab-On-A-Chip Platform for Stimulating Osteocyte Mechanotransduction and Analyzing Functional Outcomes of Bone Remodeling. *JoVE.* 2020;(e61076). doi:10.3791/61076
202. Arora S, Srinivasan A, Leung CM, Toh YC. Bio-mimicking Shear Stress Environments for Enhancing Mesenchymal Stem Cell Differentiation. *Curr Stem Cell Res Ther.* 2020;15(5):414-427. doi:10.2174/1574888X15666200408113630
203. Leclerc E, David B, Griscom L, et al. Study of osteoblastic cells in a microfluidic environment. *Biomaterials.* 2006;27(4):586-595. doi:10.1016/j.biomaterials.2005.06.002
204. Jang K, Sato K, Igawa K, Chung U il, Kitamori T. Development of an osteoblast-based 3D continuous-perfusion microfluidic system for drug screening. *Anal Bioanal Chem.* 2008;390(3):825-832. doi:10.1007/s00216-007-1752-7
205. Dash SK, Sharma V, Verma RS, Das SK. Low intermittent flow promotes rat mesenchymal stem cell differentiation in logarithmic fluid shear device. *Biomicrofluidics.* 2020;14(5):054107. doi:10.1063/5.0024437
206. Gao X, Zhang X, Xu H, Zhou B, Wen W, Qin J. Regulation of cell migration and osteogenic differentiation in mesenchymal stem cells under extremely low fluidic shear stress. *Biomicrofluidics.* 2014;8(5):052008. doi:10.1063/1.4896557
207. Mavrič B, Antolič V. Optimal mechanical environment of the healing bone fracture/osteotomy. *Int Orthop.* 2012;36(4):689-695. doi:10.1007/s00264-012-1487-8
208. Wang Y, Lee D, Zhang L, et al. Systematic prevention of bubble formation and accumulation for long-term culture of pancreatic islet cells in microfluidic device. *Biomed Microdevices.* 2012;14(2):419-426. doi:10.1007/s10544-011-9618-3

209. Shi J, Tong L, Tong W, et al. Current progress in long-term and continuous cell metabolite detection using microfluidics. *TrAC Trends Anal Chem.* 2019;117:263-279. doi:10.1016/j.trac.2019.05.028
210. Reznikov N, Bilton M, Lari L, Stevens MM, Kröger R. Fractal-like hierarchical organization of bone begins at the nanoscale. *Science.* 2018;360(6388):eaao2189. doi:10.1126/science.aao2189
211. McCoy RJ, O'Brien FJ. Influence of shear stress in perfusion bioreactor cultures for the development of three-dimensional bone tissue constructs: a review. *Tissue Eng Part B Rev.* 2010;16(6):587-601. doi:10.1089/ten.TEB.2010.0370
212. Zhao F, Chella R, Ma T. Effects of shear stress on 3-D human mesenchymal stem cell construct development in a perfusion bioreactor system: Experiments and hydrodynamic modeling. *Biotechnol Bioeng.* 2007;96(3):584-595. doi:10.1002/bit.21184
213. Cartmell SH, Porter BD, García AJ, Guldberg RE. Effects of Medium Perfusion Rate on Cell-Seeded Three-Dimensional Bone Constructs in Vitro. *Tissue Eng.* 2003;9(6):1197-1203. doi:10.1089/10763270360728107
214. Yeatts AB, Fisher JP. Bone tissue engineering bioreactors: Dynamic culture and the influence of shear stress. *Bone.* 2011;48(2):171-181. doi:10.1016/j.bone.2010.09.138
215. Sung JH, Kam C, Shuler ML. A microfluidic device for a pharmacokinetic–pharmacodynamic (PK–PD) model on a chip. *Lab Chip.* 2010;10(4):446-455. doi:10.1039/B917763A
216. Abaci HE, Gledhill K, Guo Z, Christiano AM, Shuler ML. Pumpless microfluidic platform for drug testing on human skin equivalents. *Lab Chip.* 2015;15(3):882-888. doi:10.1039/C4LC00999A
217. Esch MB, Prot JM, Wang YI, et al. Multi-cellular 3D human primary liver cell culture elevates metabolic activity under fluidic flow. *Lab Chip.* 2015;15(10):2269-2277. doi:10.1039/C5LC00237K
218. Wang YI, Shuler ML. UniChip enables long-term recirculating unidirectional perfusion with gravity-driven flow for microphysiological systems. *Lab Chip.* 2018;18(17):2563-2574. doi:10.1039/C8LC00394G
219. Wang YI, Carmona C, Hickman JJ, Shuler ML. Multiorgan Microphysiological Systems for Drug Development: Strategies, Advances, and Challenges. *Adv Healthc Mater.* 2018;7(2):1701000. doi:10.1002/adhm.201701000
220. Wang YI, Oleaga C, Long CJ, et al. Self-contained, low-cost Body-on-a-Chip systems for drug development. *Exp Biol Med.* 2017;242(17):1701-1713. doi:10.1177/1535370217694101
221. Gabetti S, Masante B, Cochis A, et al. An automated 3D-printed perfusion bioreactor combinable with pulsed electromagnetic field stimulators for bone tissue investigations. *Sci Rep.* 2022;12:13859. doi:10.1038/s41598-022-18075-1
222. Fritton SP, Weinbaum S. Fluid and Solute Transport in Bone: Flow-Induced Mechanotransduction. *Annu Rev Fluid Mech.* 2009;41:347-374. doi:10.1146/annurev.fluid.010908.165136
223. Knothe Tate ML. "Whither flows the fluid in bone?" An osteocyte's perspective. *J Biomech.* 2003;36(10):1409-1424. doi:10.1016/s0021-9290(03)00123-4
224. Beşkardeş IG, Aydın G, Bektaş Ş, Cengiz A, Gümüşderelioğlu M. A systematic study for optimal cell seeding and culture conditions in a perfusion mode bone-tissue bioreactor. *Biochem Eng J.* 2018;132:100-111. doi:10.1016/j.bej.2018.01.006
225. Chen G, Xu R, Zhang C, Lv Y. Responses of MSCs to 3D Scaffold Matrix Mechanical Properties under Oscillatory Perfusion Culture. *ACS Appl Mater Interfaces.* 2017;9(2):1207-1218. doi:10.1021/acsami.6b10745
226. Wendt D, Marsano A, Jakob M, Heberer M, Martin I. Oscillating perfusion of cell suspensions through three-dimensional scaffolds enhances cell seeding efficiency and uniformity. *Biotechnol Bioeng.* 2003;84(2):205-214. doi:10.1002/bit.10759
227. Du D, Furukawa K, Ushida T. Oscillatory perfusion seeding and culturing of osteoblast-like cells on porous beta-tricalcium phosphate scaffolds. *J Biomed Mater Res A.* 2008;86(3):796-803. doi:10.1002/jbm.a.31641
228. Bicen AO, Akyıldız IF. Molecular transport in microfluidic channels for flow-induced molecular communication. In: *2013 IEEE International Conference on Communications Workshops (ICC).* ; 2013:766-770. doi:10.1109/ICCW.2013.6649336
229. Kim L, Vahey MD, Lee HY, Voldman J. Microfluidic arrays for logarithmically perfused embryonic stem cell culture. *Lab Chip.* 2006;6(3):394-406. doi:10.1039/B511718F
230. Weinbaum S, Cowin SC, Zeng Y. A model for the excitation of osteocytes by mechanical loading-induced bone fluid shear stresses. *J Biomech.* 1994;27(3):339-360. doi:10.1016/0021-9290(94)90010-8

231. Akiva A, Melke J, Ansari S, et al. An Organoid for Woven Bone. *Adv Funct Mater.* 2021;31(17):2010524. doi:10.1002/adfm.202010524
232. Reich KM, Gay CV, Frangos JA. Fluid shear stress as a mediator of osteoblast cyclic adenosine monophosphate production. *J Cell Physiol.* 1990;143(1):100-104. doi:10.1002/jcp.1041430113
233. Yourek G, McCormick SM, Mao JJ, Reilly GC. Shear stress induces osteogenic differentiation of human mesenchymal stem cells. *Regen Med.* 2010;5(5):713-724. doi:10.2217/rme.10.60
234. Kim KM, Choi YJ, Hwang JH, et al. Shear Stress Induced by an Interstitial Level of Slow Flow Increases the Osteogenic Differentiation of Mesenchymal Stem Cells through TAZ Activation. *PLoS ONE.* 2014;9(3):e92427. doi:10.1371/journal.pone.0092427
235. Yamada S, Yassin MA, Schwarz T, Hansmann J, Mustafa K. Induction of osteogenic differentiation of bone marrow stromal cells on 3D polyester-based scaffolds solely by subphysiological fluidic stimulation in a laminar flow bioreactor. *J Tissue Eng.* 2021;12:20417314211019376. doi:10.1177/20417314211019375
236. Nakamura I, Takahashi N, Sasaki T, Jimi E, Kurokawa T, Suda T. Chemical and physical properties of the extracellular matrix are required for the actin ring formation in osteoclasts. *J Bone Miner Res Off J Am Soc Bone Miner Res.* 1996;11(12):1873-1879. doi:10.1002/jbmr.5650111207
237. Remmers S, Mayer D, Melke J, Ito K, Hofmann S. Measuring mineralised tissue formation and resorption in a human 3D osteoblast-osteoclast co-culture model. *Eur Cell Mater.* 2020;40:189-202. doi:10.22203/eCM.v040a12
238. Hagenmüller H, Hofmann S, Kohler T, et al. Non-invasive time-lapsed monitoring and quantification of engineered bone-like tissue. *Ann Biomed Eng.* 2007;35(10):1657-1667. doi:10.1007/s10439-007-9338-2
239. Stock JT. Wolff's law (bone functional adaptation). In: *The International Encyclopedia of Biological Anthropology.* John Wiley & Sons, Ltd; 2018:1-2. doi:10.1002/9781118584538.ieba0521
240. DMP1 dentin matrix acidic phosphoprotein 1 [Homo sapiens (human)] - Gene - NCBI. Accessed March 15, 2023. <https://www.ncbi.nlm.nih.gov/gene/1758>
241. Ge X, Hanson M, Shen H, et al. Validation of an optical sensor-based high-throughput bioreactor system for mammalian cell culture. *J Biotechnol.* 2006;122(3):293-306. doi:10.1016/j.jbiotec.2005.12.009
242. Oliveira CS, Leeuwenburgh S, Mano JF. New insights into the biomimetic design and biomedical applications of bioengineered bone microenvironments. *APL Bioeng.* 2021;5(4):041507. doi:10.1063/5.0065152
243. Dutch Organ-on-Chip Consortium. Vital network on Organ-on-Chip. Accessed February 21, 2023. <https://klanten.digitaalpubliceren.com/hdmt/18633/34/>
244. Mastrangeli M, Millet S, Mummery C, et al. Building blocks for a European Organ-on-Chip roadmap. *ALTEX - Altern Anim Exp.* 2019;36(3):481-492. doi:10.14573/altex.1905221
245. Dutch Foundation for Biosciences and Society. *Mini Organs-on-Chips.*; 2020.
246. Ewart L, Apostolou A, Briggs SA, et al. Performance assessment and economic analysis of a human Liver-Chip for predictive toxicology. *Commun Med.* 2022;2(1):1-16. doi:10.1038/s43856-022-00209-1
247. Vorrink SU, Zhou Y, Ingelman-Sundberg M, Lauschke VM. Prediction of Drug-Induced Hepatotoxicity Using Long-Term Stable Primary Hepatic 3D Spheroid Cultures in Chemically Defined Conditions. *Toxicol Sci Off J Soc Toxicol.* 2018;163(2):655-665. doi:10.1093/toxsci/kfy058
248. Proctor WR, Foster AJ, Vogt J, et al. Utility of spherical human liver microtissues for prediction of clinical drug-induced liver injury. *Arch Toxicol.* 2017;91(8):2849-2863. doi:10.1007/s00204-017-2002-1

Scientific Output

Journal contributions

Related to this thesis

Michelle A.M. Vis, Feihu Zhao, Nils C.H. van Creijl, Andreas M.A.O. Pollet, Jaap M.J. den Toonder, Keita Ito, Sandra Hofmann. Osteogenic differentiation on a chip using pumpless bidirectional fluid flow. (in preparation)

Michelle A.M. Vis, Feihu Zhao, Esmee S.R. Bodelier, C. Marlous Bood, Jurgen Bolsink, Marina van Doeselaar, Hossein Eslami Amirabadi, Keita Ito, Sandra Hofmann. Towards bone-remodeling-on-a-chip: self-assembling 3D osteoblast-osteoclast coculture in a microfluidic chip. (submitted) Preprint available at BioRxiv. DOI: 10.1101/2023.03.11.532167

Michelle A.M. Vis, Bregje W.M. de Wildt, Keita Ito, Sandra Hofmann. A dialysis medium refreshment cell culture set-up for an osteoblast-osteoclast coculture. *Biotechnology and Bioengineering* (2022). 120, 1120– 1132 DOI: 10.1002/bit.28314

Stefan J.A. Remmers, Bregje W.M. de Wildt*, **Michelle A.M. Vis***, Eva S.R. Spaander, Rob B.M. de Vries, Keita Ito, Sandra Hofmann. Osteoblast-osteoclast co-cultures: A systematic review and map of available literature. *PLoS ONE* (2021). 16, 11, 26 p., e0257724. DOI: 10.1371/journal.pone.0257724

Michelle A.M. Vis, Keita Ito, Sandra Hofmann. Impact of Culture Medium on Cellular Interactions in in vitro Co-culture Systems. *Frontiers in Bioengineering and Biotechnology* (2020). 8, 8 p., 911. DOI: 10.3389/fbioe.2020.00911

* Authors contributed equally

Unrelated to this thesis

Margo Tuerlings, Ilja Boone, Hossein Eslami Amirabadi, **Michelle A.M. Vis**, Eka Suchiman, Enrike van der Linden, Sandra Hofmann, Rob Nelissen, Jaap M.J. den Toonder, Yolande Ramos, Ingrid Meulenbelt. Capturing Essential Physiological Aspects of Interacting Cartilage and Bone Tissue with Osteoarthritis Pathophysiology: A Human Osteochondral Unit-on-a-Chip Model. *Advanced Materials Technologies* (2022). 7, 8, 9 p., 2101310. DOI: 10.1002/admt.202101310

Sana Ansari, Bregje W.M. de Wildt, **Michelle A.M. Vis**, Carolina E. de Korte, Keita Ito, Sandra Hofmann, Yuana Yuana. Matrix Vesicles: Role in Bone Mineralization and Potential Use as Therapeutics. *Pharmaceuticals* (2021). 14, 4, 27 p., 289. DOI: 10.3390/ph14040289

Xiaolin Cui, Bram G. Soliman, Cesar R. Alcala-Orozco, Jun Li, **Michelle A.M. Vis**, Miguel Santos, Steven G. Wise, Riccardo Levato, Jos Malda, Tim B.F. Woodfield, Jelena Rnjak-Kovacina, Khoon S. Lim. Rapid Photocrosslinking of Silk Hydrogels with High Cell Density and Enhanced Shape Fidelity. *Advanced Healthcare Materials* (2020). 9, 4, 15 p., 1901667. DOI: 10.1002/adhm.201901667

Conference contributions

Michelle A.M. Vis, Esmee S.R. Bodelier, C. Marlous Bood, Keita Ito, Sandra Hofmann. Towards bone-remodeling-on-a-chip. hDMT bone-on-chip Dec 2022, Amsterdam, the Netherlands, oral presentation

Michelle A.M. Vis, Bregje W.M. de Wildt, Keita Ito, Sandra Hofmann. A dialysis medium refreshment cell culture set-up for osteogenic differentiation of mesenchymal stromal cells and osteoclastic differentiation of monocytes in coculture. NBTE Dec 2022, Lunteren, the Netherlands, poster presentation

Michelle A.M. Vis, Esmee S.R. Bodelier, Keita Ito, Sandra Hofmann. Towards bone-remodeling-on-a-chip. EMBL-IBEC June 2022, Barcelona, Spain, poster presentation

Michelle A.M. Vis, Esmee S.R. Bodelier, Keita Ito, Sandra Hofmann. Towards bone-remodeling-on-a-chip: formation of 3D bone-like tissues. TERMIS Europe June 2022, Kraków, Poland, oral presentation

Michelle A.M. Vis, Esmee S.R. Bodelier, Keita Ito, Sandra Hofmann. Towards bone-remodeling-on-a-chip. NBTE April 2022, Lunteren, the Netherlands, oral presentation

Michelle A.M. Vis, Keita Ito, Sandra Hofmann. Recycling of culture medium for enhanced cellular interactions. TERMIS world Nov 2021, online, poster presentation

Michelle A.M. Vis, Esmee S.R. Bodelier, Keita Ito, Sandra Hofmann. Towards bone-remodeling-on-a-chip. SAFE July 2021, online, oral and poster presentation

Michelle A.M. Vis, Keita Ito, Sandra Hofmann. Recycling culture medium for enhanced cellular interactions in *in vitro* bone models. NBTE November 2020, online, poster presentation

Michelle A.M. Vis, Keita Ito, Sandra Hofmann. Recycling culture medium for enhanced cellular interactions in *in vitro* bone models. NBTE November 2019, Lunteren, the Netherlands, oral presentation

Curriculum Vitae



Michelle A.M. Vis was born on the 24th of December 1993 in Brunssum, the Netherlands. In 2012 she received her high school diploma at Sint-Janscollege in Hoensbroek. Next, she studied Biomedical Engineering at Eindhoven University of Technology where she received her bachelor's degree in 2016. At the same university, she obtained her master degree in 2019 in the Orthopaedic Biomechanics research group of Prof. Dr. Keita Ito. During her graduation project supervised by Dr. Sandra Hofmann, she focused on promoting vascularization in bone tissue engineered constructs. As part of her master degree, she completed an internship at the Christchurch Regenerative Medicine and Tissue Engineering group (CReaTE) at Otago University in Christchurch, New Zealand. There, she worked on silk fibroin hydrogels for cartilage tissue engineering applications under supervision of Dr. Khoon Lim. In 2019, she joined the Orthopaedic Biomechanics group as a PhD-student investigating bone remodeling by creating *in vitro* mini bones. The results are presented in this thesis.

Dankwoord (Acknowledgements)

Hier is het dan eindelijk! De PhD periode zit erop. Met veel plezier kijk ik terug op leuke en leerzame jaren op de TU/e. Dit proefschrift is het resultaat van vele uren samenwerking met mijn begeleiders, collega's, vrienden en familie. Ik ben dankbaar voor de steun en aanmoediging die ik van hen heb ontvangen, en zonder hen had ik deze prestatie niet kunnen bereiken.

First, I would like to thank my promotors for their support. **Sandra**, I would like to express my gratitude for your invaluable guidance and support throughout my PhD journey. Your expertise, knowledge and enthusiasm have sparked my enthusiasm about the bone field. You have generously shared your time and resources with me, providing feedback, insightful advice and constructive criticism. Your encouragement and motivation have been an inspiration to me, especially during the challenging covid times. **Keita**, I feel fortunate to have had the opportunity to work under your supervision and to benefit from your vast knowledge and experience in the field. I am honored to have you as my co-promotor. Thank you both for believing in me.

I would like to thank the members of my defense committee **prof. dr. Jaap den Toonder**, **prof. dr. Gwendolen Reilly**, **prof. dr. Jenneke Klein-Nullend**, **dr. Jeroen van den Beucken** en **dr. Eric Farrell** for spending your valuable time on evaluating my thesis. **Jaap den Toonder**, bedankt voor de introductie in de wereld van microfabricatie waardoor ik enthousiast werd over de mogelijkheden van organ-on-chips. **Gwendolen Reilly**, your review on *in vitro* bone remodeling models served as a great overview of the field at the start of my PhD. **Jenneke Klein-Nullend**, bedankt om naast de verdedigingscommissie ook deel te hebben genomen aan de gebruikerscommissie van dit project. Ook de intensive bot zomerschool in Udine diende als inspiratie voor dit werk. **Jeroen van den Beucken** and **Eric Farrell**, I am honored that you participate in my defense committee.

I want to express my gratitude to all the people that I collaborated with over the years. **Feihu**, thank you very much for all the computational work you did. It is really nice to see how the experimental and computational work complement each other. I enjoyed working with you very much. **Andreas**, bedankt voor je ontzettende behulpzaamheid en expertise op het gebied van microfluidic chips. Elke keer als ik iets niet wist, kon ik bij jou terecht voor uitgebreide uitleg. Ook mijn studenten werden uitgebreid door jou geholpen. Heel erg bedankt! **Hossein**, thank you for your advice and expertise in my fight against the bubbles. I am proud to present the set-up we came up with in this thesis. **Prof. dr. Ingrid Meulenbelt**, **dr. Yolande Ramos**, **Margo** en **Ilja** van LUMC bedankt voor de samenwerking op het gebied van joint-on-a-chip en zeker ook bedankt voor het mij wegwijs maken in het microfab lab door mij het fabricage proces van jullie chip te leren.

I am very grateful for the amazing **Bioengineering Bone group**. Dear bone girls, for me it felt as if we were not only colleagues but also friends. I really enjoyed our stay in Udine where

learning about bone while eating Italian dishes and lot's of ice cream under the sun was defined as working. **Bregje**, ik weet niet eens waar ik moet beginnen. Ik ben ontzettend blij dat jij op hetzelfde project zat. Dankzij al jou harde werken en doorzettingsvermogen heb jij grote invloed gehad op de totstandkoming van dit boekje. Bij jou kon ik terecht met al mijn vragen, problemen en frustraties. Ik heb bewondering voor jou passie voor de wetenschap en weet zeker dat er een hele mooie academische carrière voor je ligt. Heel veel succes in Zürich! Ik kan niet wachten om langs te komen en de bergen met jou te trotseren. **Sana**, you are the most kind person I know. Thank you for working together, for letting me use your ALP assay solutions and for the nice Iranian food you introduced us to. **Annelieke**, ik vond het erg gezellig toen jij de groep kwam versterken en erg leuk om jou in Krakau beter te leren kennen. Bedankt voor je behulpzaamheid. Ook **Stefan** wil ik graag even noemen. Hoewel we niet tegelijkertijd (fysiek) deel uit maakten van de BeB groep, ben ik dankbaar dat ik in de corona tijd mocht meewerken aan de systematic review. Ik ben blij dat dit mooie werk als hoofdstuk in dit proefschrift te vinden is.

Dan mijn paranimfen **Esther** en **Bart**. Es, jij past natuurlijk in heel veel lijstjes van dit rijtje, vriendengroep, onderzoeksgroep, subonderzoeksgroep, wat een voorrecht om met jou op zo veel vlakken samen te zijn. Ik was dan ook erg blij toen Sana en jij onze groep kwamen versterken toen ik net begonnen was. Zeker ook omdat jij tijdens onze master projecten mij veel geleerd hebt en mij enthousiast hebt gemaakt over het bot onderzoek. Ik vind het ontzettend bewonderenswaardig hoe jij de topsport combineert met een PhD en dat je op de een of andere manier ook nog tijd hebt om je huis te verbouwen en bij alle sociale activiteiten aanwezig te zijn. Je bent een topper! Bart, we hebben elkaar als studievrienden leren kennen en heel veel uren samen doorgebracht. Ik denk dat jij mij heel goed kent. Ik bewonder jouw vriendelijke en zorgzame karakter. We grappen wel eens dat je de ideale schoonzoon van de groep bent. Je hebt een geweldige manier om met mensen om te gaan en bent altijd bereid om anderen te helpen. Ik ben blij dat ik je als vriend mag hebben. Es en Bart, ik ben erg verheugd dat jullie aan mijn zijde staan op dit belangrijke moment.

I would like to thank all (former) members of the **Orthopaedic Biomechanics (OPB) group** for the very nice atmosphere and great enthusiasm during activities. I will never forget the amazing competitive mindset at the "meerkamp", but also at section retreat activities such as the escape room and quiz. This shows how nice of a team we are even with everybody working on their own specific "island". **Evelien**, bedankt voor het in stand houden van de gang van zaken in de groep, voor het plannen van de vele meetings en het organiseren van de section retreats. **Marina**, bedankt voor je expertise en hulp op het gebied van PCR. Hoewel mijn samples erg lastig waren, is het jou toch gelukt om RNA te isoleren en ik ben blij dat deze resultaten terug te vinden zijn in dit proefschrift. **Jurgen**, ontzettend bedankt voor de set-up die jij voor mij gebouwd hebt. Ik vind het fantastisch hoe jij elke keer weer een idee op papier kunt omzetten in een prachtig prototype. **Lucien** (hoewel geen OPB groep), ook jou wil ik bedanken voor je hulp in de werkplaats met het aan de praat houden van de pompen. Ze hebben het uiteindelijk tot het eind van mijn project gered, daar ben ik heel blij om.

Dankwoord (Acknowledgements)

Graag bedank ik de geweldige masterstudenten die ik heb mogen begeleiden: **Esmee, Claire, Marlous, Nils, Vivian** en **Neline**. Ik hoop dat jullie een leuke tijd hebben gehad en veel hebben geleerd. Ik heb in ieder geval veel van jullie geleerd. Ik ben trots op het werk dat jullie geleverd hebben en dankbaar dat gedeeltes hiervan ook duidelijk terug te vinden zijn in dit proefschrift.

I would like to thank all (former) members of **office 4.09**. Thanks for all the lunches, coffees and outings. Thanks to the **cell lab members** for sharing resources and knowledge and organizing nice activities such as the crazy 88 and the bake off. A big thank you for the **tech team** with a special shout out for **Yuana** and **Marloes** for running the cell lab during very challenging times. Our research would not have been possible without you.

Celien en **Lieke**, vanaf dag één tijdens de introductieweek van BMT hadden we een goede klik. Ik ben ontzettend blij dat we dan ook snel zijn gaan samenwonen in onze Boobytrap. En **Esther V**, eigenlijk woonde jij hier ook een beetje. Wie had toen ooit kunnen denken dat wij zo'n 5 jaar zouden samenwonen en lief en leed zouden delen. Ik ben erg blij dat Lieke calculus niet haalde (sorry Liek), omdat dat resulteerde in een ontzettend leuke vriendengroep: de Bokscheet! Hoe deze naam ontstaan is weet niemand eigenlijk, maar doordat jullie samen gingen studeren ontmoette we via Lieke allemaal leuke mensen: **Esther V, Bart, Johnick, Vincent en Willem**. Toen we elkaar in 2012/2013 leerden kennen, hadden we denk ik nooit verwacht dat we hier na al die jaren met zo veel van ons nog op de TU/e te vinden zouden zijn. Lieve Bokscheeters, bedankt voor de geweldige studenten jaren en vele kerstdiners. Ik hoop dat we dit voor altijd zullen blijven doen! Leuk ook om te zien dat de kerstdiners elk jaar drukker werden met **Jordi, Evi, Dirk, Noa, Annet, Elke, Navid en natuurlijk Len**.

Naast de Bokscheet heb ik ook nog het geluk gehad nog een hele leuke vriendengroep aan de studie over te houden: de BMT chickies. **Alicia, Elcke, Mylene, Sanne, Joni, Marissa** en ook weer **Lieke, Celien en de Esthers** bedankt voor alle gezellige etentjes, feestjes, wijn avondjes en weekendjes weg. Ik vind het erg leuk dat we elkaar blijven opzoeken, ook nu we wat verspreider door Nederland wonen. Ik kijk uit naar onze komende uitjes!

Veel mensen die ik al genoemd heb, passen in verschillende rijtjes. Ik wil nog even benadrukken hoe dankbaar ik ben dat wij met zo veel vrienden de kans hebben gehad om samen te werken. Ik denk dat het vrij uniek is dat wij na de master met z'n allen hebben besloten om nog wat extra jaartjes op de TUE te blijven hangen. **Celien, Alicia, Esther, Bart, Johnick**, zonder jullie was de PhD periode een stuk minder gezellig geweest.

Janique en **Willeke**, ik ben zo ontzettend blij met onze vriendschap. In de tweede klas van de middelbare school werden we vrienden en waar ook ter wereld wij ons allemaal hebben bevonden over de jaren, we blijven elkaar nog steeds opzoeken. Ik hoop dat onze nieuwe jaarlijkse traditie om naar Noorwegen te gaan ook nog zo lang blijft. En ik vind het heel erg leuk dat we met onze mannen **Mikis, Kevin** en **Paul** zo'n leuke groep vormen terwijl we allemaal zo verschillend zijn. Op nog vele hikes, langlaufsessies, kopjes thee en chocoladerepen!

Martin, bedankt voor alle thaibokslessen. Hoewel het misschien niet vanzelfsprekend is, hebben deze indirect wel bijgedragen aan dit proefschrift. Dat bleek zeker toen de sportscholen sloten tijdens de eerste corona lockdown. Ik kreeg binnen korte tijd last van RSI klachten. Zodra jouw (buiten) trainingen weer begonnen, verdwenen deze klachten direct. Uiteraard is thaiboksen ook heel erg geschikt tegen stress. Na een intensieve training van jou, is er geen ruimte meer voor stress in mijn hoofd.

Jan, Truke, Roland en **Irisch** ook jullie bedankt voor jullie interesse in mijn onderzoek. Ik vind het interessant om te zien dat bij jullie aan de keuken tafel niet alleen over koetjes en kalfjes gepraat wordt, maar dat er ook flink discussies over wereldzaken worden gehouden. Zo leer ik elke keer weer iets bij. Bedankt ook voor de gezelligheid, het lekkere eten en de wandelingen in het bos.

Familie **Vis** en familie **van Oppen**, bedankt voor jullie steun en interesse in wat ik doe, al weet niemand dat volgens mij precies en denken opa en oma dat ik een soort "bottendokter" ben. Ik ben blij dat wij bevoorrecht zijn met zo'n leuke familie. **Wim** en **Nicole** bedankt dat jullie altijd voor mij klaar staan. Ik heb bewondering hoe jullie ondanks je drukke banen altijd zorgen voor gezelligheid en etentjes.

Madelon, we zijn niet alleen zussen, maar ook vriendinnen. Je bent zorgzaam en staat voor iedereen klaar. Ik ben trots op jou en hoop dat we nog veel avonturen samen beleven. **Noël**, ik heb bewondering voor jou onuitputtelijke enthousiasme over sporten. Bedankt voor de dagelijkse motivatie om te blijven bewegen. Jammer dat ik de meeste Garmin challenges van je verlies, maar wie weet kan ik een keer meer stappen zetten dan jij als ik in Nepal een bergtrekking doe.

Lieve **papa** en **mama**, waar moet ik beginnen? Bedankt dat ik altijd op jullie kan rekenen. Dankzij jullie sta ik nu hier. Misschien hebben jullie mijn onderzoekers vlammetje wel aangewakkerd toen jullie mij vroeger een microscoop voor kerst cadeau deden. Ik ben blij dat jullie mij altijd steunen, of ik nou "helemaal" in Eindhoven wil gaan wonen of de wereld over wil reizen, jullie staan altijd achter mij en komen mij zelfs bezoeken als ik aan de andere kant van de wereld in Nieuw-Zeeland ben. Bedankt voor jullie onvoorwaardelijke liefde, steun en vertrouwen!

Lieve **Paul**, zonder jou had dit proefschrift hier waarschijnlijk niet gelegen. Ik ben zo blij dat ik altijd alles met jou kan delen en dat jij mij begrijpt en aanvoelt. Jij hebt mij geholpen om trots te zijn op het werk dat hier ligt door bijvoorbeeld heel enthousiast te reageren als ik jou vertelde over een resultaat waar ik zelf over twijfelde. Je hebt altijd geholpen om oplossingen te bedenken voor mijn problemen, geprobeerd om mij positief te laten denken en mij getroost als dat niet lukte. Ik ben super blij met ons fijne huisje dat door jouw kluskwaliteiten als maar mooier wordt en kijk uit naar alle avonturen die voor ons liggen!

Liefs,
Michelle